Defense Documentation Center

Defense Supply Agency

Cameron Station • Alexandria, Virginia

WT-1178

This document consists of 128 pages

No. 152 of 220 copies, Series A

Operation TEAPOT

NEVADA TEST SITE

February – May 1955

Project 37.2

DISTRIBUTION AND CHARACTERIZATION OF FALL-OUT AND AIRBORNE ACTIVITY FROM 10 TO 160 MILES FROM GROUND ZERO, SPRING 1955

12196

Issuance Date: November 17, 1958

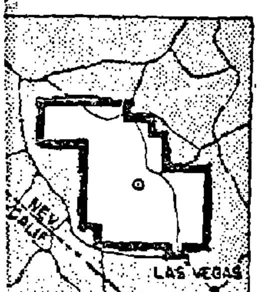

CIVIL EFFECTS TEST GROUP

4

5998

~~Report to the Test Director~~

(6)

DISTRIBUTION AND CHARACTERIZATION OF FALL-OUT AND AIRBORNE ACTIVITY FROM 10 TO 160 MILES FROM GROUND ZERO, SPRING 1955*

(10) By

L. Baurmash, J. W. Neel, W. K. Vance III,
H. M. Mork, and K. H. Larson.

(3)

Approved by: K. H. LARSON
Director
Program 37

Approved by: ROBERT L. CORSBIE
Director
Civil Effects Test Group

(5) California Univ., Los Angeles. School of Medicine.

University of California at Los Angeles
School of Medicine
Atomic Energy Project
Los Angeles, California

September 1958

(11) 17 Nov-58,

*This report supersedes parts of Report ITR-1178. The remainder of Report ITR-1178 has been superseded by Report WT-1178A.

NR

5

ABSTRACT

Fall-out patterns of four tower shots were delineated by survey-instrument methods to distances of approximately 160 miles from Ground Zero. Surface-contamination levels in terms of $\mu c/ft^2$ and fall-out particle-size distributions were determined by soil-sample analyses.

Airborne radioactivity concentrations determined by air samplers of different types and supports agreed within a factor of 4; aerosol radioactivity median diameters of $< 5\ \mu$ were determined by cascade impactors.

The solubilities of fall-out and airborne radioactivity in 0.1N HCl ranged from 20 to 30 and 65 to 85 per cent, respectively. More than 90 per cent of the fall-out from two shots was magnetic. Beta-decay slopes ranged from $T^{-0.80}$ to $T^{-1.58}$, and field gamma-decay slopes ranged from $T^{-1.07}$ to $T^{-2.10}$. Principal beta-energy peaks of 0.6 and 2.0 Mev were observed.

SECRET

ACKNOWLEDGMENTS

The authors wish to express their appreciation to the following individuals, without whose cooperative assistance the objectives of Project 37.2 would not have been realized, and to their parent organizations for making their participation possible:

D. E. Arthur, Oak Ridge National Laboratory
R. Baker, Paducah Area Office, AEC
W. Downs, University of Rochester
E. D. Graham, Idaho Operations Office, AEC
W. R. Heald, U. S. Department of Agriculture
K. Lauterbach, University of Rochester
R. G. Menzel, U. S. Department of Agriculture
P. W. Nickola, Hanford Operations Office, AEC
M. Stangler, U. S. Public Health Service
T. Toribara, University of Rochester
A. D. Warden, Oak Ridge National Laboratory
DeWitt Wood, University of Rochester

We wish to thank the division chiefs of the Atomic Energy Project at the University of California at Los Angeles (AEP/UCLA) for assigning personnel to this project. The following persons and the divisions to which they belong point up the internal cooperation:

B. L. Bachman, Radiobiology
M. Bastanchury, Administration
F. Bishop, Biophysics
H. Cook, Biochemistry
F. L. Delano, Administration
R. K. Dickey, Biophysics
R. L. Greene, Biochemistry
J. Hall, Biophysics
P. Keevan, Radiobiology
B. Kowalewsky, Radio-Ecology
J. Larson, Radiobiology
O. Smith, Administration
N. Todd, Radiobiology
D. White, Administration
D. Wright, Administration

Special appreciation is due the following:

The Health Physics Section, Biophysics Division, AEP/UCLA, under the direction of L. B. Silverman, for the handling of the beta-dosimetry work.

The Communications Section of the Test Director's Organization and the U. S. Air Force, whose assistance with communication problems greatly facilitated field operations.

The Air Weather Service for furnishing meteorological data necessary for operational planning and for evaluating much of the fall-out data.

The Test Director's Rad-Safe Unit for furnishing monitoring data to supplement our own in delineating fall-out patterns.

The personnel of Projects 37.1 and 37.3 for their helpful cooperation.

The authors wish to thank the numerous personnel of the AEP/UCLA, without whose cooperation this report could not have been completed.

CONTENTS

CONTENTS (Continued)

CONTENTS (Continued)

ILLUSTRATIONS

CHAPTER 2 METHODS AND MATERIALS

CHAPTER 3 RESULTS

[redacted]

ILLUSTRATIONS (Continued)

TABLES

CHAPTER 3 RESULTS

TABLES (Continued)

TABLES (Continued)

[redacted]

Chapter 1

INTRODUCTION

1.1 BACKGROUND

During previous continental test series, fall-out study programs were conducted either as routine safety procedures or as research programs. The on-site and off-site monitoring programs in populated areas within 200 miles of the Nevada Test Site (NTS) have been conducted by the Rad-Safe Unit of the Test Director's Organization and in the area beyond 200 miles by the AEC New York Operations Office.

The Atomic Energy Project, University of California at Los Angeles (AEP/UCLA), conducted research studies of fall-out distribution during Operations Upshot-Knothole and Tumbler-Snapper as part of the test organization.[1,2] This group also investigated the fall-out distribution from Trinity shot during the 2- to 6-yr period after the detonation.[3-5]

Other organizations have studied the fall-out problem primarily with respect to the immediate area surrounding Ground Zero (GZ). Results of these investigations are found mainly in the WT series of reports, but some information is given in other series. Two basic reports[6,7] on the subject are WT-386 and USNRDL-445.

Previous air-sampling programs used a variety of sampling instruments under various conditions. The air-sampling phases of the present investigation were designed to permit an evaluation of different sampling methods, including those which approximated isokinetic conditions. The investigation involved four types of air samplers: (1) high-volume automatic samplers operating over relatively short time intervals and using molecular filters, (2) high-volume manually changed samplers operating under different conditions of modification and using Mine Safety Appliances Company (MSA) BM-2133 filters, (3) wet-impinger samplers using several liquid media, and (4) modified cascade impactors.

The molecular filter samplers formed the basis for the determination of the influence of distance and time on radioactivity concentrations, total and radioactive particle-size distributions, and gross decay and energy characteristics of the collected sample. The manually changed high-volume samplers were used to study the effect of orifice velocity and direction on measured concentrations. They also represented the samplers most common to previous air-sampling programs. The wet-impinger samplers provided the basis for determining the immediate solubility of airborne contamination. The modified cascade impactors served as a direct field method for determining radioactive particle-size distributions.

The definition of fall-out patterns was accomplished by detailed monitoring of roads intersecting the patterns at approximately 90 deg to the midline. From these data, isodose maps depicting the area within 160 miles of GZ were plotted. The calculated short-term dosages at selected locations were supplemented by film-pack dosimetry estimates of effective beta skin dose.

Previous fall-out programs, e.g., the study cited in reference 2, have emphasized the importance of detailed sampling of fall-out material as an aid in evaluating the factors believed to influence its formation and distribution. Consequently, the detailed monitoring of roads crossing the fall-out patterns was accompanied by the collection of unit-area soil samples at selected locations. These samples provided the basis for the conversion of mr/hr to $\mu c/ft^2$ and for the determination of radioactive particle-size distributions as a function of distance. The total integrated particle-size distribution within 160 miles ultimately served as the basis for the evaluation of the influence of such factors as GZ soil characteristics, yield, height of detonation, and meteorological conditions on fall-out phenomena.

The characterization of airborne and fall-out material with respect to physical properties is essential to the definition of biological hazards. The possibility of fission-product fractionation within the cloud and, consequently, in fall-out distribution is of special interest as a possible mechanism for the occurrence of areas that are relatively high in concentration and/or availability of metabolically active isotopes. The characterization of the properties of the radioactive materials primarily involved decay, energy, and solubility investigations. The radiostrontium content of selected soil samples was also determined.

The present studies represent an effort to define further many of the phenomena described previously. It is anticipated that the information derived from these investigations will contribute substantially to the understanding of the mechanics of formation, the distribution, and the biological implications of radioactive material formed during a nuclear detonation.

1.2 OBJECTIVES

Project 37.2 studied the downwind concentrations of both airborne and primary fall-out within distances up to 160 miles from GZ. The general objectives were as follows:

1. To establish the validity of previously reported airborne concentration data and to perform measurements of concentrations and particle sizes within known limits of accuracy.
2. To define the fall-out patterns and to evaluate the several factors believed to influence the formation and distribution of the contributing fall-out particles, permitting a more complete definition of fall-out phenomena.
3. To determine some physical and chemical characteristics of airborne and primary fall-out debris, emphasizing the possible occurrence of fractionation of certain fission products as a function of distance and particle size, which may be postulated from decay schemes and the mechanics of particle formation.

1.3 DEFINITIONS

For the purposes of this report, airborne activity is defined as that activity which is suspended in air and is capable of being collected by the air samplers used for this study. Fall-out activity is defined as that activity which settles to the ground within the limits of the study area of this program. Decay constant, as used in this report, is the variable exponent of decay as used in the term $A = A_0 T^{-k}$.

REFERENCES

1. J. H. Olafson et al., Preliminary Study of Off-site Airborne Radioactive Materials, Nevada Proving Grounds. I. Fall-out Originating from Snapper 6, 7, and 8 at Distances of 10 to 50 Miles from Ground Zero, Report UCLA-243, 1953.
2. C. T. Rainey et al., Distribution and Characteristics of Fall-out at Distances Greater Than 10 Miles from Ground Zero, March and April 1953, Operation Upshot-Knothole, Report WT-811, 1954.
3. A. W. Bellamy et al., Alamogordo Report of 1947 Survey, UCLA unnumbered report, November 1947.

4. S. L. Warren, The 1948 Radiological and Biological Survey of Areas in New Mexico Affected by the First Atomic-bomb Detonation, Report UCLA-32, November 1949.
5. K. H. Larson et al., The 1949 and 1950 Radiological Soil Survey of Fission-product Contamination and Some Soil-Plant Interrelationships of Areas in New Mexico Affected by the First Atomic-bomb Detonation, Report UCLA-140, June 1951.
6. C. R. Maxwell, Nature and Distribution of Residual Contamination, Report WT-386, 1952.
7. A. L. Baietti and F. A. Devlin, Concentrations of Airborne Radioactivity Observed During Project 6.2 Field Experiments at Operation Jangle, Report USNRDL-445, 1954.

Chapter 2

METHODS AND MATERIALS

2.1 OPERATIONS

2.1.1 Nevada Test Site and Area of Operations

NTS is situated in a sparsely populated mountainous desert area within the boundaries of the Las Vegas Bombing and Gunnery Range. The two areas within NTS which were used for detonation sites during Operation Teapot were Yucca and Frenchman flats. These flats may be described as bowls surrounded by mountain ranges rising about 2500 ft above the floor of the bowls.

The areas of study extended from 7 to 160 miles from GZ in the direction of the predicted fall-out patterns. This region is characterized by mountain ranges varying up to slightly more than 10,000 ft, oriented in a north-south direction and separated by wide alluvial valleys. There are few improved roads or highways, but a large number of trails in various conditions of repair afforded access to much of the area.

2.1.2 Organization

During the maximum-effort shots a total of 20 persons were regularly involved in both field and laboratory work, with cooperative assistance from Project 37.1 personnel. Twelve persons were on temporary assignments from other AEC contractor installations, the U. S. Public Health Service, and the U. S. Department of Agriculture. The others were permanent employees of AEP/UCLA.

Three organizational groups were involved in the study of a detonation. The Field Group consisted of five teams of two men each, with another team of two being added for special assignments on selected shots. These teams were responsible for the installation and operation of sampling equipment and monitoring and field observations. The collected samples were processed by the Laboratory Group. The Administrative Group was responsible for the direction and correlation of both laboratory and field efforts, including the necessary logistics and support.

2.1.3 Basic Operational Plan

Since the fall-out pattern was dependent on meteorological conditions that varied with time, a weather unit correlated all available weather data and predicted fall-out paths to aid in the establishment of sampling stations. Meteorological information was received from the Air Weather Service and other organizational groups of the Test Director's Organization. Information on the predicted fall-out pattern which was necessary for the teams was relayed by radio and/or telephone to the field teams. The stations were established on the predicted midline of fall-out and on each side of this midline. The teams were allowed approximately 4 hr to establish their stations and to depart from the fall-out area.

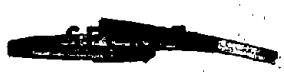

Owing to the mountainous terrain in the sampling area, which interfered with communications, it was necessary to establish an aerial relay station, which was borne aloft in a USAF C-47 flying out of Indian Springs. This relay station was in operation at approximately H−5 hr and H+30 min. The two aerial operations were required in order to send station-location directions, based on the latest possible information, to the field teams.

Because of the nonautomatic features of some of the sampling equipment, the teams were required to attend routinely the stations under their supervision. During the time between these routine trips and while checking stations, the field teams monitored the roads and trails on which they traveled. The data from the beta-gamma survey meters were reported when the teams returned to Mercury. Stations were secured at approximately H+30 hr, and all teams returned to base with equipment and samples.

2.2 FIELD SAMPLING STATIONS

2.2.1 Station Locations

Prior to the test series, various roads and trails were selected to be used as sampling areas. These approximated arcs 20, 40, 80, and 160 miles from the test site. The actual station locations on these arcs were not preassigned since weather conditions ultimately determined their positions.

2.2.2 Basic Sampling Complement

The sampling stations were defined as follows, depending on the equipment installed:

1. Routine Air-sampling Station: This station consisted of an automatic air sampler, a wet-impinger sampler, a directional high-volume sampler with throttle, a background recorder, gummed-paper assemblies, and a skin-dose film pack. These stations were installed in right and left flank positions.

2. Midline Air-sampling Station: This station consisted of all the equipment of a routine station plus extra equipment capable of obtaining data needed for correlative studies, e.g., extra gummed papers for uniformity studies, directional vs fixed high-volume samplers with and without throttle to determine which sampler gave the most representative sample of airborne concentration, a cascade impactor to be used to obtain size-analysis data, and a wind-direction and velocity recorder (Fig. 2.1).

3. Tray Station: This station consisted of a pair of gummed-paper assemblies. The tray stations were located between air-sampling stations and on either side of the flank stations.

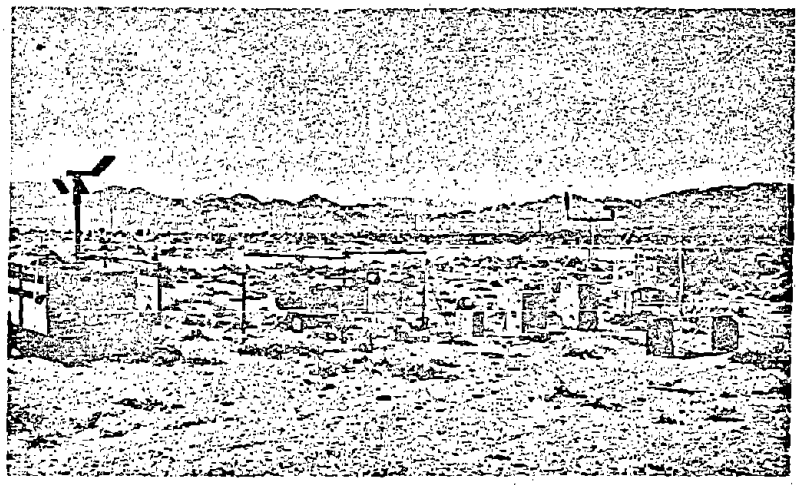

Fig. 2.1 — Typical midline air-sampling station.

2.3 FIELD SAMPLING EQUIPMENT AND TECHNIQUES

The selection of field-sampling equipment was based fundamentally on the greatest anticipated yield of information describing biological hazard and aiding in the formulation of a theory to explain the various fall-out patterns. The requisites of such equipment were portability, reliability, and consistency of operation.

All air sampling was done at 3 to 4 ft above the ground. Gummed papers and film packs were also exposed at this height. Survey-meter readings were taken 3 ft above the ground and at least 50 ft away from any buildings or vehicles.

2.3.1 Modified High-volume Automatic Air Sampler

Basically this unit consists of the automatic air sampler described in a previous report.[1] Several modifications have been made in the design of this unit to improve the over-all performance. During Operation Upshot-Knothole it was noted that the filter seal was not adequate. A positive filter seal was assured by the use of a screw type retaining ring. A d-c indexing motor replaced the rotary solenoid in the original unit, thus the positioning of the filters in the sampling orifice was positive. The samplers were adjusted to sample for 2-hr periods. Initiation of sampling was set at a suitable period, usually 1 hr prior to predicted fall-out time, by means of a delay-timing mechanism, which yielded delay times up to 20 hr. The samplers were placed on card tables with the sampling orifice 42 in. from the ground and facing GZ (Figs. 2.2 and 2.3).

The filter medium used in these units was a molecular filter (Millipore) backed by an MSA all-purpose dust pad, type BM-2133, for support. With this filtering combination the rate of air flow averaged 8 ft^3/min.

2.3.2 Modified High-volume Air Sampler

A vacuum-cleaner type of sampler was modified to sample through flat filters. In order to compare the effect of sampling velocity, several units were equipped with a reducing orifice to obtain a velocity equivalent to 38.14 mph. These units were compared to units which sampled at a velocity of 5.2 mph under unrestricted flow conditions. The two types were suspended from a support by means of nylon cord, and vanes were attached to the rear of the unit so that the sampler faced upwind. At the same location a sampler was placed in a fixed direction, toward GZ, with the orifice throttle in place (Figs. 2.4 and 2.5). The concentration data obtained by these three sampling methods were compared to determine the effect of orifice velocity and direction on measured airborne concentration.

These units used the MSA all-purpose dust pad, type BM-2133, as the filtering medium. The sampling rate with the throttle in place was 38 ft^3/min, and without the throttle the rate was 40 ft^3/min. The filters on these units were changed manually approximately every 4 hr.

2.3.3 Jet-impinger Air Sampler

The jet impinger, or wet impinger, as it is commonly designated, consisted of two units: a polyethylene container (3-pint capacity) and a Lucite impinger assembly, consisting of a 0.75-in.-I.D. outlet tube and a 1-in.-I.D. intake tube ending in a five-jet impinger. Three baffles, evenly spaced along the tube with alternately positioned perforations, served to decrease both splashing and bubble size.

The liquid-sampling unit consisted of four impingers whose outlet tubes were connected to a central reservoir, the entire unit being enclosed in a 14.5- by 14.5- by 18.5-in. wooden case. At the beginning of the sampling period, individual impinger containers received 350 ml of one of the following solutions: (1) distilled water, (2) 0.1N HCl, (3) 0.1N $Na_2S_2O_3$, or (4) sodium diphosphate–citric-acid buffer solution at pH 7.6. The reservoir was connected by rubber tubing to the intake of a Parson's air sampler operated without a magazine. In order to prevent freezing of the solutions, a 100-watt heater tape connected to the electrical circuit of the unmodified sampler was placed around the impinger containers (Figs. 2.6 and 2.7).

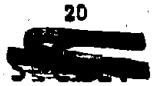

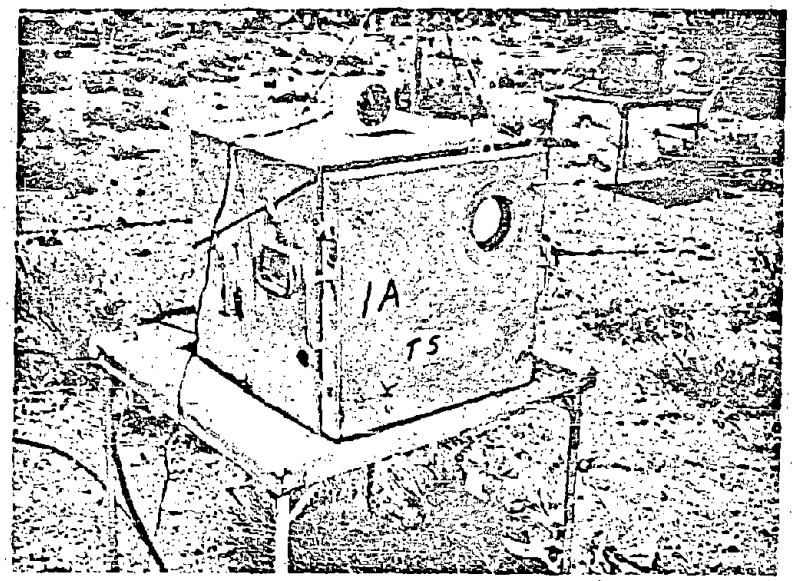

Fig. 2.2—Modified automatic air sampler in position for fall-out sampling.

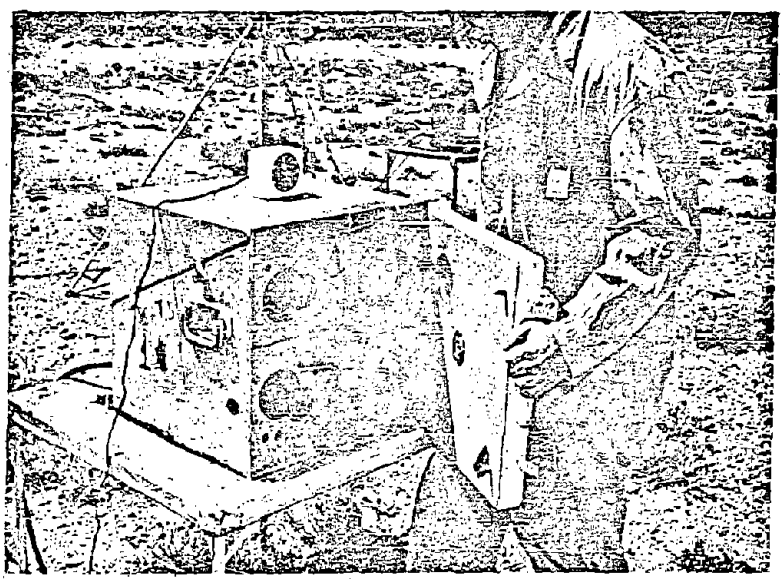

Fig. 2.3—Automatic air sampler, showing method of changing magazines.

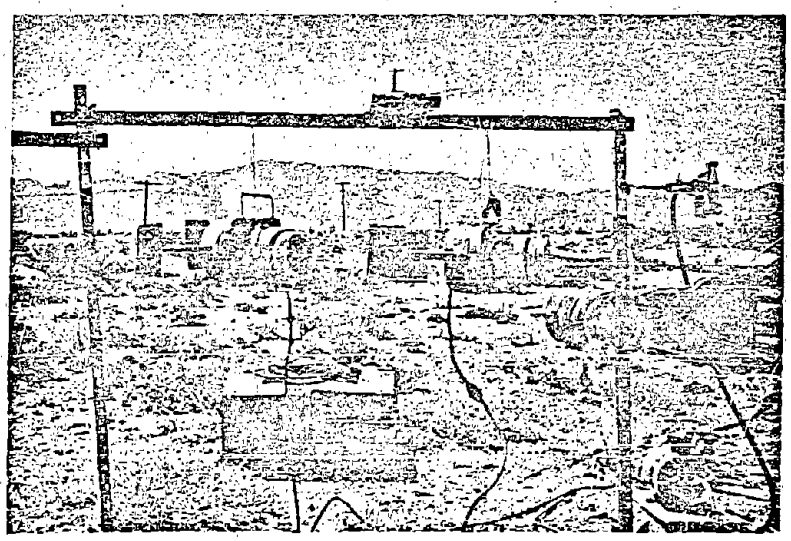

Fig. 2.4—High- and low-inlet velocity directional samplers and method of installation. Cascade impactor is located on fence post at upper right.

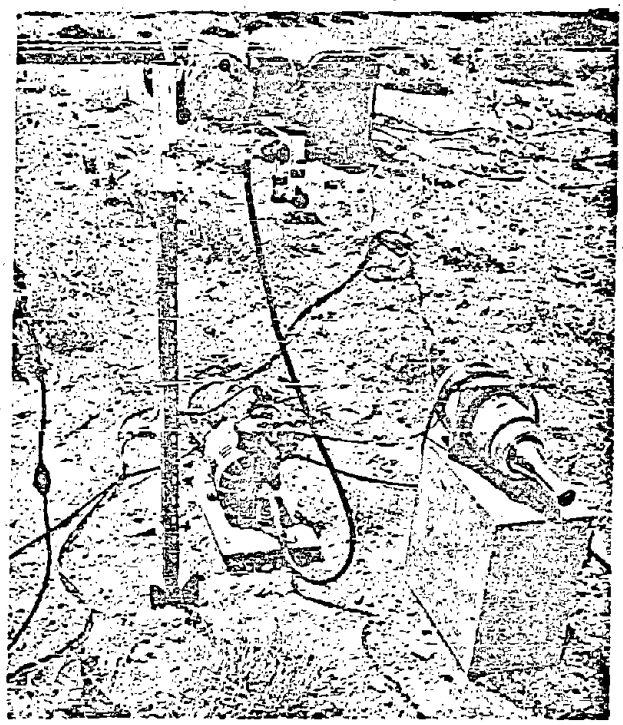

Fig. 2.5—Fixed-directional sampler with high-velocity nozzle. The Casella cascade impactor is located on fence post in center.

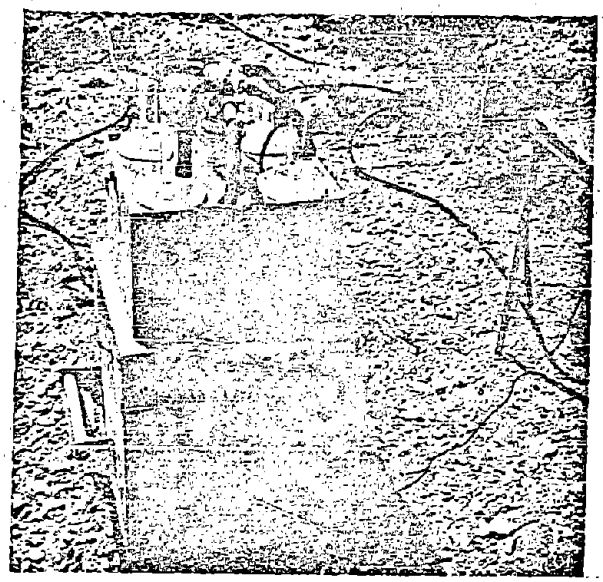

Fig. 2.6—Relation of plastic impinger units and pump section.

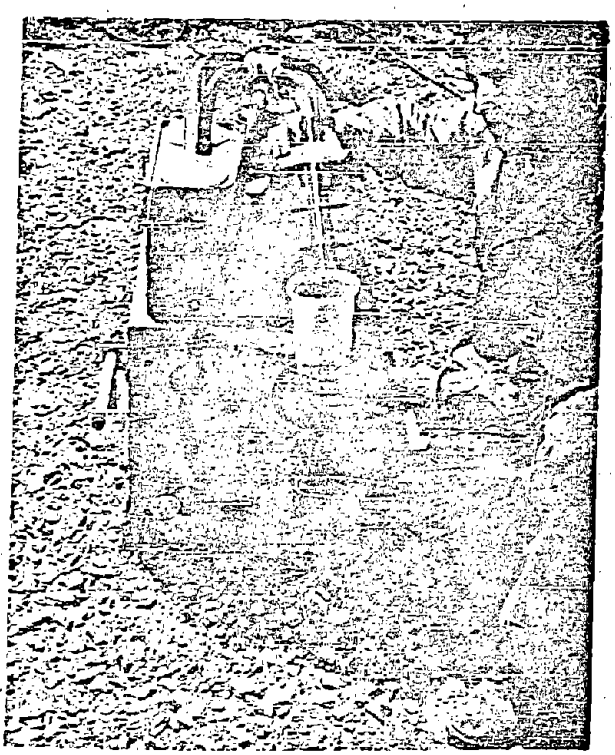

Fig. 2.7—Plastic impinger unit, showing nozzles and diffusion plates.

The initiation of sampling coincided with that of the modified high-volume automatic samplers (Sec. 2.3.1), and the samplers operated continuously for approximately 8 hr. The reduction of solution volume through vapor loss (approximately 100 ml/hr/impinger) required periodic additions of the solution during the sampling period to maintain a minimum volume of 200 ml. At the conclusion of the sampling period, the intake orifice of each impinger was sealed with a rubber stopper for transport to the laboratory.

2.3.4 Modified Casella Cascade Impactor

These units consisted of the standard Casella impactor with an added fifth stage consisting of a Whatman No. 41 filter (Figs. 2.4 and 2.5). The impactors were operated in sequence and changed manually.

2.3.5 Gummed-paper Fall-out Sampler

The determination of primary fall-out concentrations was initiated by the collection of fall-out particles on 8- by 9-in. adhesive-covered cellophane sheets. The sheets were mounted on galvanized-iron plates 4 ft above the ground. Normally, two gummed papers were used at each installation to increase the sampling area (Fig. 2.6), but four gummed papers were used for some studies.

At the midline stations a study was made of the persistence and migration of the fall-out material. After several hours of exposure the exposed gummed papers were removed, and fresh papers were installed. Fresh papers were also exposed 6 in. above the ground at this time. On termination of station operation, these papers were removed and returned to the laboratory.

2.3.6 Background Recorder

An essential phase of the study of fall-out phenomena was the determination of fall-out time and the duration of fall-out. This was accomplished by means of a background recorder consisting of a Neher-White ionization chamber connected to a d-c–operated current amplifier whose output drove an Esterline-Angus recorder (Fig. 2.9). All the components were installed in a metal case, and the detecting unit was exposed only to the radiation penetrating the cabinet. The response of the detector and amplifier was logarithmic and ranged up to 100 r/hr. The time at which a rise in activity to 1 mr/hr was noted was designated as the fall-out time, and the time from the initial rise until the radiation level began to decrease below the maximum was designated as the duration.

2.3.7 Film-pack Dosimetry

A description of the techniques and analytical procedures associated with this phase of fall-out documentation has been issued separately.[2]

2.3.8 Field Monitoring

The fall-out pattern was defined on the basis of radiation-intensity measurements across the path of fall-out. The data were obtained by the regular station teams and special monitoring teams using Precision model 106 G-M type beta-gamma survey meters and Jordan model AG-500 ionization-chamber type gamma survey meters.

On the passage of the fission cloud, the teams traversed their respective arcs. Readings were taken every 2 miles until an increase in radiation was observed, at which time the teams moved until a reading of 1 mr/hr was obtained. During some tests, teams then proceeded to make readings across arcs at 1-mile intervals until a value of 1 mr/hr was again reached. This information was brought to Mercury by the teams, and the data were plotted. During shots of particular interest the location of 1 mr/hr was again the starting point for the monitoring survey. However, in these cases, readings were taken at 0.5-mile intervals until a value of 1 mr/hr was again reached. The teams rough-plotted their data to determine the approximate midline, and then they took instrument readings at 0.1-mile intervals for a distance of 0.5 mile on either side of this midpoint. This information was also brought to Mercury for plotting.

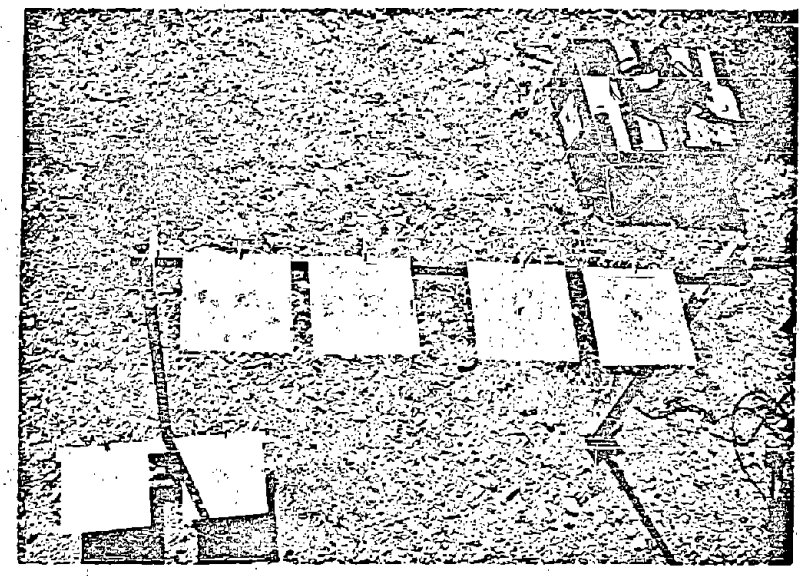

Fig. 2.8—Method of exposing gummed papers, showing relative position of ½- and 4-ft samplers.

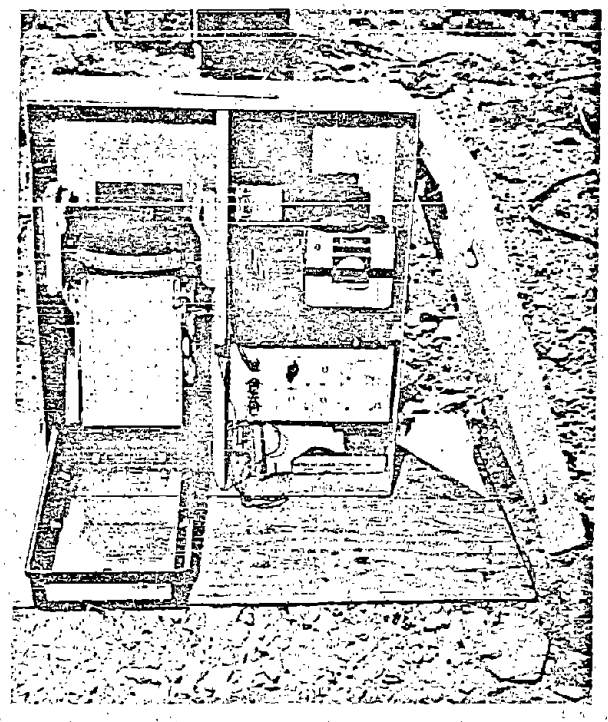

Fig. 2.9—Internal mechanism of battery-operated background recorder, showing relative positions of components.

2.3.9 Wind-direction Recorder

Two stations, 20 and 80 miles from GZ, were equipped with wind-direction recorders. The equipment used was the commercially available cup anemometer and vane instrument supplied by The Instruments Corporation and trademarked Anemograph. This instrument records wind velocity and direction on the same strip chart. The velocity range was from 3 to 75 mph, and the direction was 360 deg in scope. The instrument gave information for correlation with air-sampling results.

2.3.10 Soil-sample Collection

The locations for soil sampling depended on the isodose plots that defined the fall-out patterns. If the field teams were not notified on the morning of D+1 day as to the location of the midline of the fall-out, they used the maximum radiation-intensity location as the midline. A sample consisting of 3 ft^2 of surface soil was collected at this point by the use of a 1-ft^2 template (Fig. 2.10). Samples of similar areas were taken at intervals on either side of the midpoint until the activity had decreased to 1.0 mr/hr. These samples were then brought back to the laboratory.

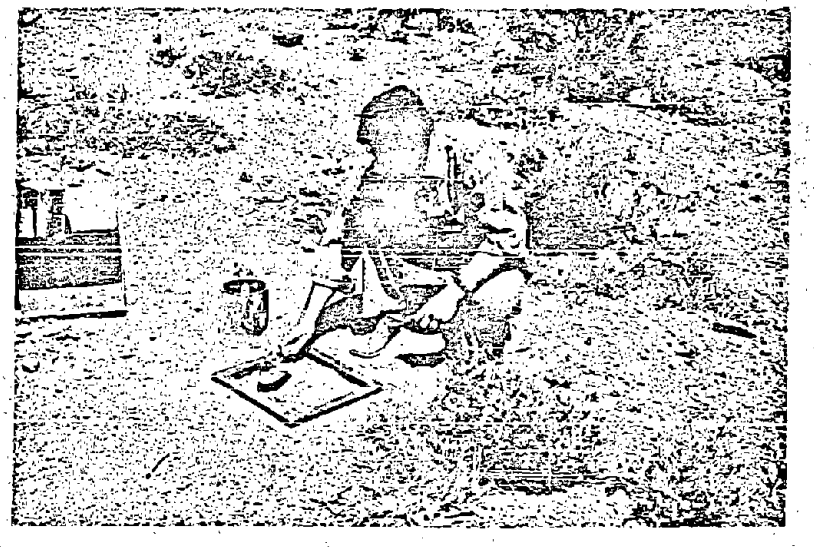

Fig. 2.10 — Method of collecting 1-ft^2 soil-surface sample using steel template.

2.4 SAMPLE PROCESSING

2.4.1 High-volume Air Samples

Each group of high-volume samples from an individual sampler was assembled as a unit in sequential order. The filters were placed in cellophane bags, and a code designation was assigned. All the members of a series were placed together in an envelope with a cover sheet identifying the unit. The complete set of filters was then ready for radioassay.

2.4.2 Jet-impinger Samples

On the completion of a sampling run, the field team in charge stoppered the impinger units and returned the complete set of four to the laboratory. Each container with its liquid was handled as a separate entity. The filtration equipment consisted of an all-glass filtering funnel and Millipore filters. The contaminated suspension was poured from the impinger flask into the upper section of the funnel, and the filtrate was collected in a 500-ml volumetric flask.

When all the original suspension had been filtered, sufficient washings of the same liquid were used to bring the volume to 500 ml. The flask was then marked with the identifying code. A 25-ml aliquot was taken and placed in a Petri dish. The liquid sample and the Millipore filter were then dried and counted. If sufficient activity was found in the solution, the balance in the volumetric flask was placed in polyethylene storage bottles.

2.4.3 Cascade-impactor Samples

Each cascade unit was dismantled in the laboratory, and each stage was marked. The five stages of the samples were counted in sequence in the same scaling unit. Individual units in the sampling sequence were handled in this manner, and the data were tabulated in serial order.

2.4.4 Gummed-paper Fall-out Samples

After the sample papers had been exposed and were ready for collection, two trays were placed face to face for transport to the laboratory. At the laboratory the exposed areas were removed from the trays, and the papers were cut in half to yield two 4- by 9-in. counting samples. These papers were placed in cellophane bags and marked.

Gummed papers were radioassayed on flat-plate counters. Selected samples were saved for decay and energy studies. Other samples were selected for autoradiographic studies.

2.4.5 Soil Samples

If wet, soil samples were initially dried by the use of gas hot plates. After drying, the total quantity of soil was sieved through a 2-mm sieve, and the weight of material <2 mm was obtained. Triplicate 100-g samples of the <2-mm soil were placed in 4- by 9- by 1-in. boxes and counted in flat-plate counters.

One of the 100-g samples was placed in a sieve nest (Fig. 2.11) and shaken for 60 min to yield the following size fractions, in microns:

2000–500	250–177
500–420	177–125
420–350	125– 88
350–300	88– 44
300–250	44– 0

The fraction of 0 to 44 μ was subjected to further fractionation in a roller particle-size analyzer (Fig. 2.12) to yield the following size fractions, also in microns:

44–20
20– 5
5– 0

Each of the above fractions was weighed and radioassayed for total radioactivity.

Selected soil fractions were treated with distilled water, 0.1N HCl, 0.1N $Na_2S_2O_3$, and sodium diphosphate–citric-acid buffer solution at pH 7.6 to determine soluble components. Samples weighing 0.1 or 0.5 g were suspended in 50 or 250 ml of solution for 30 min, respectively, with occasional shaking. The suspensions were filtered through Millipore filters, and the residue and a 25-ml aliquot of the filtrate were dried at approximately 100°C. The dried samples were radioassayed, with appropriate self-absorption correction factors being applied to the residual samples.

2.5 RADIOACTIVITY ASSAYS

2.5.1 Equipment and Techniques

Two types of radiation counting equipment were used. Small samples, such as cascade-impactor stages, wet-scrubber samples, and a number of soil samples selected for decay and

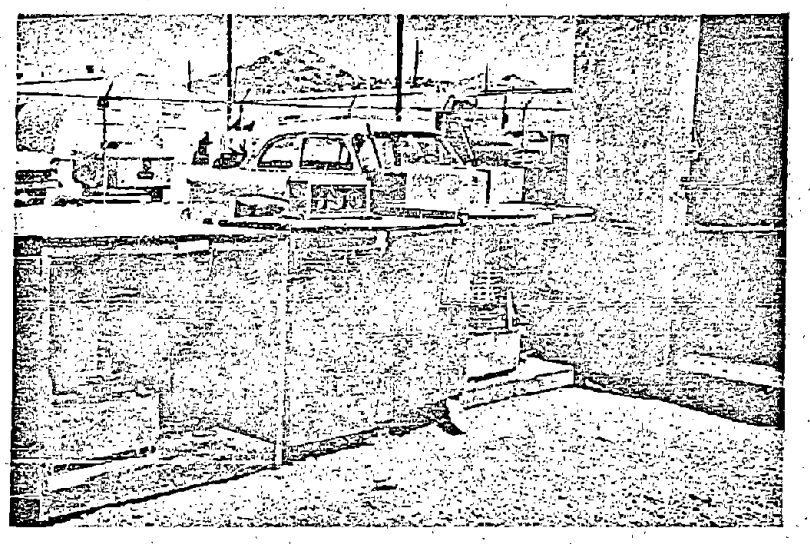

Fig. 2.11—Soil sieve nest in position on shaking mechanism.

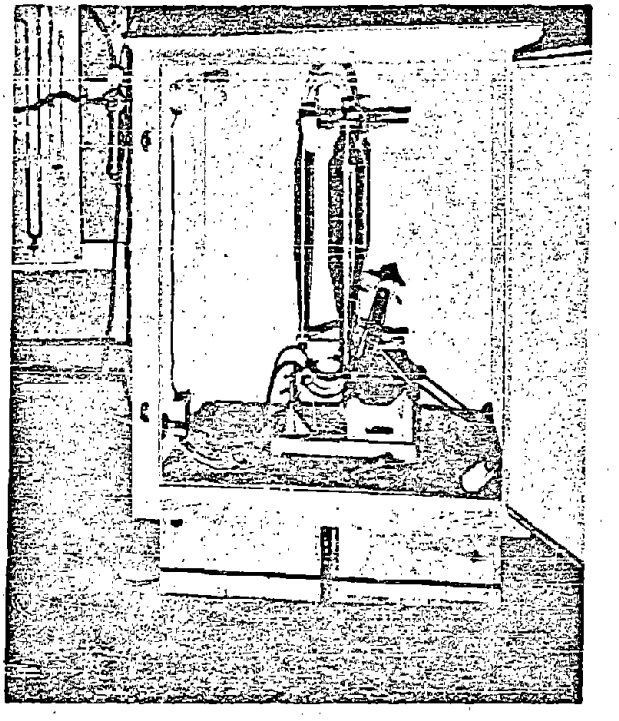

Fig. 2.12—Roller particle-size analyzer with separation chamber used to remove 5- to 20-μ fractions.

energy investigations were radioassayed by halogen-filled Anton No. 10017 tubes having window thicknesses ranging from 1.4 to 2.0 mg/cm^2 in conjunction with IDL or Nuclear scalers. The tubes were mounted in 2-in.-thick aluminum-lined lead shields. Individual samples were counted for a total of 1000 counts or 5 min, whichever required less time, at geometries ranging from 2 to 30 per cent.

The large-area samples, such as air filters, gummed papers, and soil samples, were counted in flat-plate methane-flow proportional counters (Figs. 2.13 to 2.15). These units, which were fabricated at Los Alamos Scientific Laboratory, have a higher count acceptance than the G-M type. Each unit consisted of an unshielded flat-plate counter having an aluminum-coated Mylar film window (0.8 mg/cm^2) followed by a linear amplifier and a binary scaler. Samples were counted routinely for a minimum of 40,000 counts or 5 min, whichever required less time; thin samples were counted at a geometry of 30 per cent, whereas thick or exceedingly radioactive samples were counted at geometries ranging to 4 per cent.

Counting efficiencies were determined by the use of Ra-D and -E standards prepared by adding aliquots of standardized Ra-D and -E solutions to Whatman No. 1 filter paper. All standards were enclosed in a 1-mil thickness of aluminum to absorb the soft-beta components. The standards approximated the dimensions of the samples to be radioassayed, and they were compared under the same counting conditions.

Coincidence correction values were determined by the method of counting two samples individually and together.

The size analysis of suspensions derived from air-filter samples was accomplished by using a thin anthracene crystal in conjunction with a photomultiplier tube and rate meter to measure the rate of change of activity while the suspension was allowed to settle (Fig. 2.16).

Corrections for the decay of field samples were based on the following equation, describing the decay of mixed fission products:

$$A = A_0 T^{-1.2}$$

where A = activity or dose rate at any time t
A_0 = activity or dose rate at any reference time t_1
T = ratio of time t to time t_1

Radioactivity values are expressed in terms of microcuries as derived from the equivalency of 1 μc to 2.22×10^6 d/min.

2.5.2 Determination of Airborne Activity Concentration

Air samplers were calibrated prior to sampling with respect to sampling rate, and the total volume of air sampled per filter was calculated. The total activity divided by the latter value yielded the activity concentration at the time of counting. This value was corrected for decay to the midtime of sampling and to H + 12 hr. Since all samples were then on a common basis, comparisons could be made regarding the rate of cloud travel and the rate of deposition of fission product.

2.5.3 Determination of Fall-out Activity per Unit Area

Fall-out activity per unit-area values were determined by two methods: (1) gummed papers and (2) soil samples. Duplicate or quadruplicate gummed-paper samples, each representing 0.5 ft^2, were averaged to yield unit-area activities.

Triplicate 100-g samples of the <2-mm soil material were placed in 4- by 9- by 1-in. cardboard boxes and radioassayed by gas-flow counters. Radioactivity values were extrapolated to zero mass by sample self-absorption factors, which were determined by counting increasing weight increments of contaminated soil. These factors were determined periodically throughout the counting period to account for energy variation with time. The average radioactivity of 100 g of soil was then related to activity per unit area through the total weight of <2-mm soil collected per 3 ft^2.

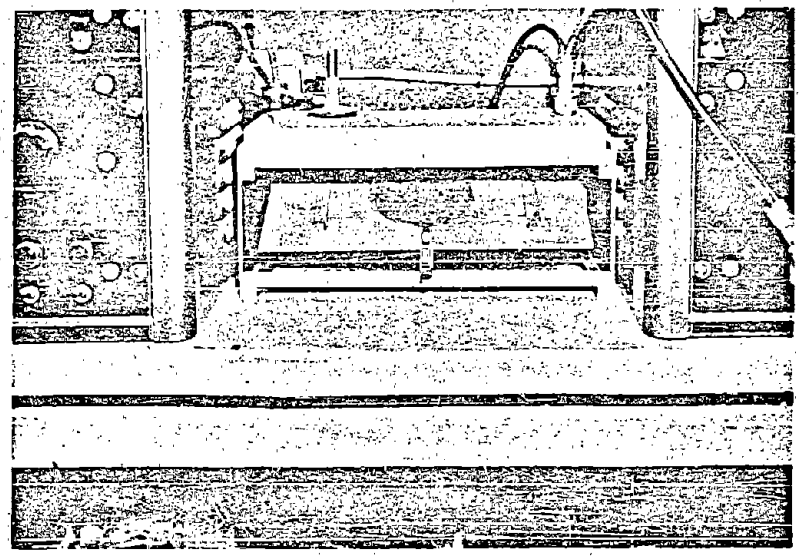

Fig. 2.13—Flat-plate methane-flow proportional counter with air filter in position for counting (after shelf is closed).

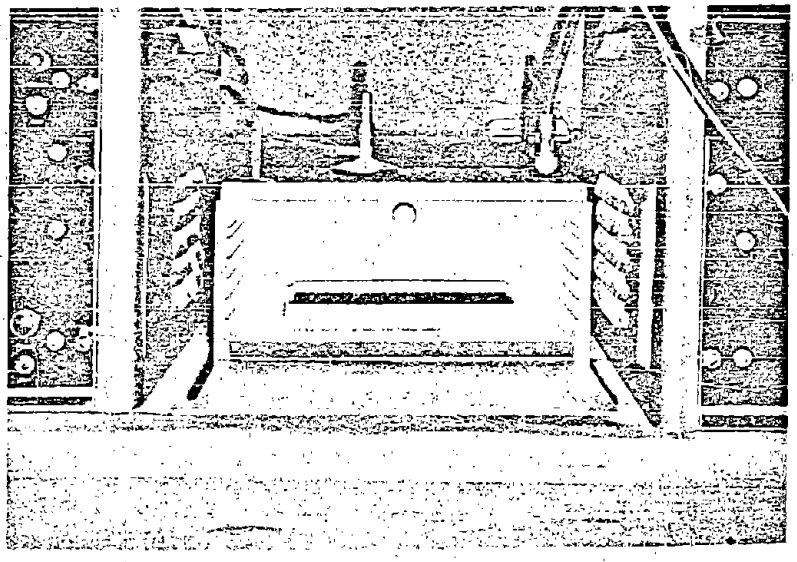

Fig. 2.14—Proportional counter with 100-g soil sample in position for counting.

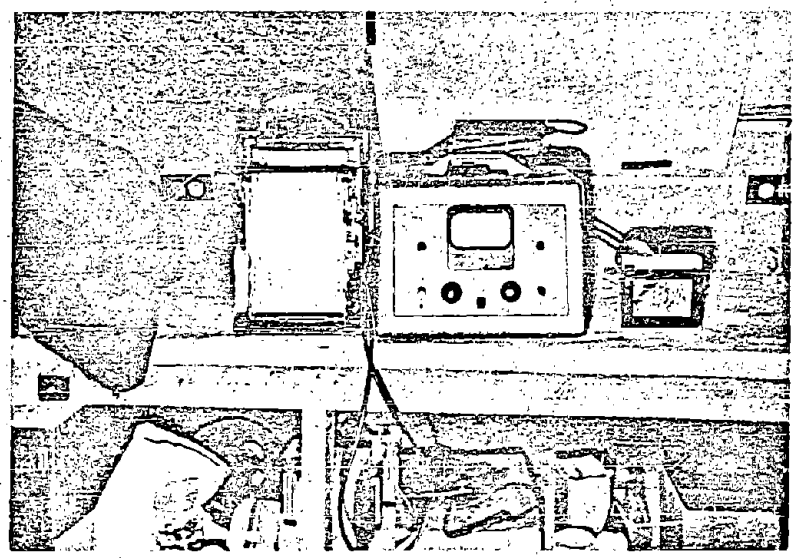

Fig. 2.15—Gas-flow detecting element and proportional counter with soil-sample fraction in counting position.

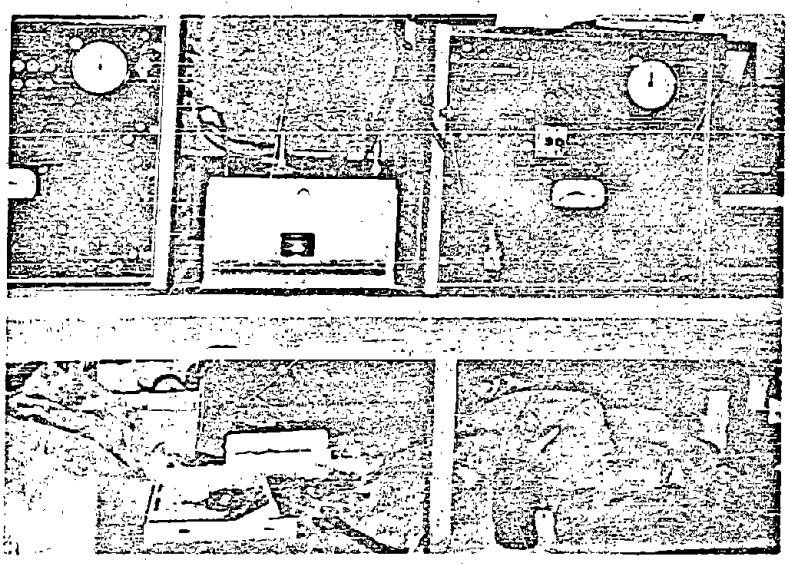

Fig. 2.16—Components of radiosedimentation unit with detecting elements at right. Other parts are rate meter and recorder.

For purposes of comparison, all activity per unit-area values were corrected for decay to H+12 hr.

2.5.4 Determination of Particle Size of Fall-out Material

Two types of samples were measured for their size distribution. The soil samples fractionated by sieve nest and roller particle-size analyzer yielded a direct weight analysis. Each of these fractions was measured for total radioactivity yielding the activity distribution with size.

The air samples were analyzed by two different techniques. A simple and commonly used method was that of the cascade impactor. The distribution of the activity was an indication of the size distribution of the airborne activity.

The particulate matter on selected molecular filters was also size-analyzed after the total activity was determined. A molecular filter was dissolved in 20 ml of 40 per cent acetone and 60 per cent Cellosolve. This suspension was placed in a polyethylene test tube so that the level of the liquid was 1.25 cm above a 0.25-in.-thick anthracene crystal. As the suspension settled, the light output of the crystal decreased. This output was detected by a photomultiplier tube connected to a recording rate meter. By the use of Stokes' law, the activity contribution by each size fraction was determined from the trace.

2.5.5 Radiostrontium Analysis of Soils

In order to obtain a measure of the fractionation of radiostrontium in fall-out material, a series of soils from Tesla and Met shots were assayed radiochemically for this isotope. All the soils were dry-sieved to obtain the various size fractions. The predominant particle size and the 0- to 44-μ size were then analyzed. Using the Tesla soils, the total activity and radiostrontium content were determined. For the Met soils, the same activities were measured, in addition to the determination of exchangeable total and radiostrontium activities.

Total activities of soils were determined by treating a 5-g sample with $HClO_4$ and HF. The residue was dissolved in dilute HNO_3, and the volume was made up to 100 ml. Aliquots were plated on planchets for radioassay.

Radiostrontium determinations were made by first fusing the soil aliquot with Na_2CO_3 at 900°C for 1.5 hr. The melt was dissolved in dilute HCl, evaporated to dryness in Pyrex beakers, and baked for 1 hr at 110°C to dehydrate the silica. Fifteen milliliters of concentrated HCl was added to the dried residue and allowed to wet the solids completely, after which 225 ml of water was added. The suspension was heated gently until only the silica remained undissolved. The silica was filtered and washed with a 1:20 dilution of HCl. The dried silica was checked for activity. Significant activity was found to be associated with the silica at this point. Forty-eight per cent of HF was added to convert SiO_2 to SiF_4, which was volatilized by evaporating to dryness. The small amount of insoluble residue containing the activity was again fused with Na_2CO_3, and silica was separated as described above. No activity was found in the silica at this stage. Strontium carrier was added to the combined filtrates from the above separations, and they were then neutralized to pH 4 to 5 with NaOH; Na_2CO_3 was added, and the resulting precipitate was filtered. The precipitate was dissolved in dilute HCl and evaporated to dryness. Water and fuming HNO_3 were added to the residue to give a final concentration of 75 per cent HNO_3. This served to dissolve most of the salts present, other than barium and strontium nitrates. The strontium was redissolved from this precipitate with water, and the resulting solution was scavenged with $Fe(OH)_3$ and $BaCrO_4$. The strontium was precipitated from the filtrate as the oxalate.

The exchangeable activity was determined by leaching the soil sample with normal $NH_4C_2H_3O_2$ (pH 7.0). The leachate was dried, ashed, and then put into solution with water. Aliquots of this solution were used to determine total exchangeable activity. Strontium carrier was added to the remainder of the solution and to the strontium-isolated oxalate precipitate, as in the above procedure.

REFERENCES

1. C. T. Rainey et al., Distribution and Characteristics of Fall-out at Distances Greater Than 10 Miles from Ground Zero, March and April 1953, Operation Upshot-Knothole, Report WT-811, 1954.
2. R. K. Dickey et al., Beta Skin-dose Measurements by Specially Designed Film-pack Dosimeters, Operation Teapot, Report WT-1178A.

Chapter 3

RESULTS

3.1 SHOT PARTICIPATION

Six detonations of varying characteristics, as summarized in Table 3.1, represented the major effort of Project 37.2. The data derived from the several detonations varied to some extent with regard to quantity and type, depending on the characteristics of the detonation and program requirements.

Special samples were collected from Moth fall-out, and they were characterized on request of the Fall-out Prediction Unit of the Test Director's Organization. The data from this study are in Appendix A.

On the request of the Division of Biology and Medicine, samples collected by an airplane flying through the cloud from Hornet shot were analyzed and characterized. At that time, some decontamination studies were made on the samples, and these data are given in Appendix B.

TABLE 3.1—PROJECT 37.2 SHOT PARTICIPATION

Shot*	Date (1955)	Time	Height, ft	Yield, kt
Tesla	1 March	0530 PST	300	6.9 ± 0.2
Turk	7 March	0520 PST	500	43.0 ± 2.0
Bee	22 March	0505 PST	500	8.1 ± 0.3
Apple I	29 March	0455 PST	500	15.5 ± 2.0
Met	15 April	1115 PST	400	23 ± 1.5
Apple II	5 May	0510 PDT	500	30.0 ± 3.0

* Met was fired on Frenchman Flat; all other shots were fired on Yucca Flat.

3.2 METEOROLOGY

3.2.1 Forecasts

During the period 12 February through 5 May 1955, 51 12-hr operational forecasts (midline of fall-out) were made. The approximate accuracy of these midline forecasts was 68 per cent, and, on this basis, four of the six shots worked should have been fall-out "hits." In practice, two direct fall-out hits were realized; and, in two other cases, the fission cloud went directly over the midline sampling stations. It is believed that the latter two cases would have been hits if the proper cloud heights could have been forecast.

3.2.2 Trajectories

Constant-layer air movement determinations were calculated for the six shots of interest to Project 37.2. Based on these data, surface positions and times of arrival of particles falling from within the debris cloud were determined. For the four shots that were studied in detail, the computed predominant particle sizes are included.

The surface positions and times of arrival of particles falling from within the cloud were computed as follows:

The atmosphere was divided into equal layers of 5000 ft parallel to mean sea level, and it was assumed that a reported wind was representative for the entire layer and that a given wind held for a period of time midway between the reported time and that of the next observation. If more than one wind was reported within any given layer, the vector resultant was determined, with speed equal to the length of this resultant vector divided by the number of winds reported for that layer. Streamline isotach maps were analyzed for each layer and for each observation time from shot time to the limit of the data in time and/or area. A particle was then started at the top of each 5000-ft layer and projected until it reached the ground. Assumptions used in these computations included the following:

1. Any given particle spent equal amounts of time in each layer during its descent.
2. A particle was advected exactly with the wind, and instantaneous velocity occurred.
3. It was possible for all particles in the 0- to 1000-μ-diameter range to reach all levels with the cloud.

No diffusion or vertical motions were taken into account in any of the computations, and the cloud was considered as a line source; therefore, no particle distribution across any given layer was considered. To demonstrate the change of wind with time in a layer and over the area considered, constant-layer trajectories were computed. The trajectories demonstrated the path of particles remaining in a layer throughout a given time interval. The diagram of constant-layer trajectories (Figs. 3.1 to 3.6) and surface positions and times of arrival of particles (Figs. 3.7 to 3.12) show GZ and a portion of the NTS area as outlined on standard aeronautical charts of scale 1:500,000. The times shown at each position along a given altitude or layer are Pacific Standard Time. Table 3.2 lists the approximate height of cloud and shot time for each of the six detonations considered.

TABLE 3.2—SHOT TIME AND CLOUD HEIGHTS USED IN TRAJECTORY ANALYSES

Shot	Shot time (PST)	Cloud height, ft above MSL
Tesla	0530	27,000
Turk	0520	42,000
Bee	0505	40,000
Apple I	0455	31,000
Met	1115	42,000
Apple II	0410	40,500

The computations of predominant-size particles at the various ground positions were accomplished using an equation developed by Rubey, namely:

$$v\mu = -\frac{6\mu}{\rho_0 d} + \frac{36\mu^2}{\rho_0^2 d^2} + \frac{2g}{9}\frac{\rho - \rho_0}{\rho_0} d$$

where μ = viscosity of air
ρ_0 = density of the air
d = diameter of the particle
g = acceleration of gravity
ρ = density of the particle
$v\mu$ = terminal velocity of the particle

(Text continues on page 44.)

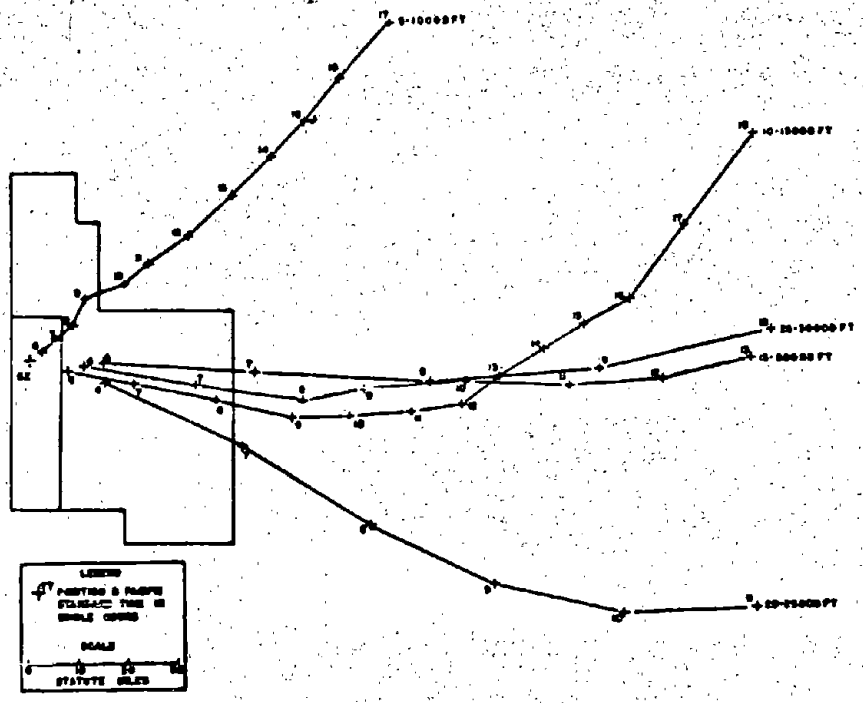

Fig. 3.1—Constant-layer trajectories, Tesla.

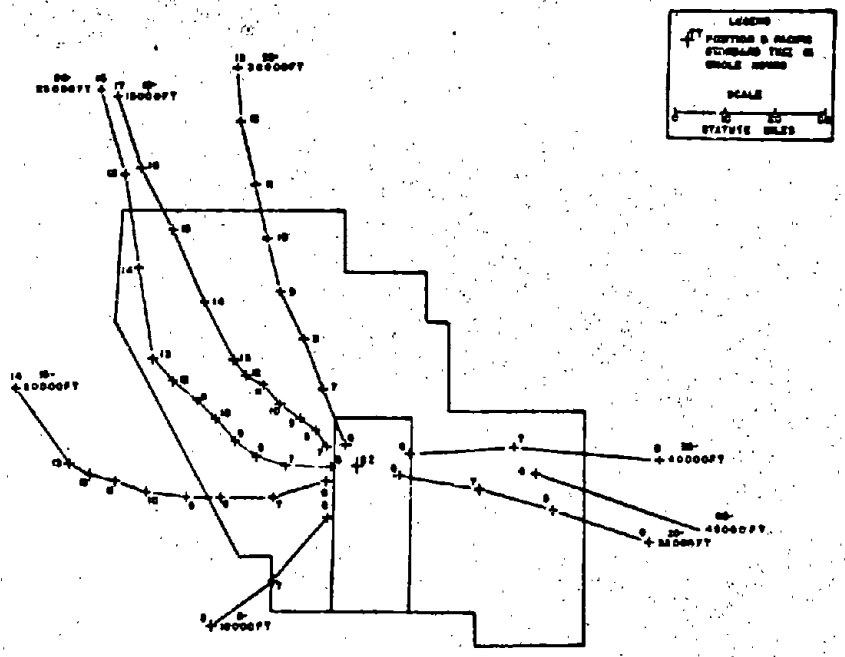

Fig. 3.2—Constant-layer trajectories, Turk.

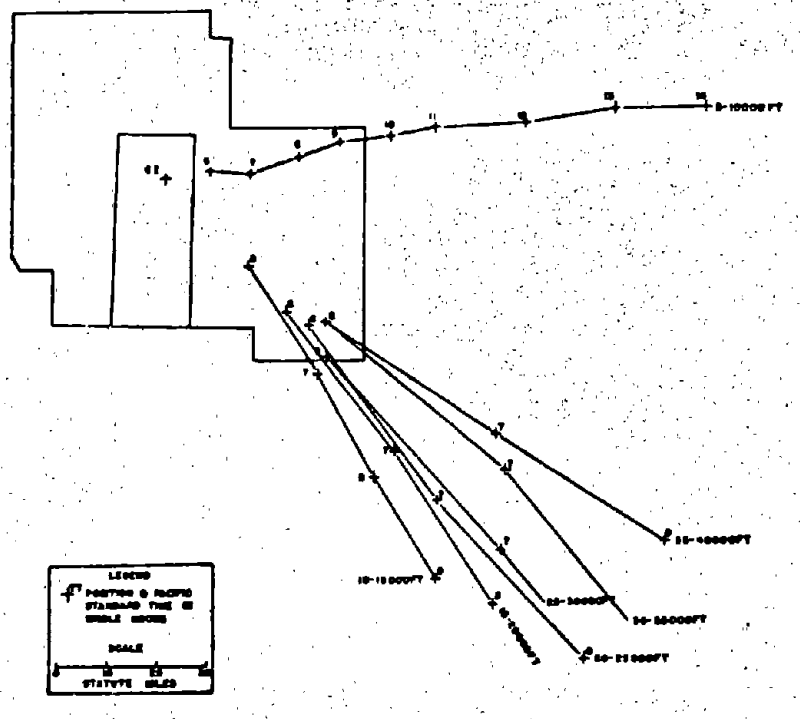

Fig. 3.3—Constant-layer trajectories, Bee.

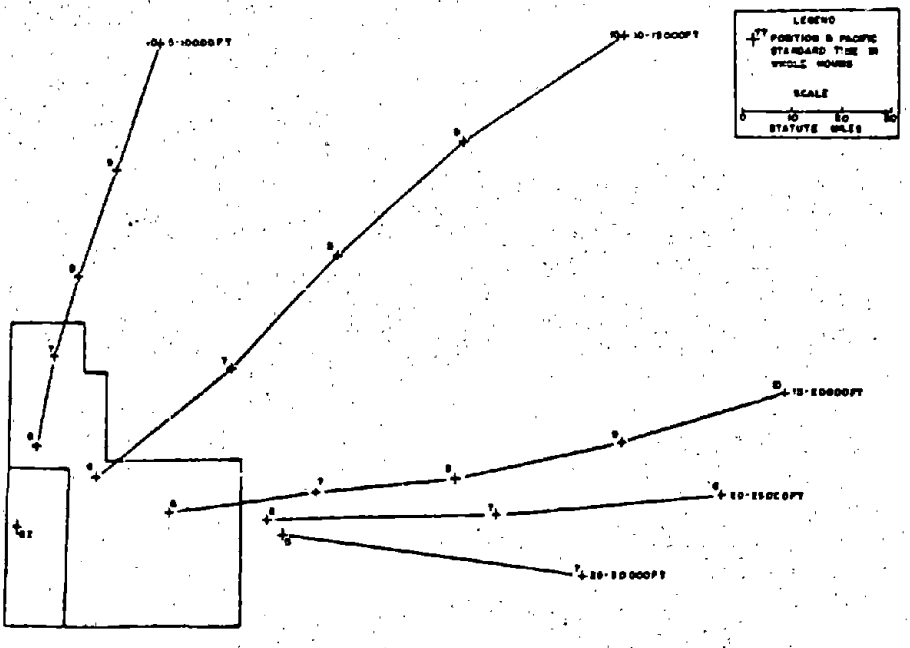

Fig. 3.4—Constant-layer trajectories, Apple I.

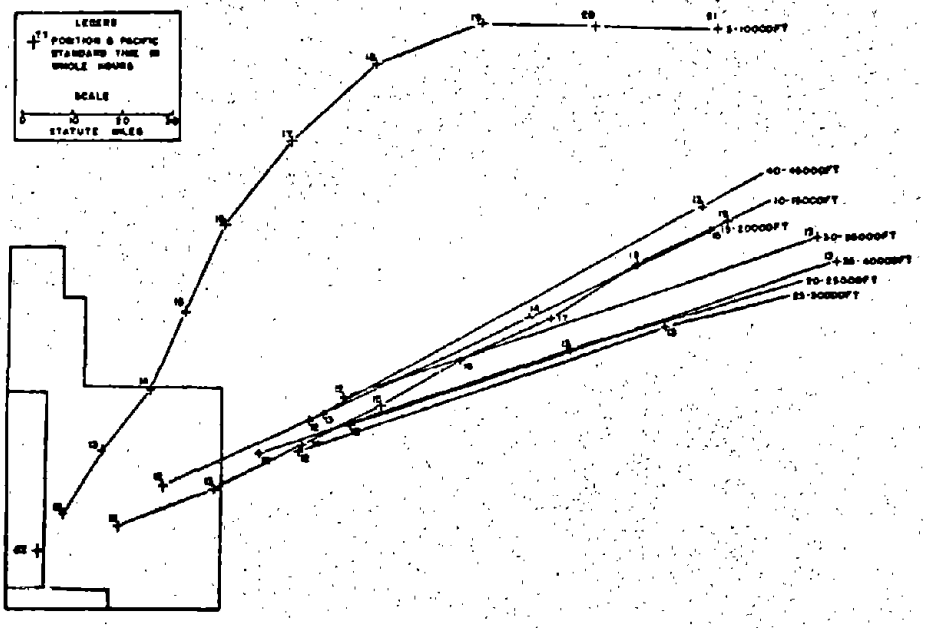

Fig. 3.5—Constant-layer trajectories, Met.

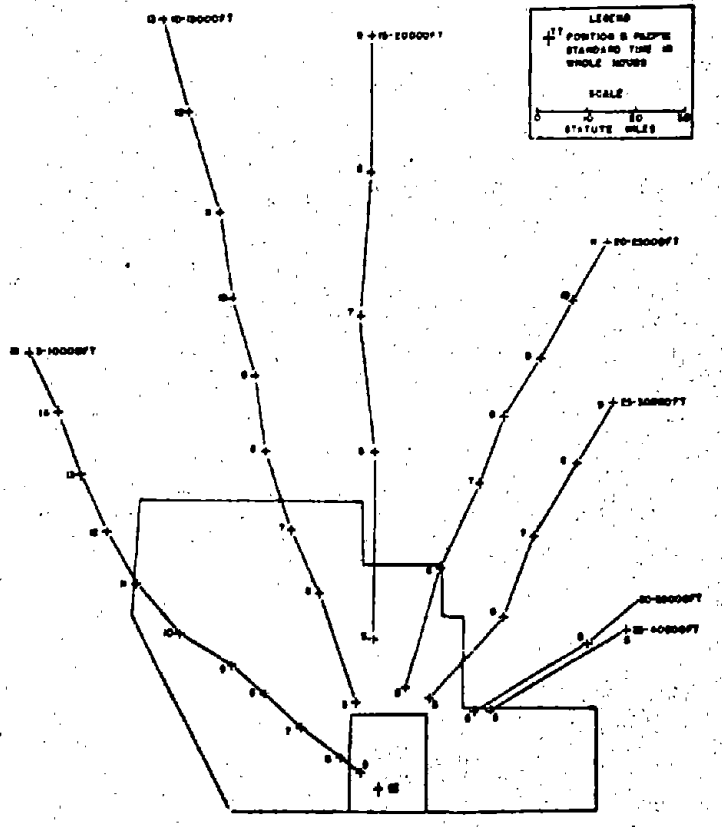

Fig. 3.6—Constant-layer trajectories, Apple II.

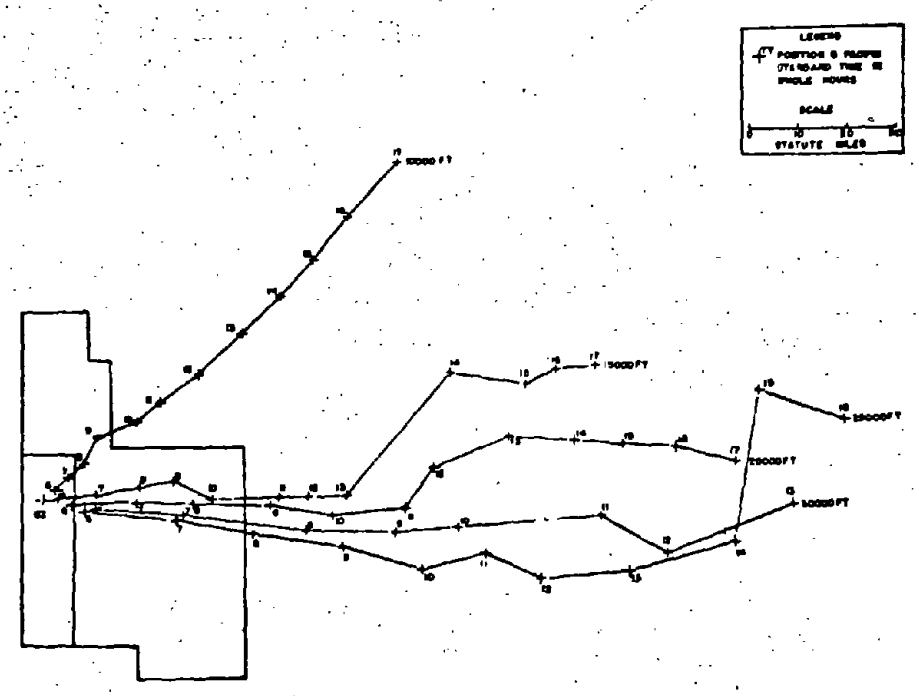

Fig. 3.7—Surface position and time of arrival, Tesla.

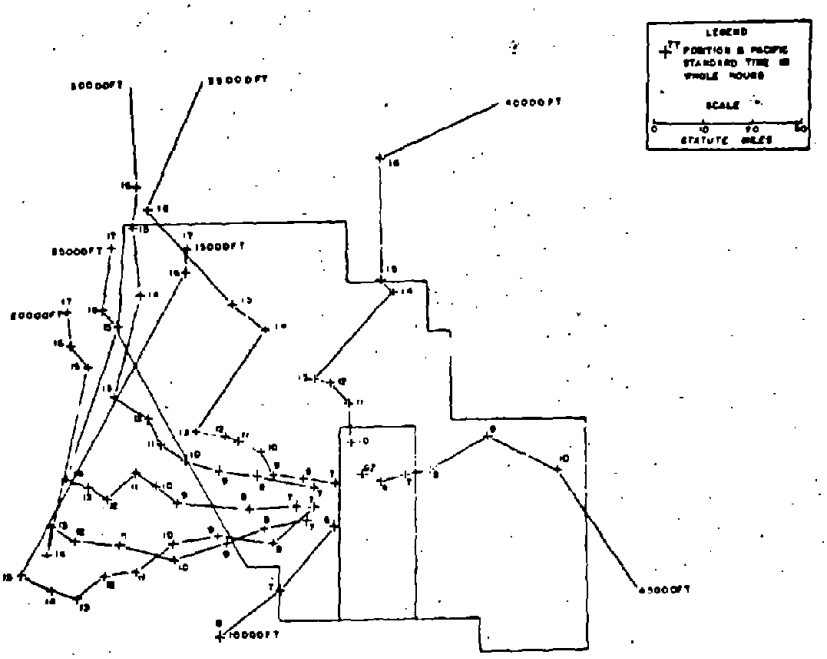

Fig. 3.8—Surface position and time of arrival, Turk.

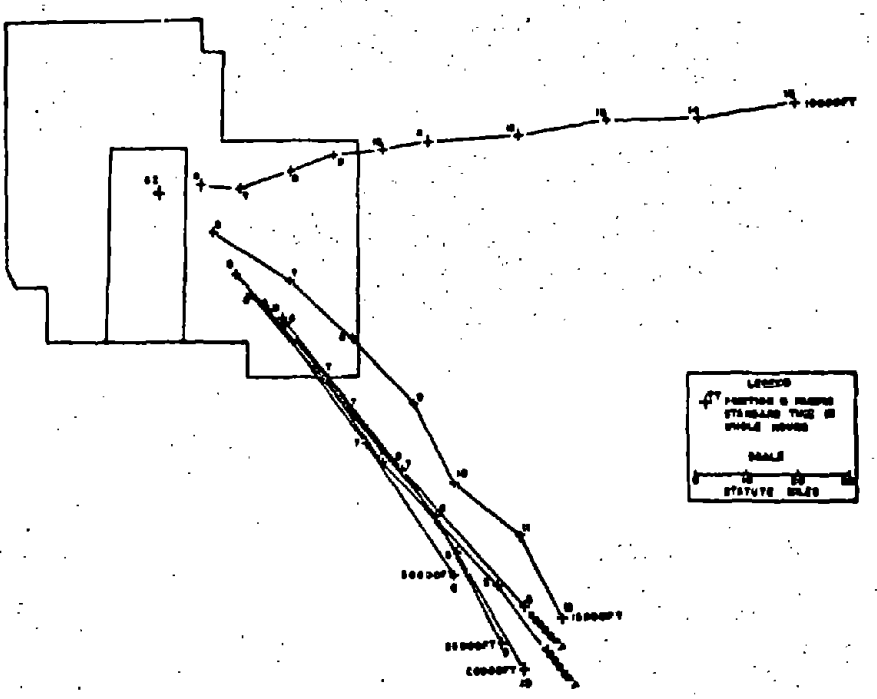

Fig. 3.9—Surface position and time of arrival, Bee.

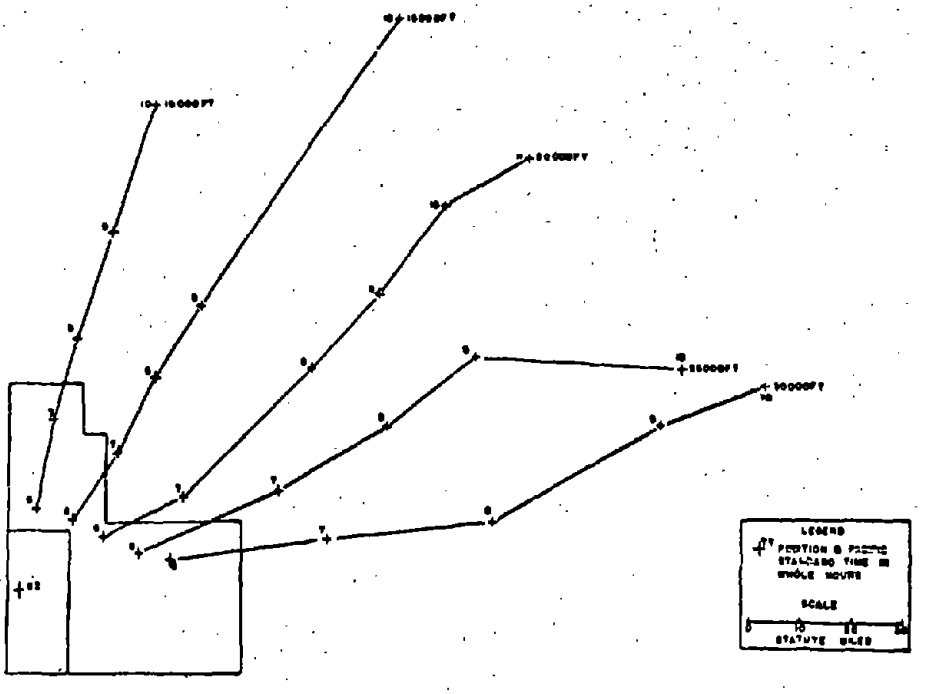

Fig. 3.10—Surface position and time of arrival, Apple I.

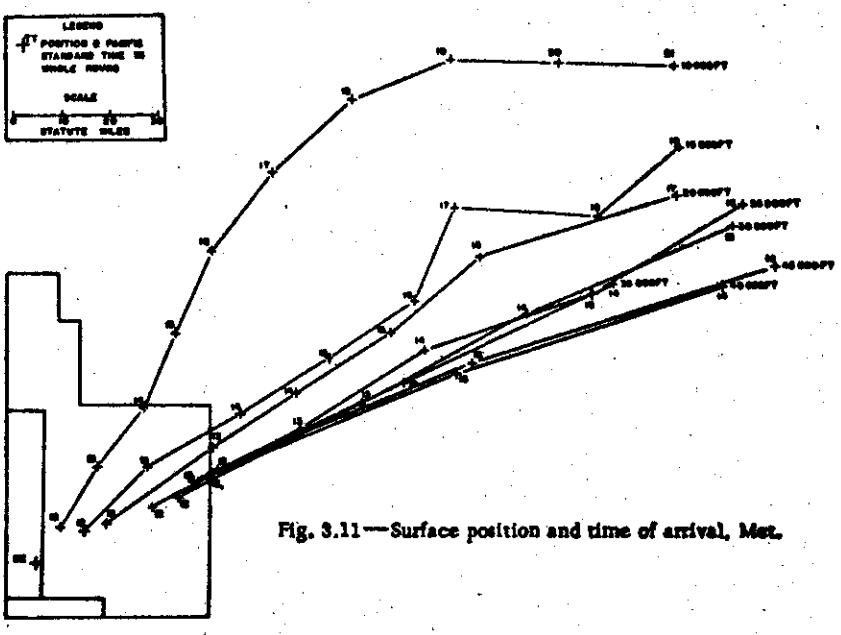

Fig. 3.11—Surface position and time of arrival, Met.

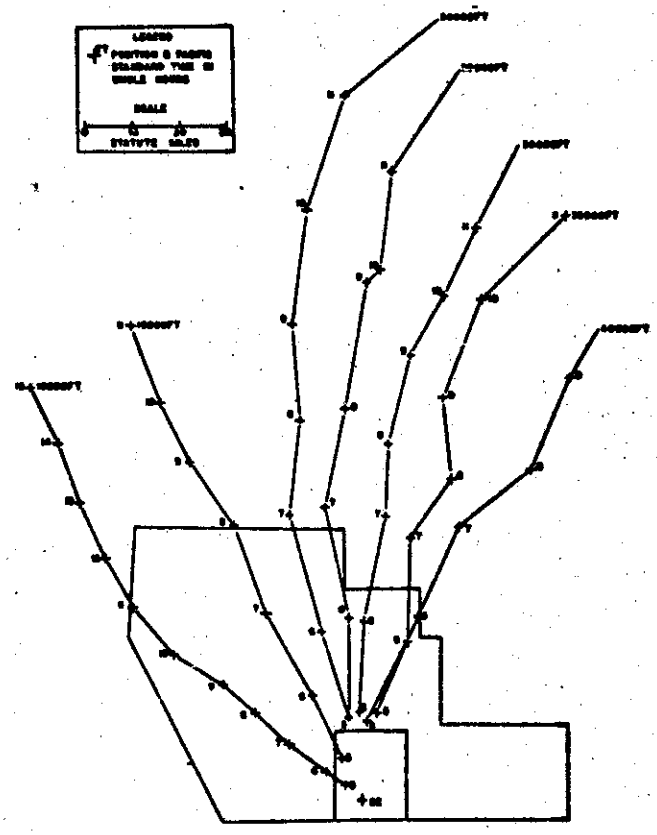

Fig. 3.12—Surface position and time of arrival, Apple II.

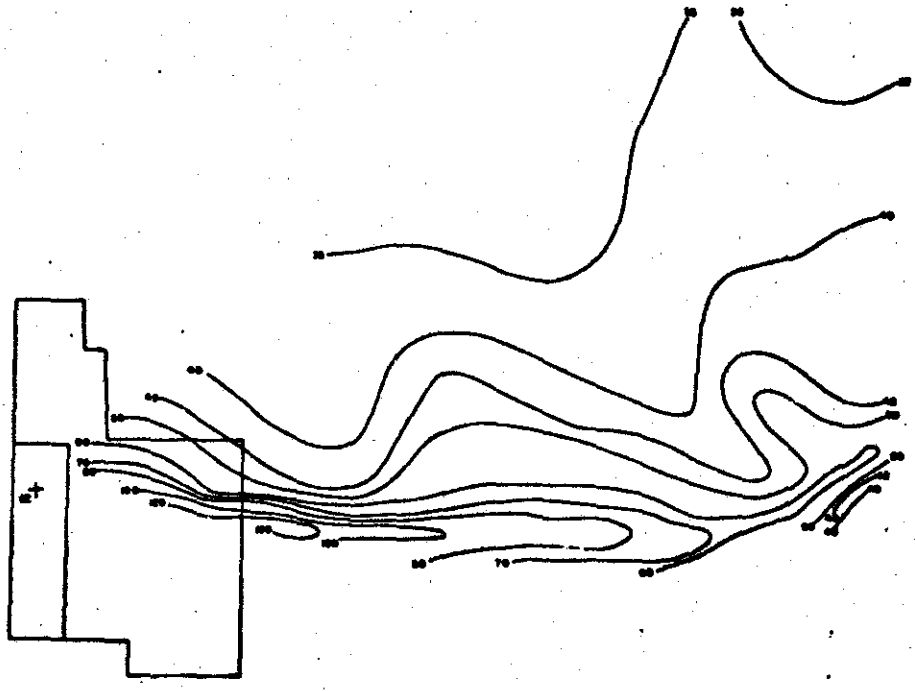

Fig. 3.13—Predominant particle size (in microns) on surface, Tesla.

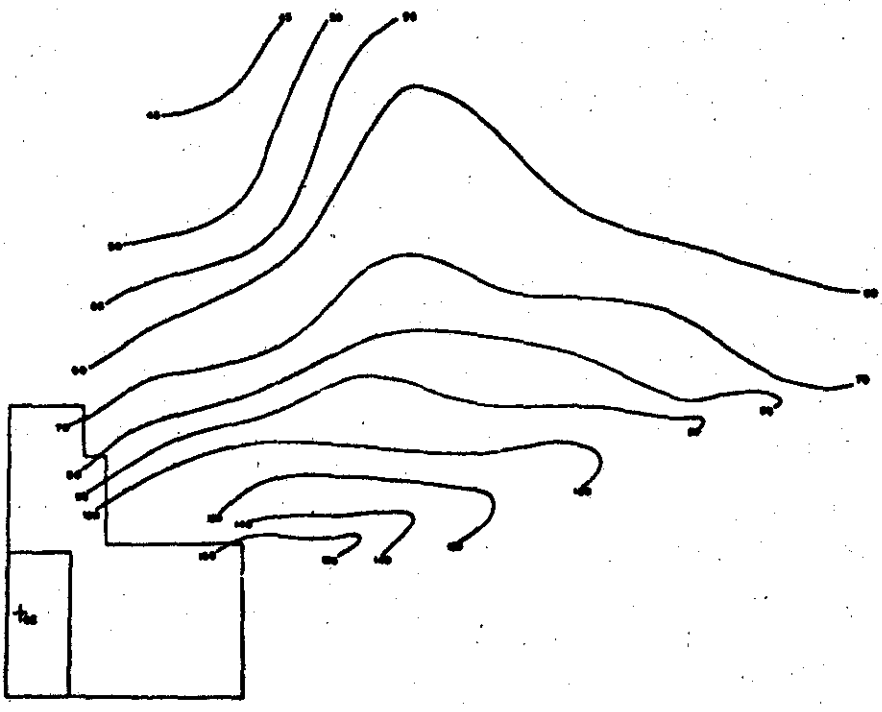

Fig. 3.14—Predominant particle size (in microns) on surface, Apple I.

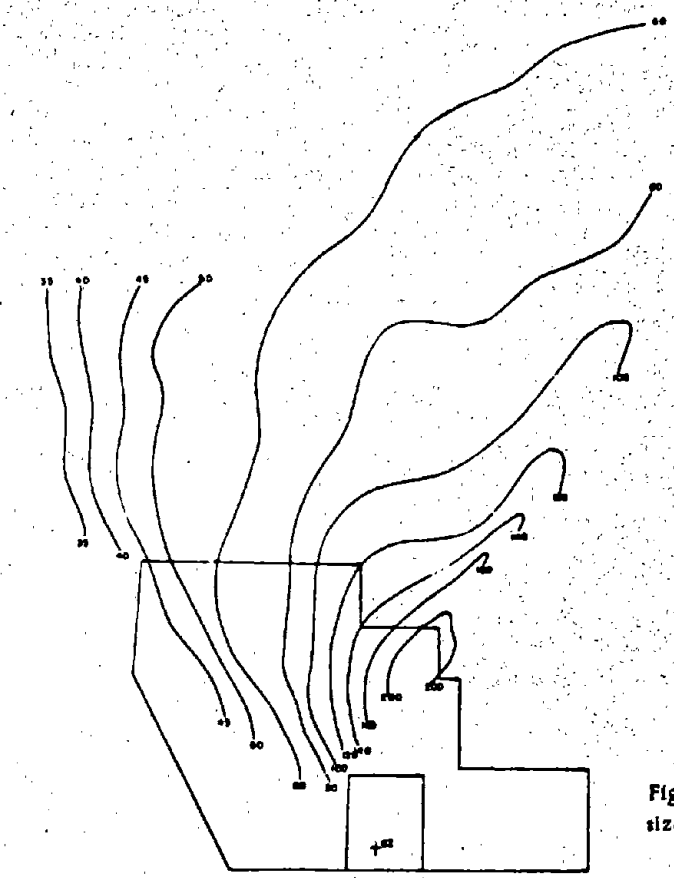

Fig. 3.15—Predominant particle size (in microns) on surface, Met.

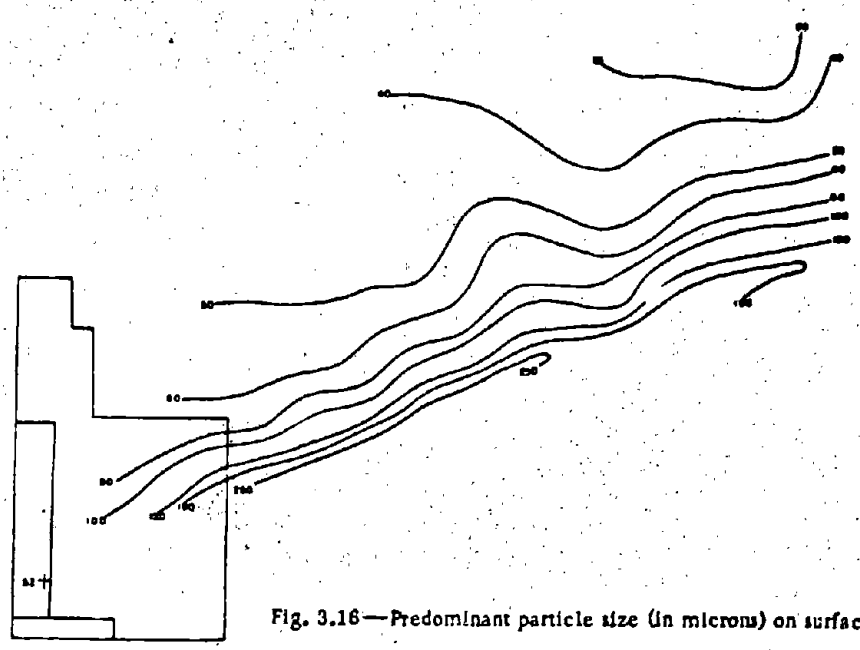

Fig. 3.16—Predominant particle size (in microns) on surface, Apple II.

To obtain a workable solution of the above equation, certain assumptions, in addition to those mentioned previously, were made, namely:

1. That a particle reaches terminal velocity in a very short time after beginning its descent.
2. That the atmosphere is homogeneous with a constant density of 7×10^{-4} g/cm^3 and a constant viscosity of 1.63×10^{-4} poise.
3. That the average density of particles is 2.5 g/cm^3.

Using the vertical distance to the surface and the hour of arrival after shot time at each surface position, the approximate predominant particle diameter was computed. Four computed particle-size analysis maps are shown (Figs. 3.13 to 3.16).

3.3 FALL-OUT CONTAMINATION

3.3.1 Fall-out Patterns in Terms of Infinite Dose

On the day following the Tesla shot, seven monitoring teams were sent into the field to determine radiation intensities on seven roads and trails that crossed the fall-out pattern. The pattern, which lay in an easterly direction from NTS, is described in Fig. 3.17.

The fall-out pattern on the Turk shot was not defined due to the general inaccessibility of the area receiving the primary fall-out. Generally, low levels of surface activity precluded the definition of the Bee fall-out pattern.

Apple I was a postshot participation, and six teams were sent out on D+1 day to obtain radiation intensity data and soil samples. The results of the radiation-intensity data have been plotted in Fig. 3.18.

Owing to the quantity of equipment used and the data collected in the Met shot participation, radiation intensities were measured on only three arcs. The data from these measurements and from Off-site Rad-Safe have been plotted to yield the isodose map shown in Fig. 3.19.

Since the Apple II shot participation involved the postshot maintenance of air-sampling equipment, only three arcs could be studied for radiation-intensity levels. Data from both this project and Off-site Rad-Safe were used to plot the isodose map, showing the fall-out pattern, given in Fig. 3.20.

The above figures are suggested as references for the identification of sampling locations described in the succeeding sections.

During Met and Apple II shots, fall-out intensity recorders were operating. Two of the records from Met were suitable for more intensive analysis than merely time-of-arrival measurements. These were from stations 20 and 58 miles from GZ. The data obtained from the recording charts are given in Table 3.3.

3.3.2 Soil-sample Collections

The results of soil-sample analyses, on which the determinations of unit-area activities and particle-size distributions are based, are given in the appendixes.

A total of 77 soil samples were collected on seven arcs crossing the Tesla fall-out pattern. These data, presented with respect to distance from GZ, appear in Appendix C.

TABLE 3.3—ANALYSIS OF TIME-INTENSITY RECORDS FROM MET SHOT

Distance, miles	Time of arrival, hr	Time of peak activity, hr	Peak activity, r/hr	Integrated dose to time of arrival +12 hr	Gamma decay slopes			
					H+1.25 to 3.0 hr	H+3.5 to 8.57 hr	H+10.75 to 15.75 hr	H+16.75 to 23.75 hr
20	H+0.3	H+0.66	500*	760 r*	−1.07	−1.49	−2.10	
58	H+2.3	H+2.83	1.1	4.0		−1.51	−1.30	−1.79

* These results are based on extrapolations of measured off-scale values obtained from the background recorder.

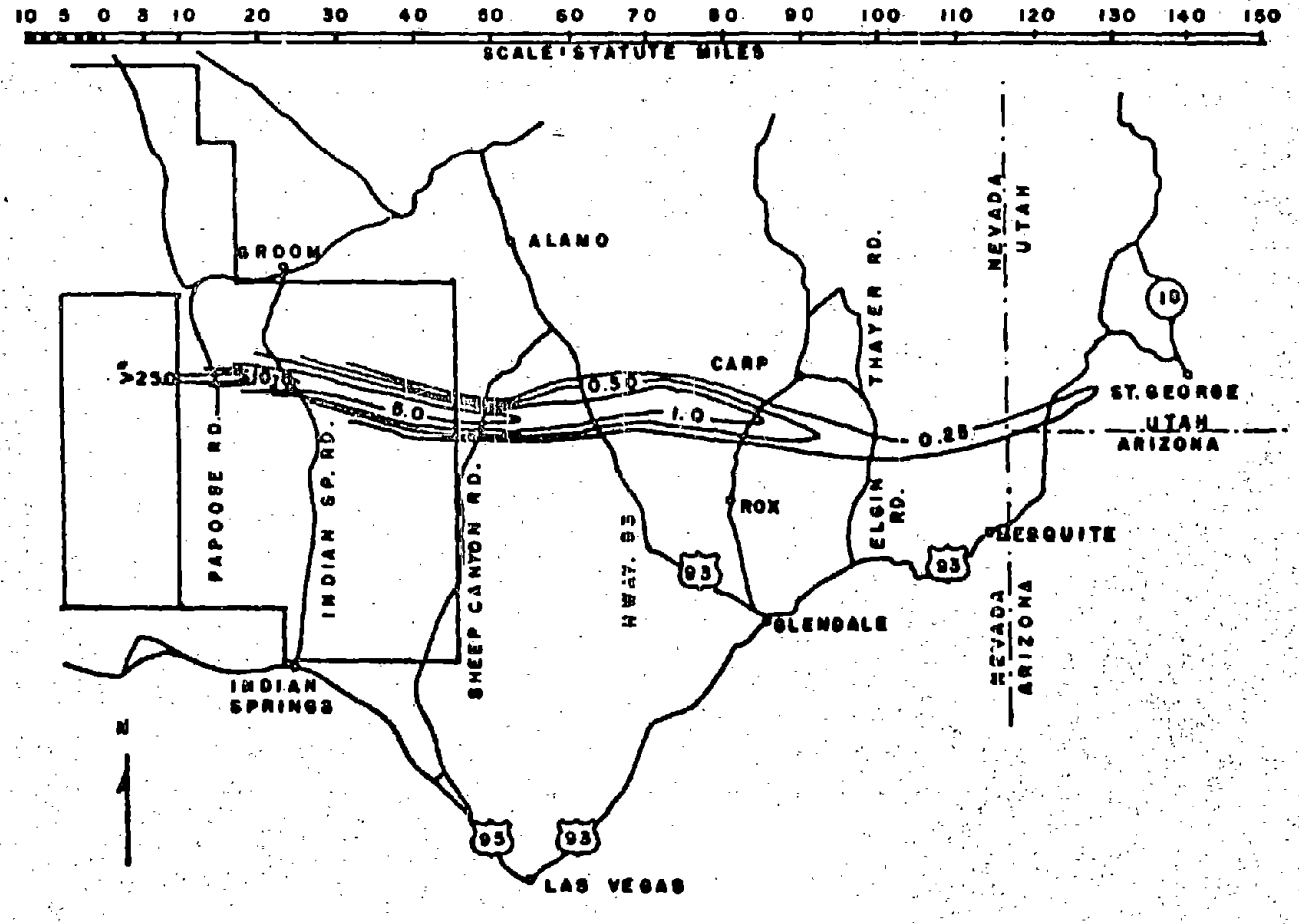

Fig. 3.17—Infinite dose plot for Tesla shot.

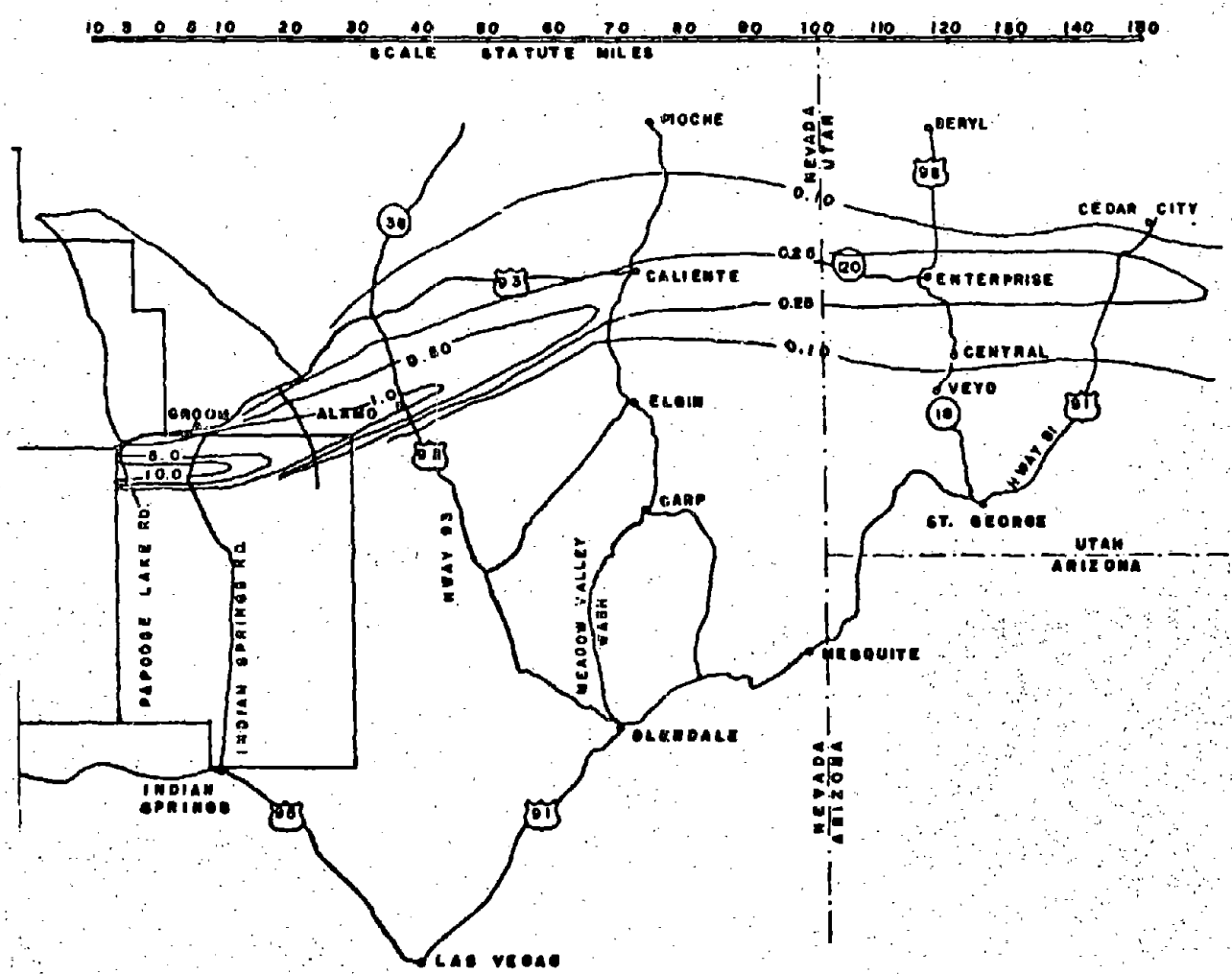

Fig. 3.18 — Infinite dose plot for Apple I shot.

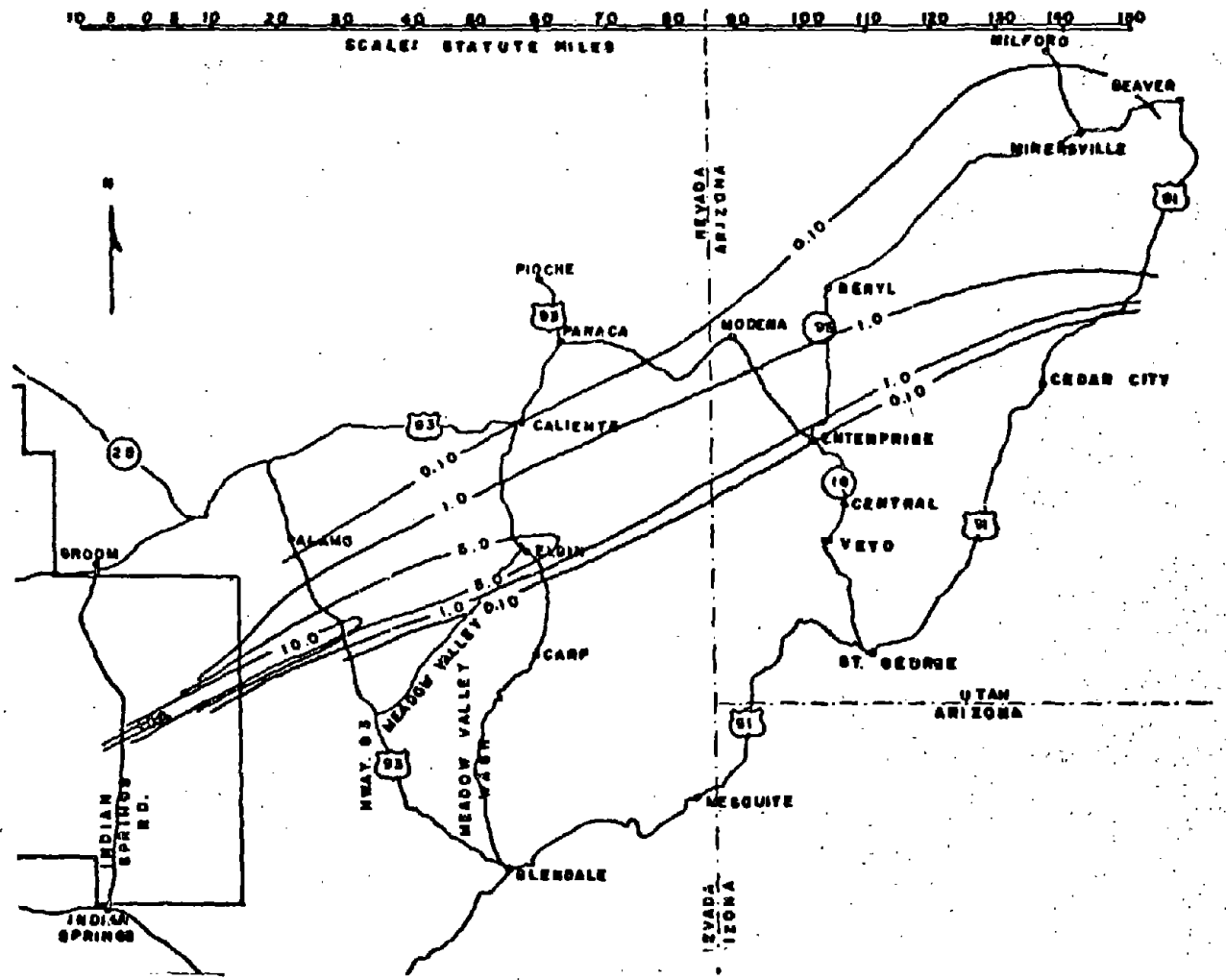

Fig. 3.19—Infinite dose plot for Met shot.

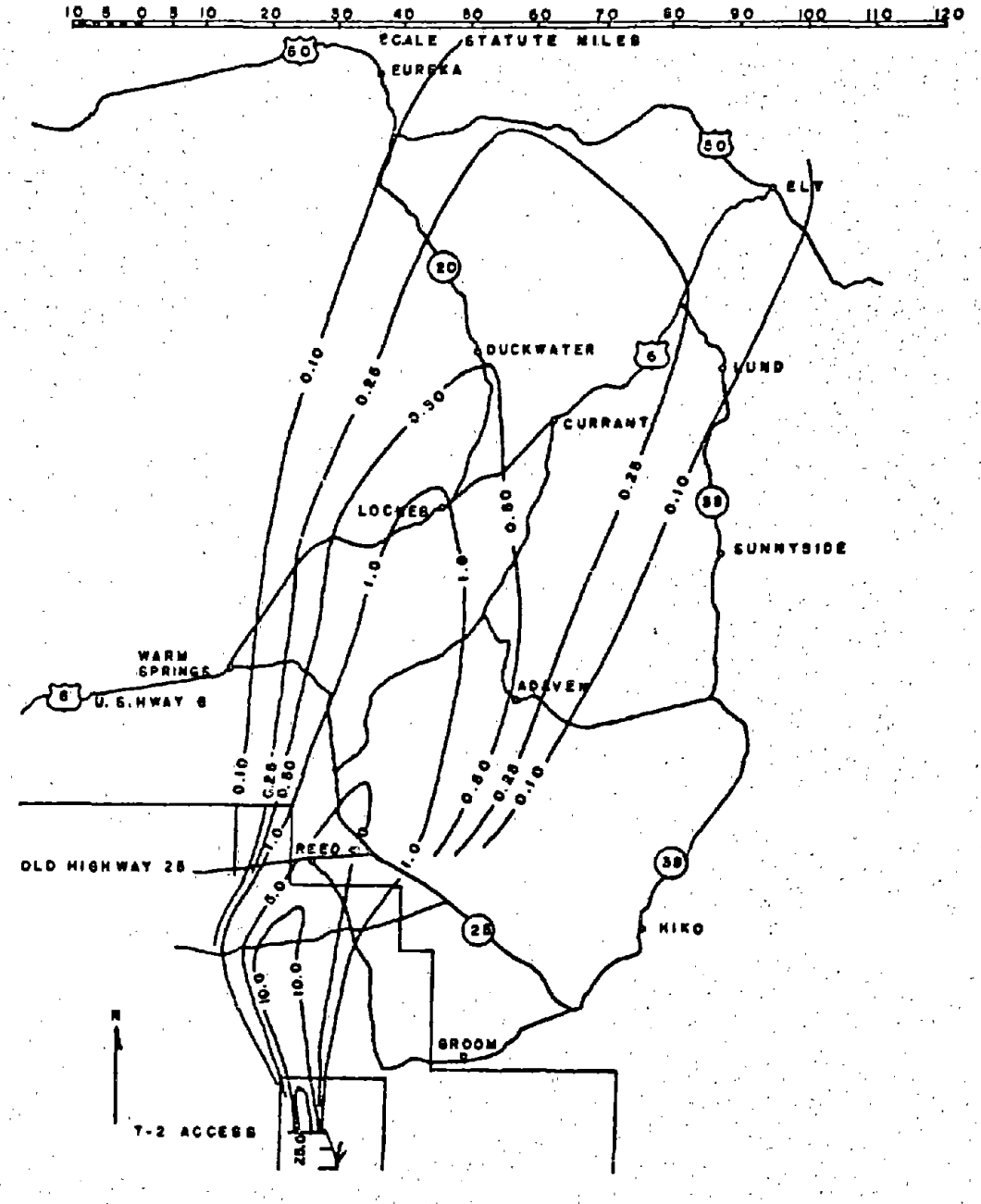

Fig. 3.20—Infinite dose plot for Apple II shot.

The Turk fall-out pattern was sampled at only one distance, 11.5 miles west-southwest of GZ. The results of four soil-sample analyses are given in Appendix D.

The Apple I fall-out pattern was sampled on six arcs, yielding 76 individual soil samples. These data are given in Appendix E.

Soil samples were collected on three arcs crossing the Met and Apple II fall-out patterns. The results are given in Appendixes F and G, respectively.

3.3.3 Fall-out Distribution As a Function of Distance from GZ

Determinations of the total fall-out contamination at specific distances from GZ were made by plotting observed radiation-intensity (mr/hr) and surface radioactivity ($\mu c/ft^2$) values with respect to distance across the fall-out pattern and then integrating the areas beneath the curves by measurements with a polar planimeter. The integrated values have the dimensions of mr/hr × ft or $\mu c/ft$; however, these units have little physical significance, and the data are presented as if all the activity across an arc were located at a point a specific distance from GZ. Figures 3.21 to 3.24 give total fall-out contamination as a function of distance from GZ for the Tesla, Apple I, Met, and Apple II shots.

The total fall-out contamination curves based on both mr/hr and $\mu c/ft^2$ values generally demonstrated a rapid initial decline to a distance of approximately 50 miles and a less rapid decline at greater distances. The Apple II shot was an exception in that an increase in total contamination between 7 and 48 miles was indicated. A slight tendency for the total contamination curve of the Tesla shot to increase beyond 78 miles also occurred.

If the data from the Tesla, Apple I, and Met shots are plotted on log-log paper, straight-line relations are apparent. However, the data from Apple II would seem to indicate that the information was not complete enough to obtain the total fall-out pattern at 7 miles from GZ. The equations of radiation-intensity and surface contamination vs time, as determined from Figs. 3.25 to 3.27, are as follows:

For Tesla,

$$\frac{mr}{hr} \times ft = 3.17 \times 10^6 \, T_f^{-1.43}$$

$$\frac{\mu c}{ft} = 57.5 \times 10^6 \, T_f^{-1.81}$$

For Apple,

$$\frac{mr}{hr} \times ft = 3.26 \times 10^6 \, T_f^{-1.17}$$

$$\frac{\mu c}{ft} = 26.3 \times 10^6 \, T_f^{-1.76}$$

For Met,

$$\frac{mr}{hr} \times ft = 6.45 \times 10^6 \, T_f^{-0.81}$$

$$\frac{\mu c}{ft} = 40.6 \times 10^6 \, T_f^{-1.04}$$

where T_f is fall-out time in hours and mr/hr × ft and $\mu c/ft$ are integrated values across the fall-out pattern.

Utilizing data on Tumbler-Snapper 7 from Report UCLA-243, Upshot-Knothole 5 and 7 from Report WT-811, and Bee and Zucchini from Off-site Rad-Safe reports of the Operation Teapot series, the same line of relation is evident. The equations, as obtained from Fig. 3.28, are as follows:

(Text continues on page 58.)

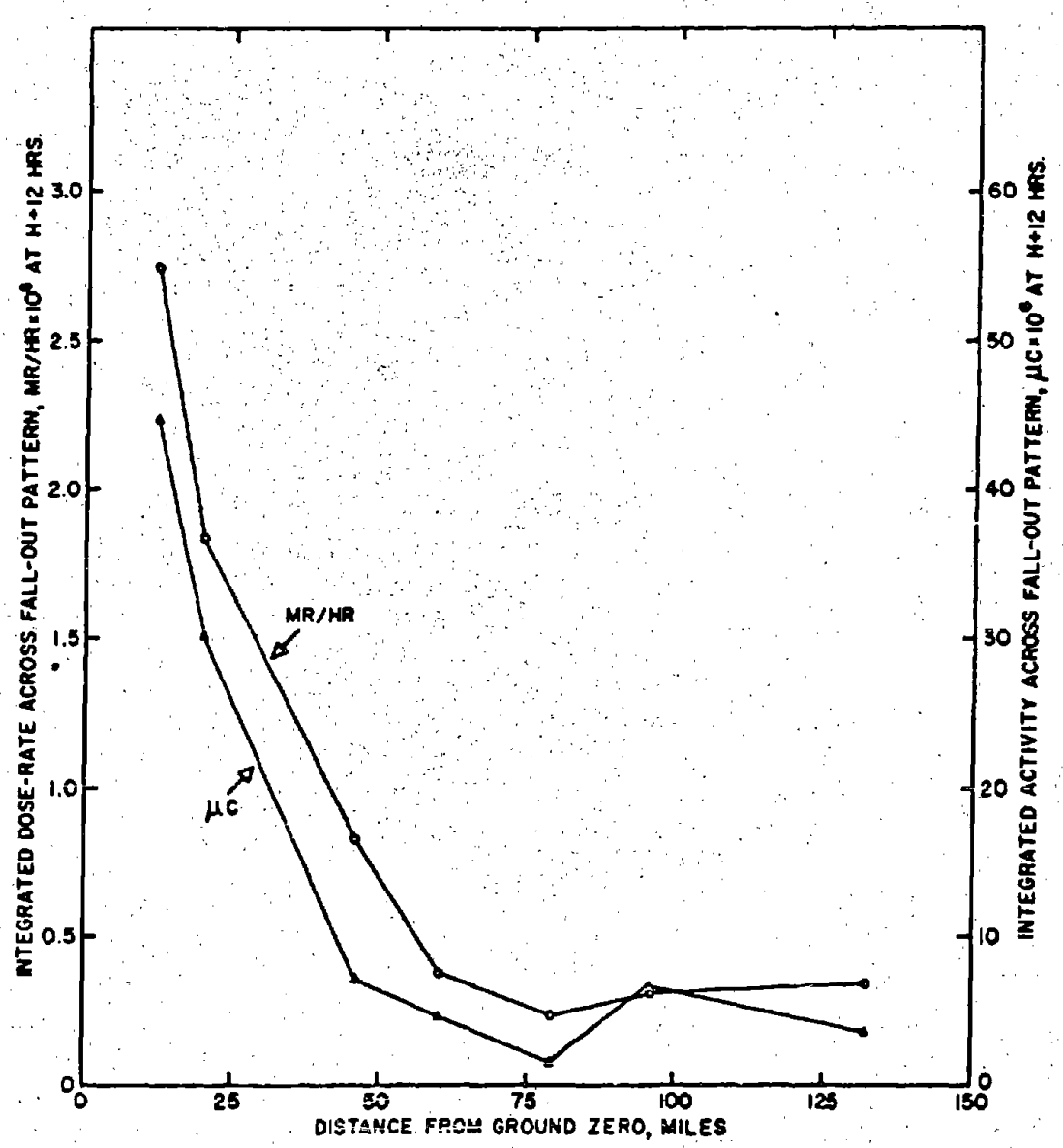

Fig. 3.21 — Variation of surface activity and radiation intensity with distance from GZ, Tesla. Values are determined by integration across fall-out pattern.

[redacted]

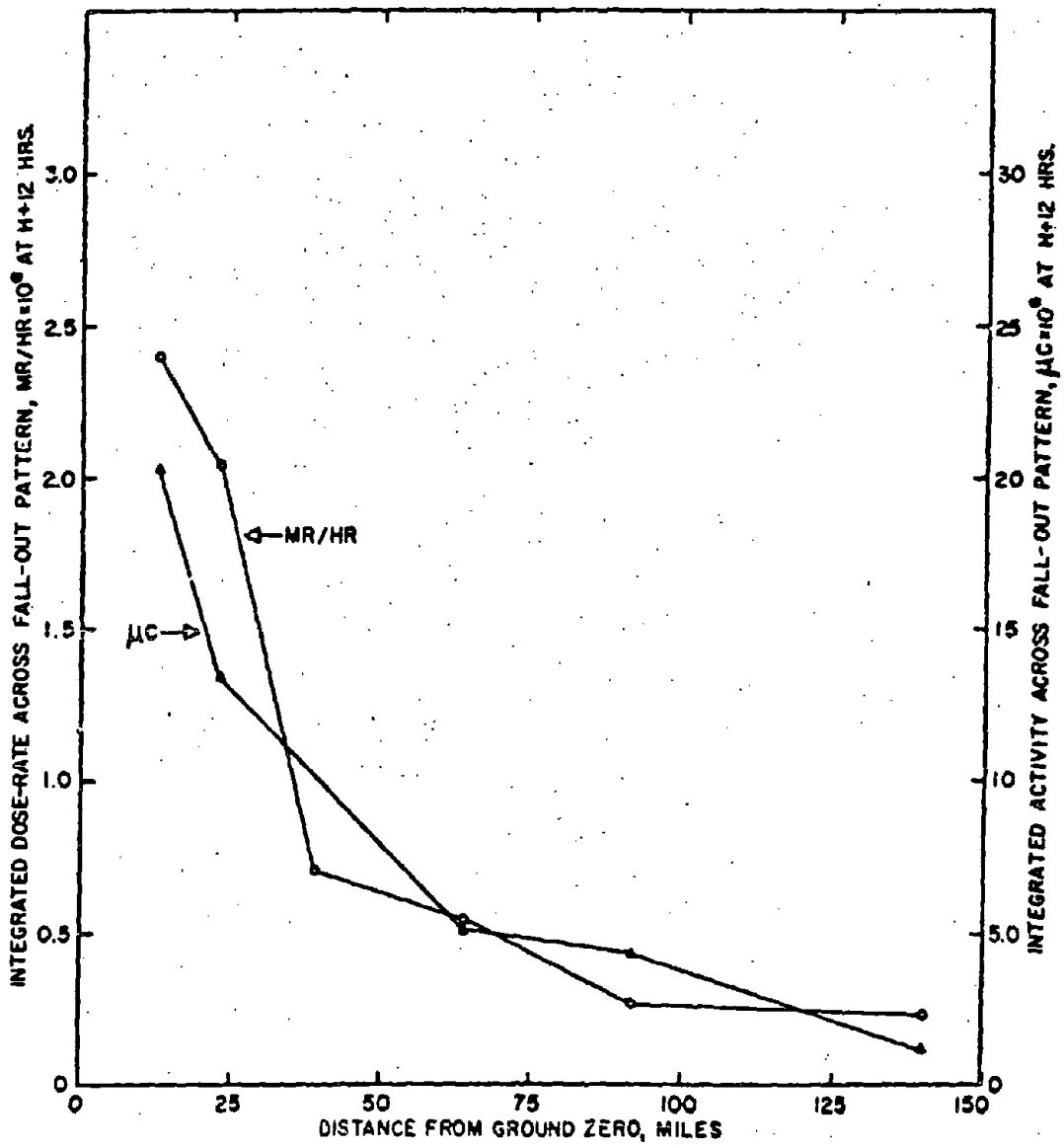

Fig. 3.22—Variation of surface activity and radiation intensity with distance from GZ, Apple I. Values are determined by integration across fall-out pattern.

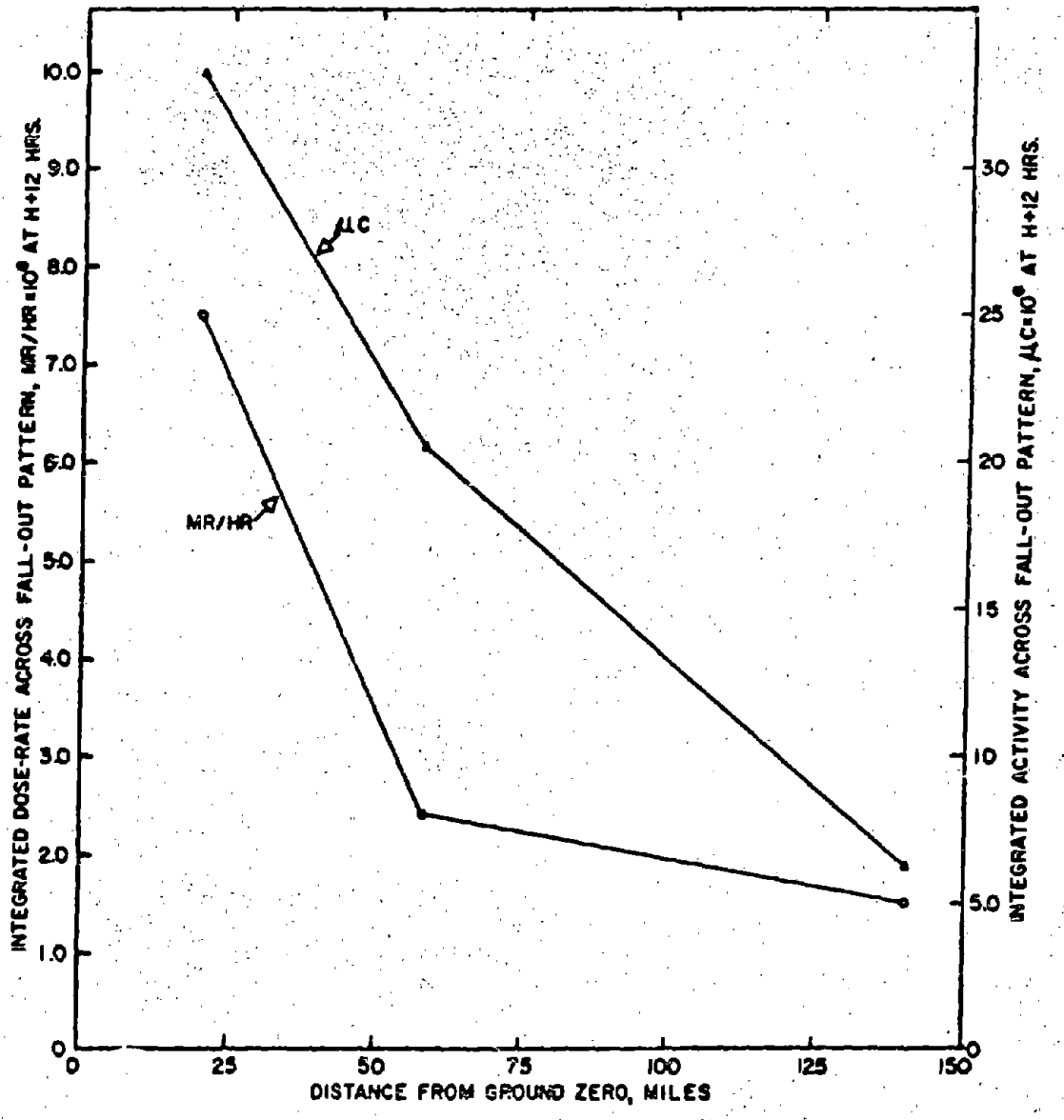

Fig. 3.23 — Variation of surface activity and radiation intensity with distance from GZ, Met. Values are determined by integration across fall-out pattern.

[redacted]

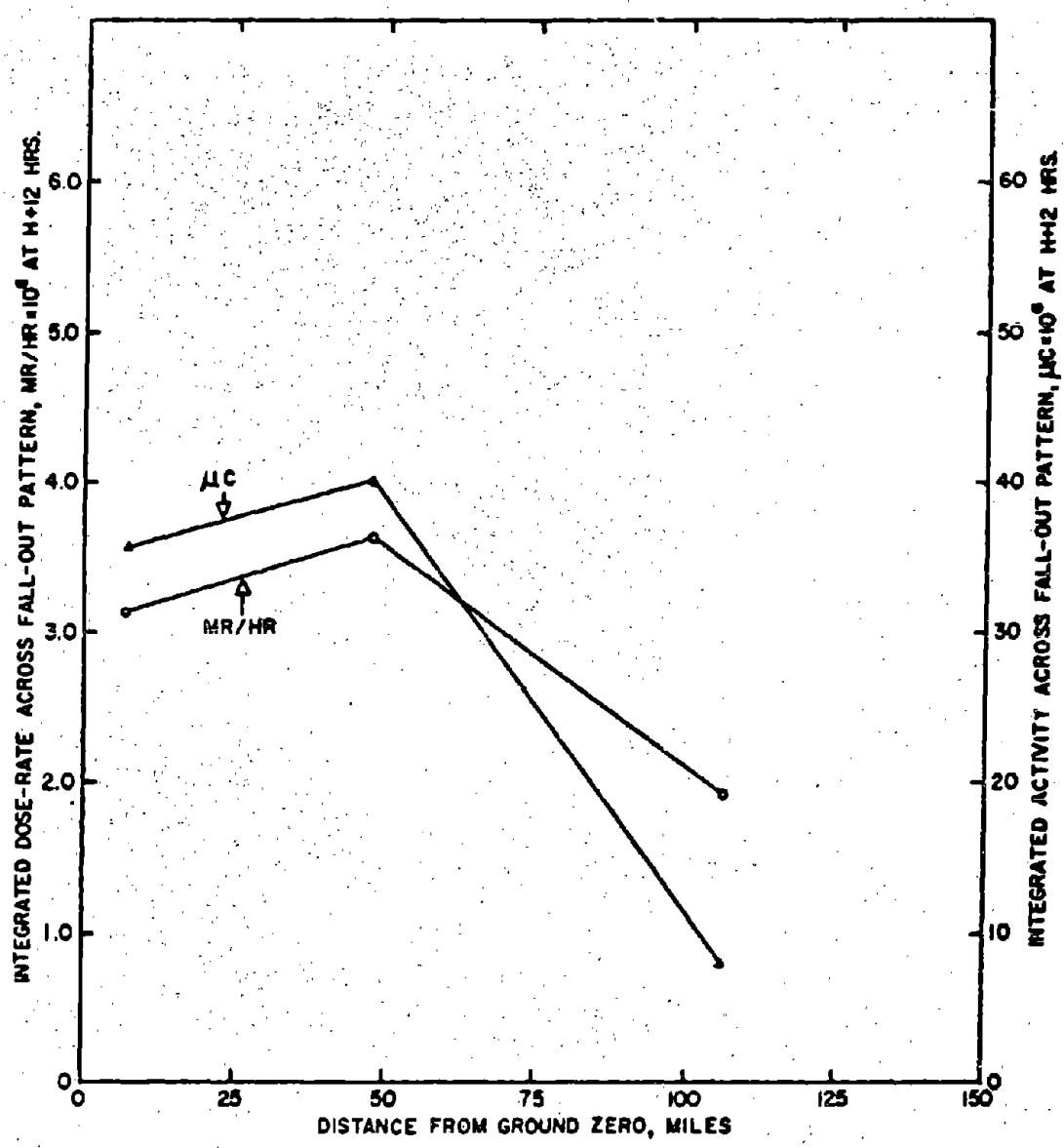

Fig. 3.24 — Variation of surface activity and radiation intensity with distance from GZ, Apple II. Values are determined by integration across fall-out pattern.

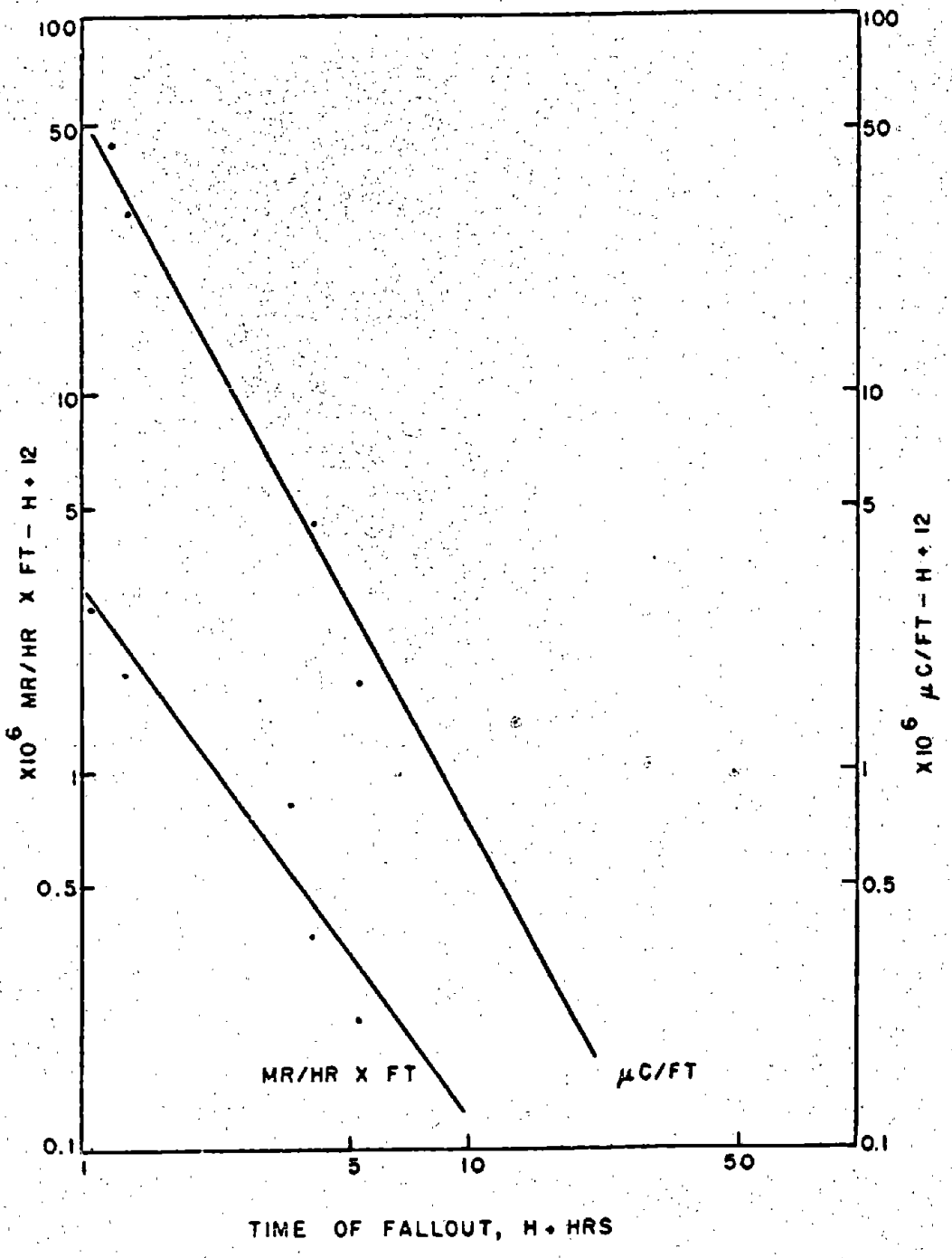

Fig. 3.25—Radiation intensity and surface contamination as related to fall-out time, Tesla.

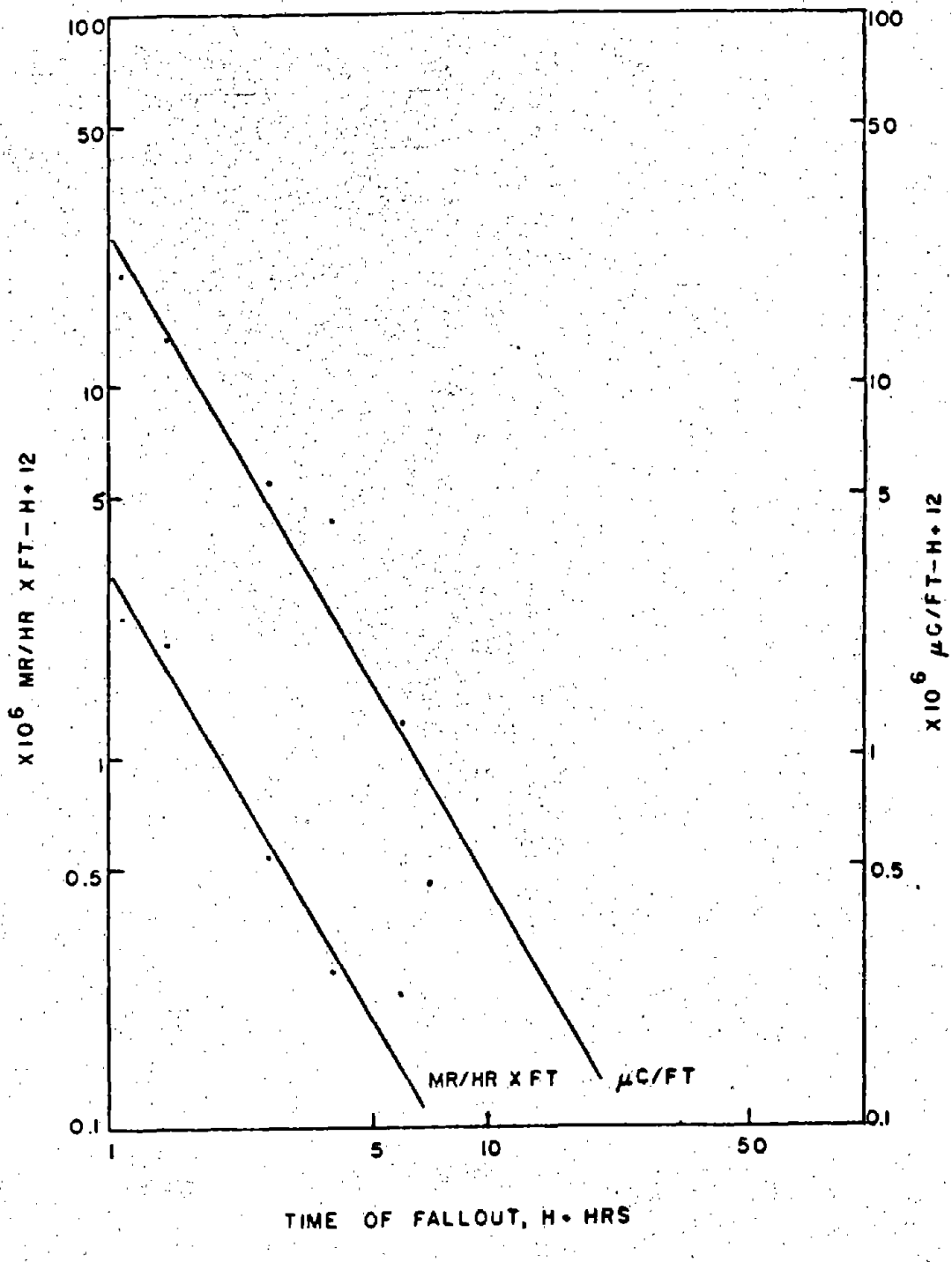

Fig. 3.26—Radiation intensity and surface contamination as related to fall-out time, Apple 2.

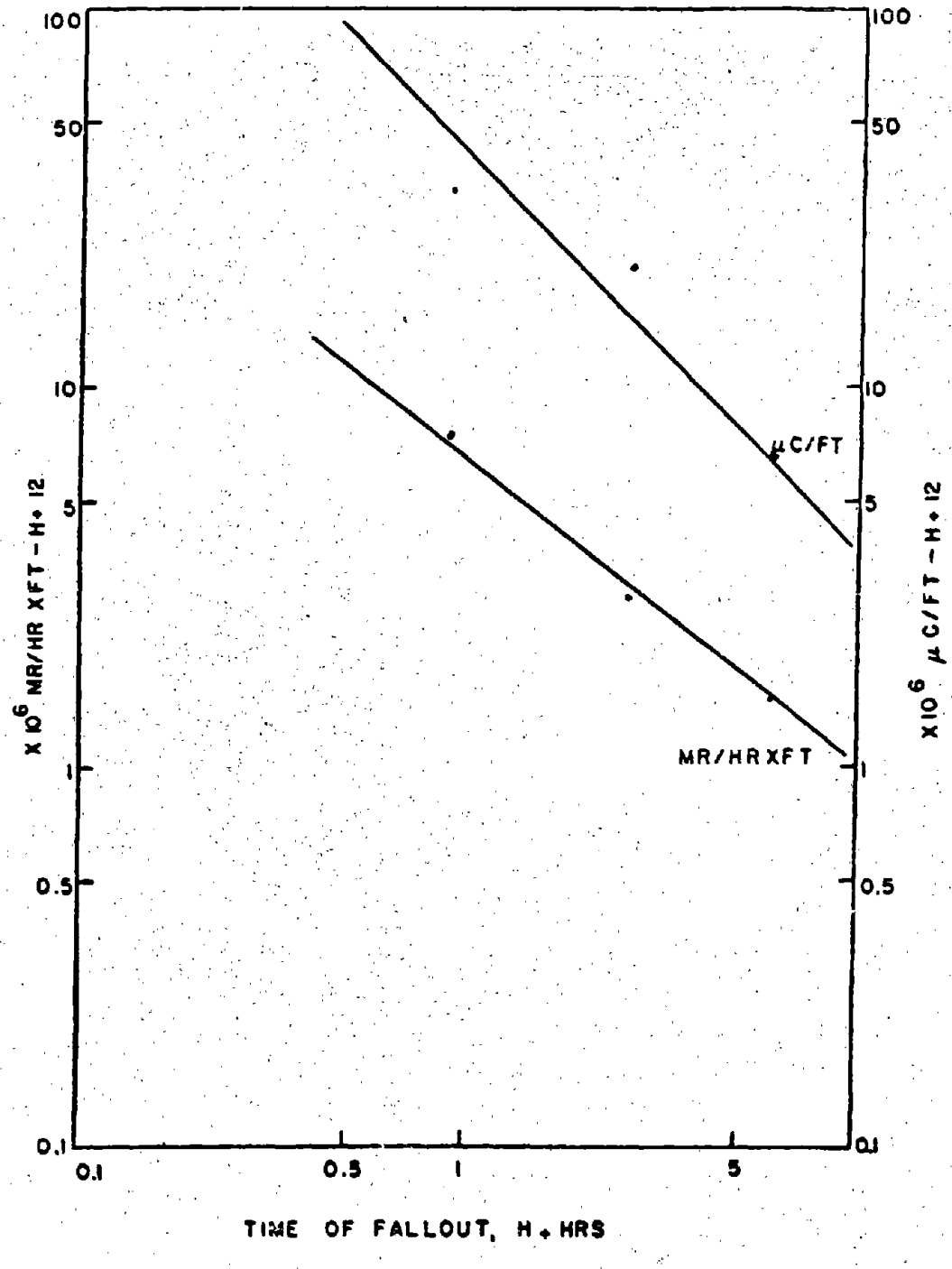

Fig. 3.27—Radiation intensity and surface contamination as related to fall-out time, Met.

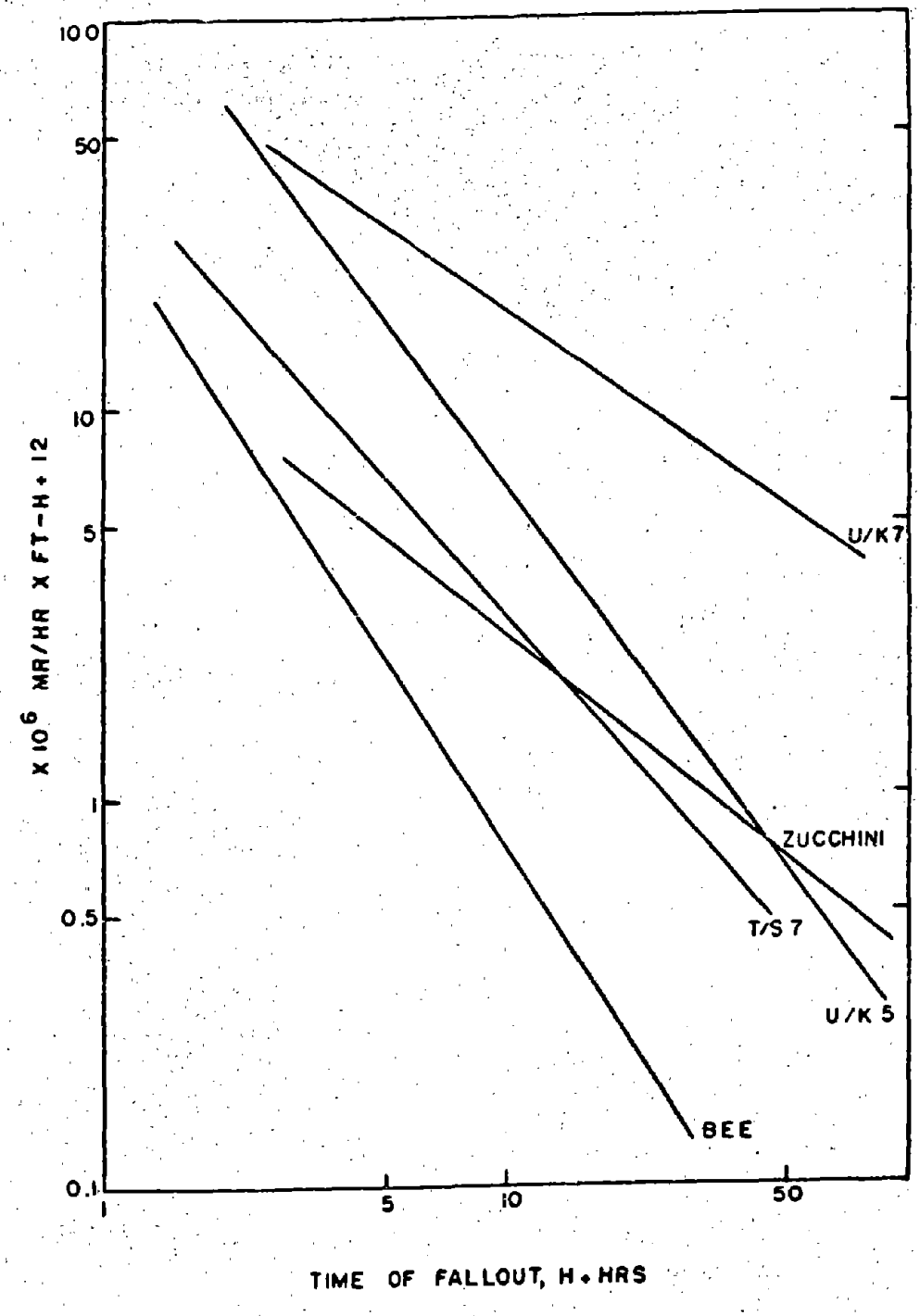

Fig. 3.28—Radiation-intensity relation with fall-out time for Bee, Zucchini, Tumbler-Snapper 7, and Upshot-Knothole 5 and 7.

For Tumbler-Snapper 7,

$$\frac{mr}{hr} \times ft = 2.87 \times 10^6 \, T_f^{-1.18}$$

For Upshot-Knothole 5,

$$\frac{mr}{hr} \times ft = 6.27 \times 10^6 \, T_f^{-1.41}$$

For Upshot-Knothole 7,

$$\frac{mr}{hr} \times ft = 17.4 \times 10^6 \, T_f^{-0.73}$$

For Bee,

$$\frac{mr}{hr} \times ft = 0.731 \times 10^6 \, T_f^{-1.61}$$

For Zucchini,

$$\frac{mr}{hr} \times ft = 2.53 \times 10^6 \, T_f^{-0.82}$$

3.3.4 Radiation-Intensity Levels As a Function of Weapon Yield and Tower Height

Radiation-intensity values were first plotted vs distance across the fall-out pattern at varying distances from GZ. The integrated values obtained by this method were then plotted vs distance from GZ (Figs. 3.21 to 3.24). Graphical integration of this plot between fixed distances from GZ would indicate the total contamination to be found within these distance limits.

In order to compare fall-out activities between various shots, it was necessary to integrate the fall-out plots between limits of distance that coincide with fall-out times of H+0.8 and H+2.2 hr. These times were selected since all the shots studied had these fall-out times in common. Figure 3.29 shows the relation between yield at two tower heights to levels of contamination.

The total fall-out of Apple II did not agree with the experimental data from the other 500-ft tower shots. There appeared to be twice as much activity from this shot as would be expected from a device of this yield on the basis of the plot. After studying fall-out data and fall-out patterns, it appeared that the value for Apple II may have been low, and this would make the fall-out from Apple II even more than twice the experimental value. No reason for this variation was apparent on the basis of information available to this Project; however, it might be postulated that differences in shielding material and equipment in the tower cab caused more of the activity to fall out close to GZ, with a corresponding decrease in the amount scattered over the rest of the fall-out area.

3.3.5 Comparison of $\mu c/ft^2$: mr/hr Ratios

The failure of the $\mu c/ft^2$ and mr/hr curves in Figs. 3.21 to 3.24 to remain parallel reflects differences in the $\mu c/ft^2$: mr/hr ratio at different distances, and a similar variation for the several detonations is indicated by differences in the ordinate units. A summary of individual $\mu c/ft^2$: mr/hr ratios determined at different distances from GZ for the Tesla, Apple I, Met, and Apple II shots is given in Table 3.4.

The data revealed considerable variation in the values obtained at any one distance from GZ, which tended to obscure any relation that may exist between the ratio and distance. Similarly, the differences in the ratio with respect to the several shots are difficultly defined.

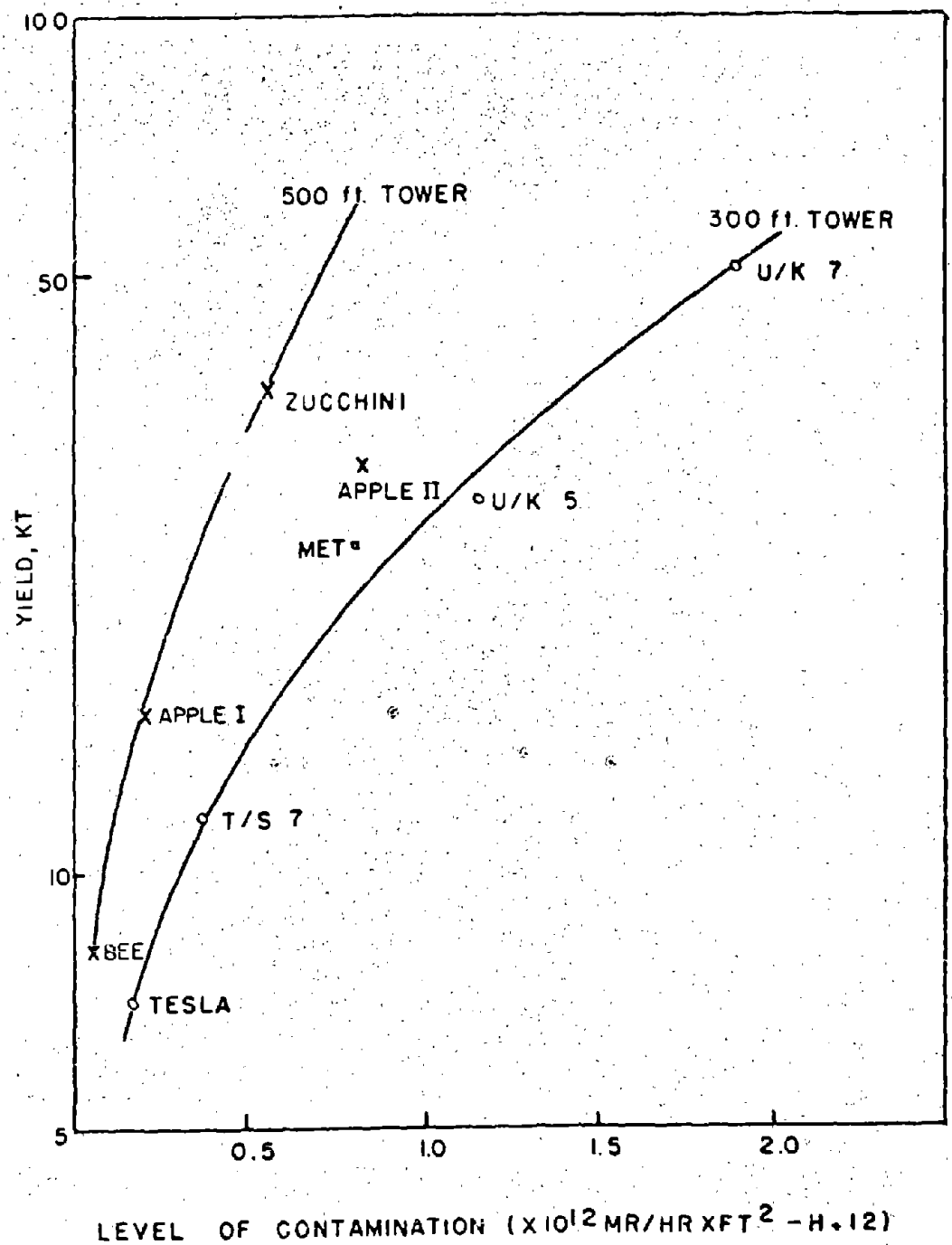

Fig. 3.29—Relation of yield and tower height to fall-out levels.

TABLE 3.4—$\mu c/ft^2$: mr/hr RATIOS DETERMINED FOR THE TESLA, APPLE I, MET, AND APPLE II SHOTS AT DIFFERENT DISTANCES FROM GZ

Distance from GZ, miles	No. of cases	Average ratio, $\mu c/ft^2$: mr/hr	Standard deviation
	Tesla		
12	12	15.05	8.23
20	20	10.75	2.13
46	9	8.88	4.51
60	9	11.41	4.05
79	6	7.47	2.69
96	8	15.77	8.86
132	10	15.80	2.63
12–132	76	12.13	6.68
	Apple I		
15	3	8.01	1.02
23	12	7.07	3.58
64	20	19.43	7.48
92	17	19.25	13.3
140	5	5.68	4.68
13–140	57	14.97	10.6
	Met		
20	14	6.38	3.21
56	18	6.63	1.93
140	11	3.51	2.54
20–140	43	5.33	2.72
	Apple II		
7	8	9.40	3.54
48	15	10.71	3.71
106	9	8.03	3.75
7–106	32	9.62	3.70

However, the ratios of $\mu c/ft^2$: mr/hr determined at all distances across the Met pattern were consistently lower than those obtained for the other shots. The average ratio of $\mu c/ft^2$: mr/hr for the four shots, based on all individual values, was 10.54 with a minimum value of 3.51 and a maximum value of 19.43.

3.3.6 Particle-size Distribution with Respect to Distance and Fall-out Time

Median-diameter values, based on mean particle-size percentages along individual arcs across the Tesla, Apple I, Met, and Apple II fall-out patterns, are plotted with respect to distance from GZ in Fig. 3.30.

All curves demonstrated a general decrease in median diameter with distance from GZ, although both the Tesla and Apple I curves indicated slight increases at greater distances.

The percentage and activity distributions of the 0- to 5-μ-diameter fall-out material were of special interest because of biological inhalation and ingestion considerations. The 0- to 5-μ-diameter mean percentages and activity distributions (determined by the application of the mean percentages to total arc activities, as shown in Figs. 3.21 to 3.24) are plotted with respect to distance from GZ in Figs. 3.31 to 3.34.

The percentage contributions of the 0- to 5-μ material tended to increase with distance, with declines in the Tesla and Apple I curves at distances corresponding to increases in median diameter. The levels of 0- to 5-μ-diameter radioactivity generally tended to reflect the total radioactivity distributions.

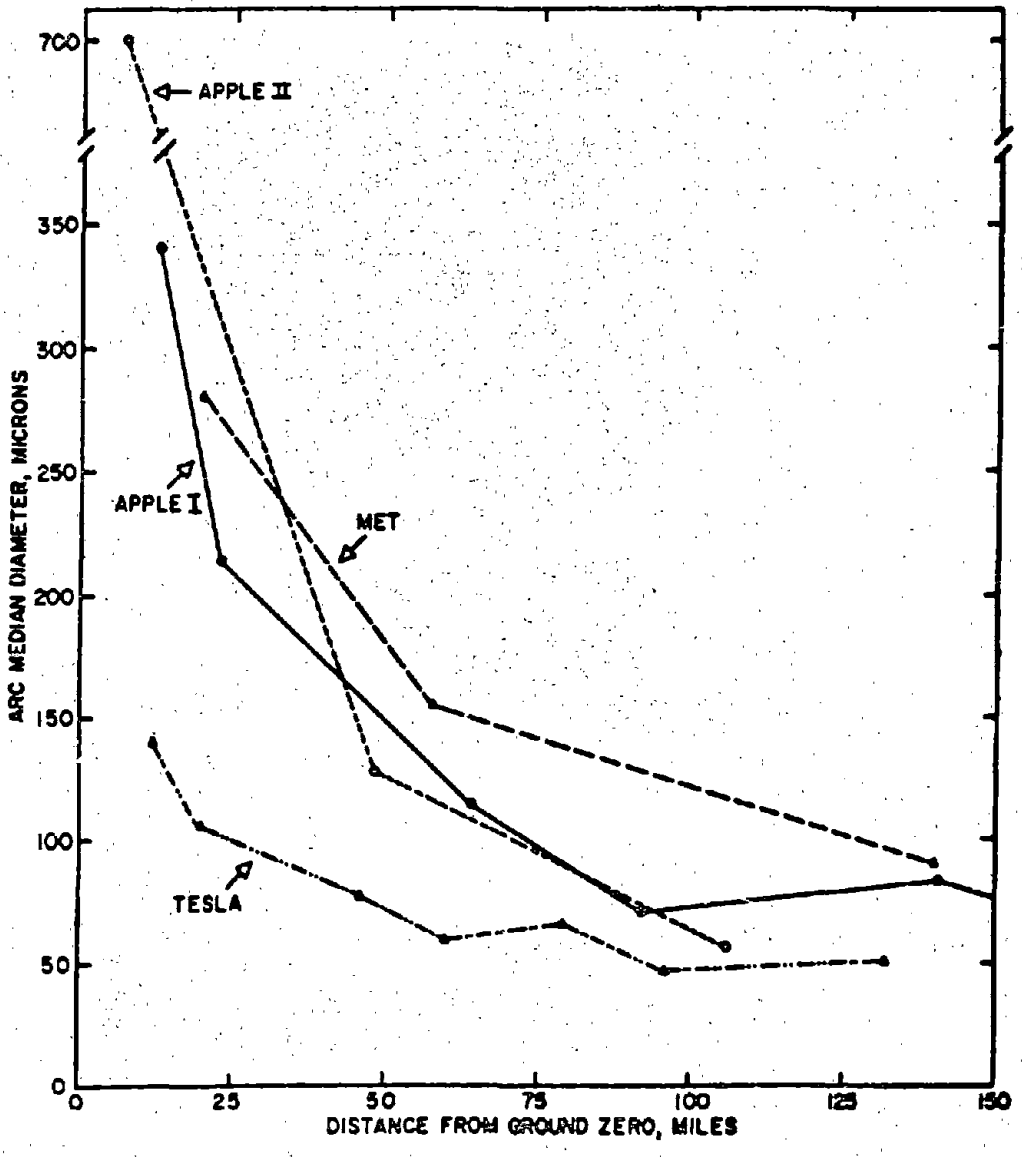

Fig. 3.30—Arc median diameters of the Tesla, Apple I, Met, and Apple II shots at various distances from GZ.

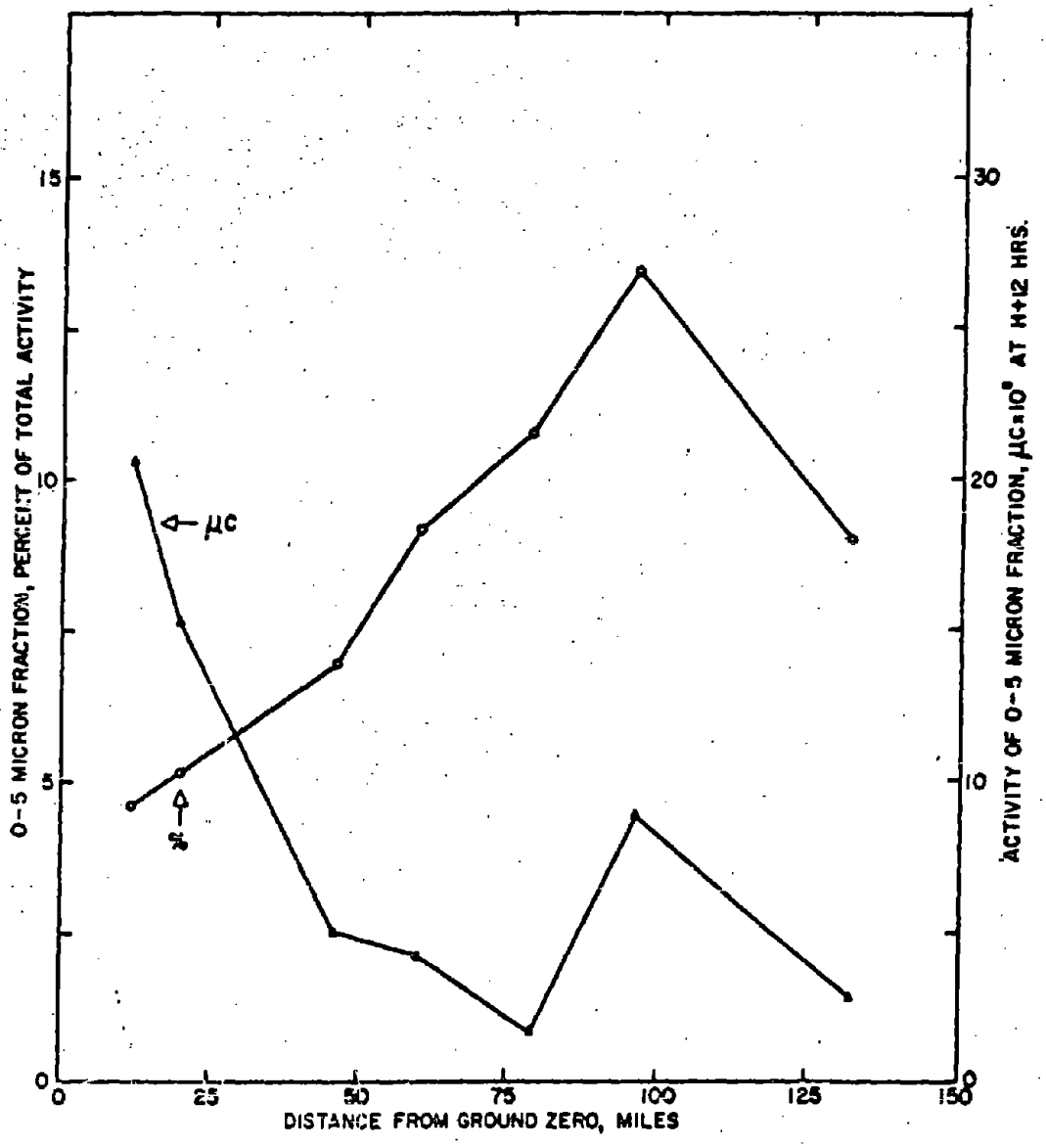

Fig. 3.31—Percentage and activity distributions of 0- to 5-μ fraction with respect to distance from GZ, Tesla.

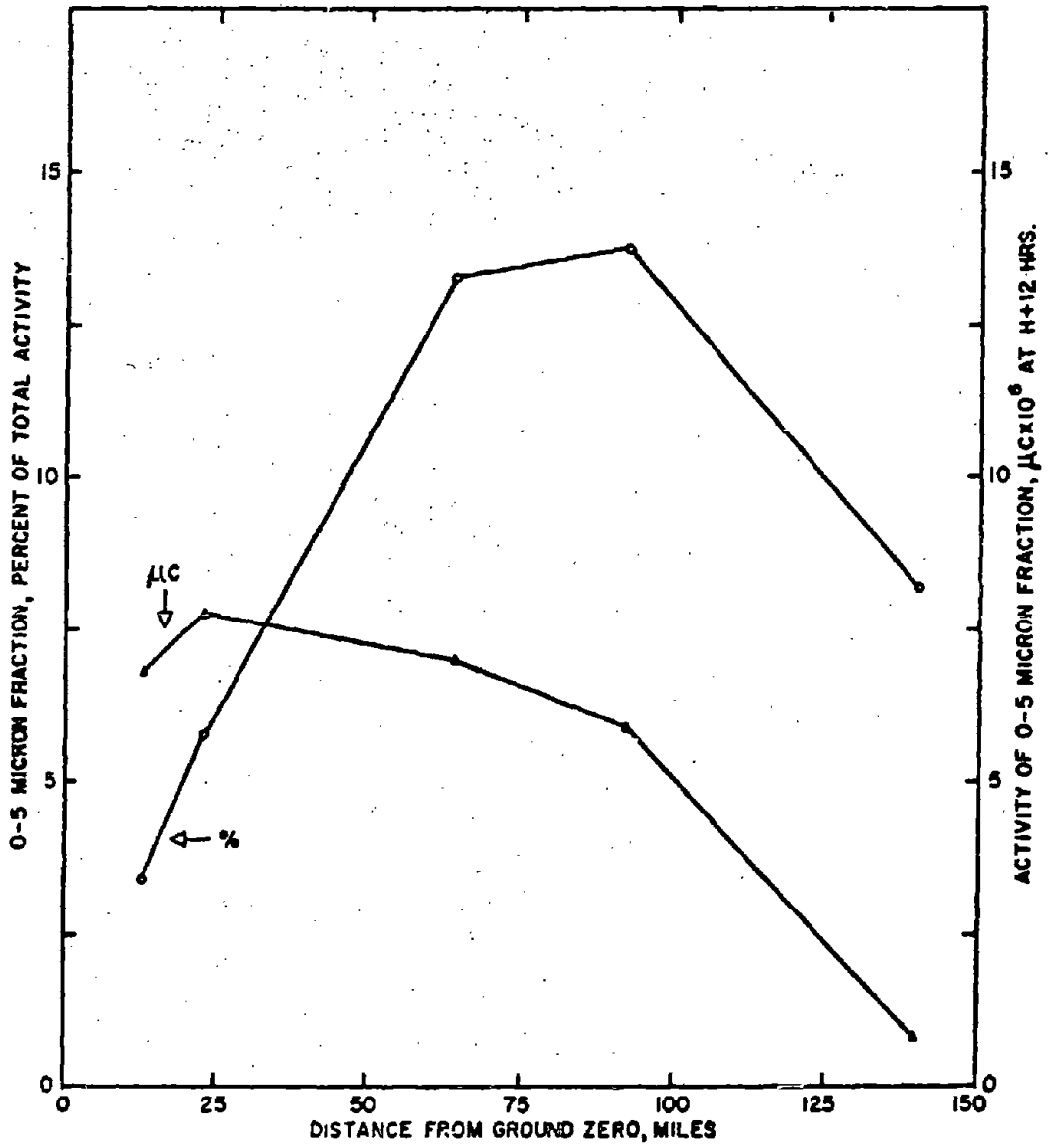

Fig. 3.32—Percentage and activity distributions of 0- to 5-μ fraction with respect to distance from GZ, Apple I.

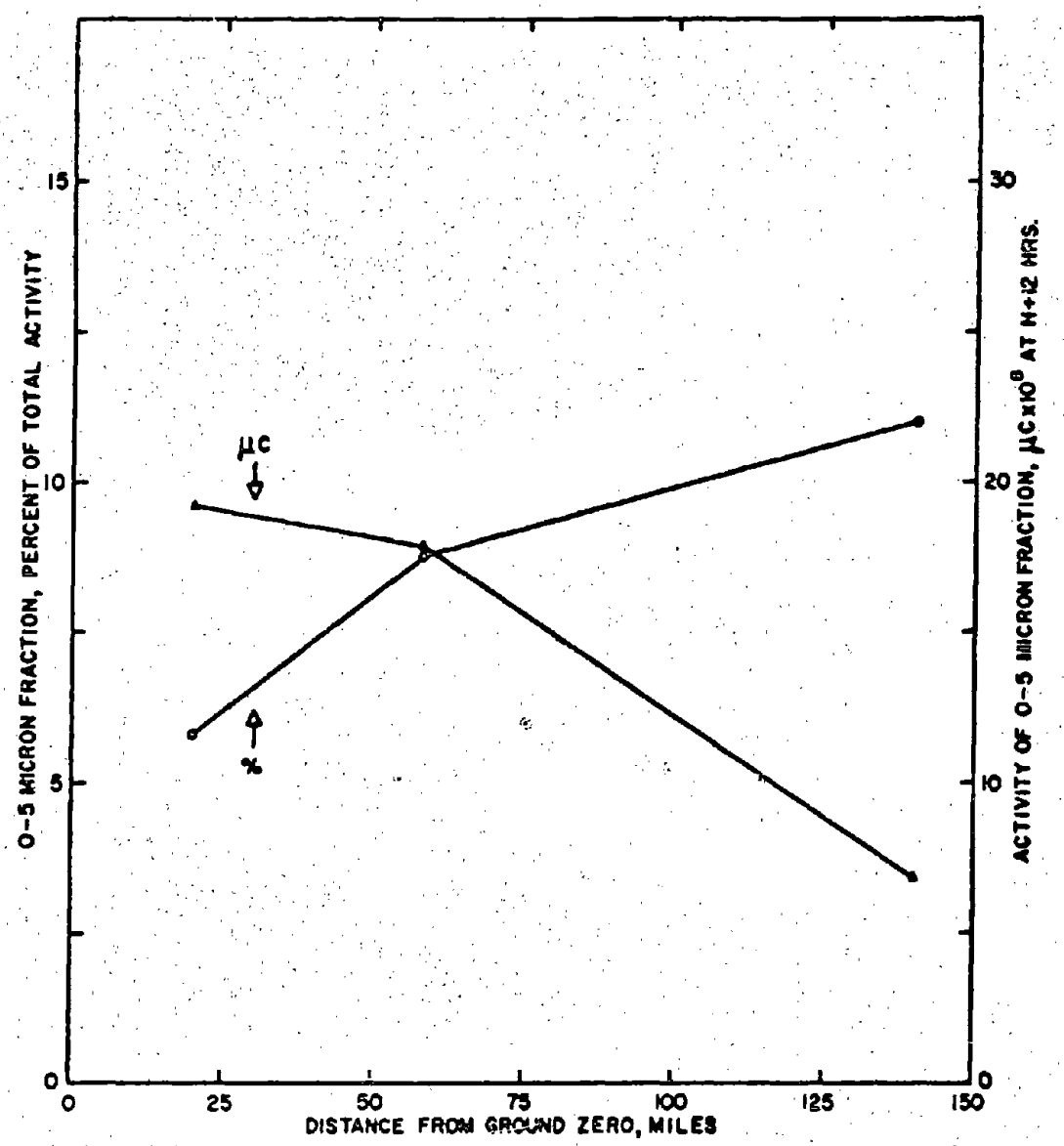

Fig. 3.33 — Percentage and activity distributions of 0- to 5-μ fraction with respect to distance from GZ, Met.

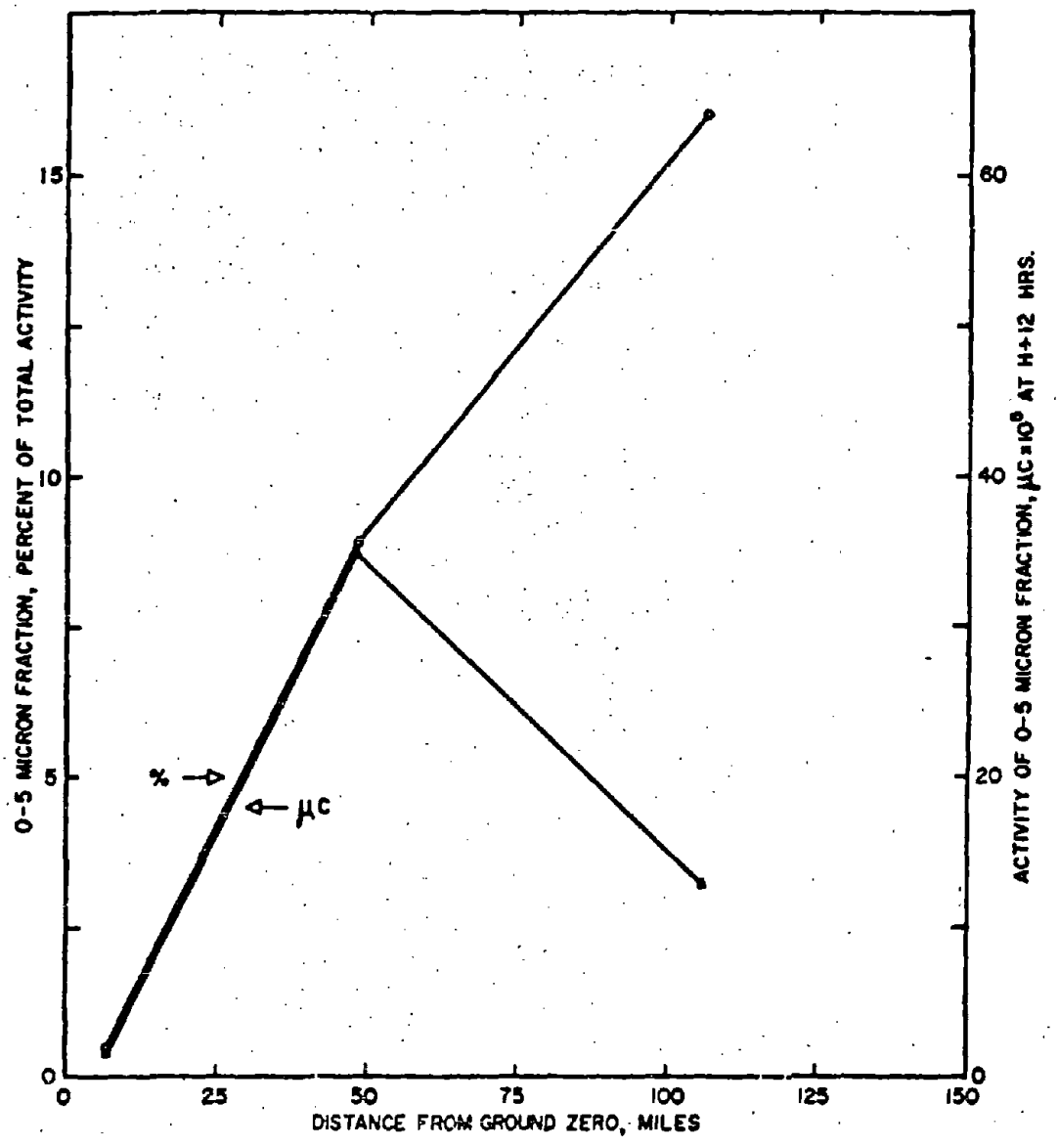

Fig. 3.34—Percentage and activity distributions of 0- to 5-μ fraction with respect to distance from GZ, Apple II.

If the particle distributions for the Tesla, Apple I, and Met shots (Appendixes C, E, and F) were first integrated across the fall-out pattern and then the results were integrated with distance from GZ, it was possible to determine the size distribution of the fall-out within the limits studied. A typical correlation is given in Table 3.5.

3.3.7 Radiostrontium Distribution with Respect to Distance and Particle Size

The soil samples of fall-out contamination from the Tesla and Met shots were analyzed for radiostrontium approximately 1.75 yr after deposition. Table 3.6 gives the data at this date on the basis of area contamination.

TABLE 3.5—TOTAL PARTICLE-SIZE DISTRIBUTION OF FALL-OUT

	Tesla	Apple I	Met
Distance range, miles	12–132	23–165	20–140
Time of fall-out, H+hr	1.2–9.2	1.45–7.0	0.3–6.0
Total activity	7.77	4.28	11.70
Percentage distribution by particle-size range			
0 to 44 μ	15.05	22.20	9.08
44 to 88 μ	30.78	12.34	9.67
88 to 125 μ	13.90	16.15	14.95
125 to 177 μ	19.95	19.85	17.25
177 to 250 μ	9.78	11.64	16.31
250 to 300 μ	3.73	6.42	11.03
300 to 350 μ	2.45	5.58	12.75
350 to 420 μ	2.45	2.22	3.54
420 to 500 μ	1.03	1.66	3.07
500 to 2000 μ	0.90	2.05	2.13

The fall-out from Shot Tesla indicated that the radiostrontium content reached a peak value at approximately 80 miles from GZ both in terms of total radiostrontium per square foot and in percentage of the total activity in the 44- to 88-μ range. The radiostrontium content of the 0- to 44-μ material appeared to be uniformly distributed at all the distances studied. The analyses of the Met samples indicated higher levels of contamination both in total radiostrontium content and in percentage of the total activity.

Table 3.7 lists the data concerning the availability of total fission-product activity and radiostrontium from Met fall-out as measured by $NH_4C_2H_3O_2$ extraction. On the basis of these few samples, it appeared that the radiostrontium was more available than the total fission-product material by approximately a factor of 10, suggesting surface phenomena. It was not conclusively proved, but there appeared to be a trend toward increasing radiostrontium availability with increasing distance.

3.3.8 Gummed-paper Samples

The Met and Apple II shots resulted in the most complete contamination of prelocated gummed-paper stations. Although soil samples were used as the primary basis for unit-area activity measurements because of the detail permitted by postshot sampling, the comparison of gummed-paper and soil-sample values was important from the points of view of methodology and relation to previous unit-area activity measurements. Table 3.8 gives the Met and Apple II gummed-paper (approximately 30-hr exposure) and soil-sample activity values and their respective ratios at different sampling locations.

Considerable variation in the ratio of gummed-paper to soil-sample activity occurred for both detonations. It might be expected that gummed-paper values would generally be more variable than corresponding soil-sample values because of the greater sampling area in the latter case. When the two 0.005 ratio values were omitted, the average ratio of gummed-paper to soil-sample activity was 0.83.

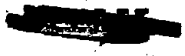

TABLE 3.6 — RADIOSTRONTIUM DISTRIBUTION IN SELECTED PARTICLE-SIZE RANGES

Shot	Distance from GZ, miles	Particle size, μ	Total soil activity, d/min/ft²	Total soil radio-strontium, d/min/ft²	Radio-strontium fraction, %
Tesla	12	0 – 44	9,140	27.3	0.3
		177 – 250	394,000	1,683.0	0.4
	20	0 – 44	44,500	153.5	0.3
		125 – 177	263,500	461.0	0.2
	46	0 – 44	18,400	127.0	0.7
		44 – 88	71,800	281.0	0.4
	60	0 – 44	15,280	79.9	0.5
		44 – 88	506,000	364.0	0.7
	79	0 – 44	18,160	68.5	0.4
		44 – 88	67,900	986.0	1.5
	96	0 – 44	24,500	0.0	0.0
		44 – 88	48,300	828.0	1.7
	132	0 – 44	7,780	34.8	0.5
		44 – 88	5,130	36.3	0.7
Met	20	0 – 44	96,200	856.0	0.9
		250 – 297	637,000	6,250.0	1.0
		297 – 350	369,500	8,730.0	2.4
	58	0 – 44	49,200	344.0	0.7
		125 – 177	101,000	812.0	0.8
		177 – 250	47,950	849.0	1.8
	140	0 – 44	20,900	991.0	4.7
		88 – 125	19,450	136.7	0.7
		125 – 177	2,025	153.5	7.7

TABLE 3.7 — AVAILABILITY OF RADIOSTRONTIUM IN MET FALL-OUT

Distance from GZ, miles	Particle size, μ	Total β activity available, d/min/ft²	Total activity available, %	Radio-strontium available, d/min/ft²	Radio-strontium available, %	β activity available as radio-strontium, %
20	0 – 44	5980.0	6.09	571.0	65.70	0.582
	250 – 297	355.0	0.06	180.0	2.88	0.028
	297 – 350	274.5	0.07	34.1	0.39	0.009
58	0 – 44	1555.0	3.16	105.5	30.70	0.214
	125 – 177	743.0	0.74	40.6	5.00	0.040
	177 – 250	863.5	0.76	128.4	15.12	0.268
140	0 – 44	550.0	2.63	68.0	6.86	0.325
	88 – 125	210.0	1.08	24.9	18.20	0.128
	125 – 177	196.5	9.70	19.7	12.84	0.373

The influence of time of exposure and height above ground on gummed-paper radioactivities were also investigated in Met and Apple II fall-out areas. These results are given in Tables 3.9 and 3.10.

The data indicated that detectable quantities of radioactive material were in motion for relatively long periods of time after initial fall-out, representing either the migration of deposited material or a continuation of fall-out. Regardless of origin, the comparatively low levels of activity may be significant with respect to biological aspects, particularly if it is assumed that the smaller size ranges are involved. No consistent relation was apparent between the late-exposure values obtained by sampling at 0.5 and 4 ft above the ground surface.

TABLE 3.8—COMPARISON OF GUMMED-PAPER AND SOIL-SAMPLE ACTIVITY VALUES

Location	Approx. distance from GZ, miles	Gummed-paper activity, $\mu c/ft^2$ (H + 12 hr)	Soil activity, $\mu c/ft^2$ (H + 12 hr)	Gummed-paper/soil ratio
	Met			
22 miles N of Indian Springs AFB	20	0.50	8.69	0.06
25 miles N of Indian Springs AFB		2217.4	5541.9	0.40
20 miles N of Meadow Valley	58	156.0	196.9	0.79
18 miles N of Meadow Valley		317.85	321.5	0.99
16 miles N of Meadow Valley		274.05	658.4	0.42
14 miles N of Meadow Valley		671.05	376.5	1.78
12 miles N of Meadow Valley		7.55	9.14	0.83
10 miles N of Meadow Valley		3.95	2.19	1.81
8 miles N of Meadow Valley		2.54	1.82	1.40
16 miles N of Enterprise	140	20.40	67.0	0.31
12 miles N of Enterprise		17.35	100.5	0.18
9 miles N of Enterprise		25.40	71.1	0.36
6 miles N of Enterprise		24.80	38.2	0.65
	Apple II			
4.1 miles W of Mercury Hwy.	7	2347.9	2475.5	0.95
2.6 miles W of Mercury Hwy.		920.6	2070.1	0.45
0.8 mile W of Mercury Hwy.		0.37	74.5	0.005
12 miles W of Reed	48	6.45	20.0	0.32
9 miles W of Reed		64.55	34.0	1.90
6 miles W of Reed		191.75	108.7	1.77
3 miles W of Reed		156.90	490.1	0.32
Reed		384.55	646.6	0.60
3 miles E of Reed		199.65		
8 miles W of Warm Springs	106	2.85		
0.4 mile NE of Warm Springs		19.80		
0.5 mile NE of Warm Springs		3.67		
8.0 miles NE of Warm Springs		22.55	19.9	1.14
16.0 miles NE of Warm Springs		34.4	39.8	0.87
24.0 miles NE of Warm Springs		0.13	25.5	0.005

3.4 AIRBORNE CONTAMINATION

Airborne concentrations originating from the Bee, Met, and Apple II shots were sampled by the several types of air samplers. The primary data are recorded with respect to distance from GZ, sample interval, and type of sampler in Appendixes H, I, and J.

3.4.1 Comparison of Air Samplers

The different conditions of sampling represented by the several samplers used are summarized in Table 3.11, and the comparative results obtained by the various instruments during three shots are given in Table 3.12.

The average concentrations over the entire sampling period obtained by the respective samplers at individual locations generally agreed within a factor of 4, although considerably higher variation occurred over shorter sampling intervals (as indicated in Appendixes H to J), particularly in cases of extremely low concentration levels. Although variations occurred in

TABLE 3.9—INFLUENCE OF TIME OF EXPOSURE AND HEIGHT OF COLLECTOR ON GUMMED-PAPER SAMPLES, MET

Location	Distance from GZ, miles	Height above ground, ft	Exposure period, H+hr	Activity, $\mu c/ft^2$ (H+12 hr)
22 miles N of Indian Springs AFB	20	4	0.33–27.50	0.50
		4	0.33– 5.75	0.31
		4	5.75–27.50	0.05
		0.5	6.75–27.50	0.02
25 miles N of Indian Springs AFB		4	0.33–30.00	2217.40
		4	0.33– 5.75	2203.0
		4	5.75–30.00	14.42
		0.5	7.00–30.00	6.58
18 miles N of Meadow Valley on Hwy. 93	68	4	1.16–30.25	317.88
		4	6.75–30.25	2.13
		0.5	6.75–30.25	1.30
14 miles N of Meadow Valley on Hwy. 93		4	1.08–30.50	671.05
		4	1.08– 6.25	475.15
		4	6.25–30.50	1.24
		0.5	6.00–30.50	2.13
10 miles N of Meadow Valley on Hwy. 93		4	1.00–31.15	3.95
		4	5.15–31.15	0.25
		0.5	5.15–31.15	0.16
12 miles N of Enterprise	140	4	3.50–27.3	17.33
		0.5	6.00–27.3	0.84
6 miles N of Enterprise		4	3.50–30.15	24.80
		4	3.50– 7.00	56.50
		4	7.00–30.15	0.18
		0.5	7.00–29.00	0.39

both directions, the values obtained by the directional sampler without throttle and the fixed sampler with throttle exceeded those of the directional sampler with throttle by an average factor of 1.6. The average concentration levels determined by the UCLA sampler and the directional sampler with throttle were approximately the same.

3.4.2 Relations Between Airborne and Fall-out Concentrations

Table 3.13 gives the Met and Apple II average airborne concentrations determined over the total sampling period and corresponding soil-surface activities at different distances from GZ and the midline of fall-out.

The airborne concentrations demonstrated little correlation with surface contamination, other than the fact that high surface activities were generally accompanied by relatively high airborne concentrations. The transient nature of airborne material was emphasized, however, by the occurrence of comparatively high concentrations in areas of low surface contamination. The influence of distance from GZ on airborne concentrations was obscured by the variable distances from the fall-out midline; however, the rate of decrease for maximum airborne-concentration values with distance from GZ was generally less than that for soil contamination.

3.4.3 Concentration Variation with Respect to Time

The variations in concentration levels with time at individual sampling locations were generally similar to those previously observed, i.e., the rapid decline of initial concentrations

TABLE 3.10—INFLUENCE OF TIME OF EXPOSURE AND HEIGHT OF COLLECTOR ON GUMMED-PAPER SAMPLES, APPLE II

Location	Distance from GZ, miles	Height above ground, ft	Exposure period, H+hr	Activity, $\mu c/ft^2$ (H+12 hr)
4.1 miles W of Mercury Hwy. on T-2 Access Rd.	7	4	0.13–31.83	2347.88
		4	0.13– 8.83	2140.13
		4	8.83–31.83	0.20
		0.5	8.83–31.83	0.12
2.6 miles W of Mercury Hwy. on T-2 Access Rd.		4	0.20–32.33	920.02
		0.5	9.83–32.33	0.05
0.8 mile W of Mercury Hwy. on T-2 Access Rd.		4	0.25–30.42	0.37
		0.5	10.67–30.42	0.01
12.0 miles W of Reed	48	4	1.50–30.83	6.45
		4	7.77–30.83	10.00
		0.5	7.83–30.83	0.02
9.0 miles W of Reed		4	1.67–31.50	64.57
		4	7.33–31.50	0.04
		0.5	7.33–31.50	0.04
6.0 miles W of Reed		4	1.83–32.00	191.76
		4	1.83– 6.70	192.91
		4	6.70–32.00	0.09
		0.5	6.70–32.00	1.07
3.0 miles W of Reed		4	1.58–32.33	156.88
		4	1.58– 8.17	164.24
		4	8.17–32.33	0.04
		0.5	8.17–32.33	0.07
Reed		4	1.00–31.17	384.53
		4	5.50–31.17	0.79
		0.5	5.50–31.17	3.62
3.0 miles E of Reed		4	1.67–30.33	199.63
		4	5.25–30.33	1.17
		0.5	5.25–30.33	0.28
8.0 miles W of Warm Springs on Hwy. 6	106	4	2.67–30.83	2.85
		0.5	8.33–30.83	0.15
0.4 mile NE of Warm Springs on Hwy. 6		4	3.08–30.08	18.78
		0.5	8.00–30.08	0.47
0.5 mile NE of Warm Springs on Hwy. 6	106	4	3.25–30.33	3.67
		0.5	8.83–30.33	0.83
8.0 miles NE of Warm Springs on Hwy. 6		4	3.67–32.83	22.57
		4	3.67– 7.33	25.54
		4	7.33–32.83	0.21
		0.5	7.33–32.83	1.53
16.0 miles NE of Warm Springs on Hwy. 6		4	3.08–31.83	34.39
		0.5	7.58–31.83	1.00

TABLE 3.11—COMPARISON OF SAMPLING CONDITIONS REPRESENTED BY DIFFERENT AIR SAMPLERS

Sampler	Filter type	Orifice velocity, m/min	Sampling rate, m^3/min
UCLA	Millipore	30.5	0.23
High-volume directional with throttle (Dir-T)	MSA	1023	1.08
Fixed with throttle (fixed-T)	MSA	1023	1.08
Directional without throttle (Dir-NT)	MSA	140	1.13

TABLE 3.12—COMPARISON OF CONCENTRATIONS OBTAINED BY VARIOUS SAMPLING PROCEDURES

Location	Sample time, H+hr	Concentration,* $\mu c/m^3 \times 10^{-6}$ (H+12 hr)	Concentration ratio		
			Fixed-T/ Dir-T	Dir-NT/ Dir-T	UCLA/ Dir-T
	Bee				
4.0 miles N of Nye Canyon Rd. on White Flag Rd.	1.00–12.00	9,058	1.15	1.15	0.68
7.0 miles N of Nye Canyon Rd. on White Flag Rd.	1.50–12.00	37,801			0.52
	Met				
25.0 miles N of ISAFB† on Indian Springs Rd.	0.33–14.25	193,116			0.92
22.0 miles N of ISAFB	0.33–13.75	1,163	1.39	1.74	1.57
18.0 miles N of Meadow Valley on Hwy. 93	1.00–26.00	40,213			0.93
14.0 miles N of Meadow Valley	1.08–27.50	77,750	0.86	1.47	0.33
12.0 miles N of Enterprise on Utah Hwy. 18	3.50–27.50	13,563			1.35
6.0 miles N of Enterprise	3.50–28.92	11,570		3.43	
	Apple II				
4.1 miles W of Mercury Hwy. on T-2 Access Rd.	0.13–15.83	11,015	3.92	2.38	2.05
2.6 miles W of Mercury Hwy.	0.20–30.67	35,847			1.21
6.0 miles W of Reed on Old Hwy. 25	1.83–17.33	8,467	1.73	2.67	0.68
3.0 miles W of Reed on Old Hwy. 25	1.58–30.33	6,837	1.74	13.61	0.14
8.0 miles W of Warm Springs	2.67–30.83	1,582			0.27
0.5 mile NE of Warm Springs	3.25–11.33	2,490		0.48	
4.0 miles NE of Warm Springs	3.25–30.08	2,937			0.61
8.0 miles NE of Warm Springs	3.08–33.33	4,863		0.82	2.29
16.0 miles NE of Warm Springs	3.08–33.50	7,980			0.64

* Concentration data obtained from directional sampler with throttle.
† Indian Springs Air Force Base.

TABLE 3.13—COMPARISON OF AVERAGE AIRBORNE CONCENTRATION TO SOIL FALL-OUT CONCENTRATION

Distance from GZ, miles	Distance from midline,* miles	Av. airborne concentration,† $\mu c/m^3 \times 10^{-6}$	Soil activity, $\mu c/ft^2$
		Met	
20	0.0	60,866	5,541.9
	3.0 S	1,691	8.7
	6.0 S	100	
58	3.2 N	35,396	321.5
	0.0		890.5
	0.8 S	24,185	376.5
	4.8 S	532	2.19
	8.8 S	756	
140	0.0 N	12,061	100.48
	6.0 S	11,570‡	38.18
	11.0 S	515‡	1.04
		Apple II	
7	0.9 W	12,592	2,475.5
	0.0		5,913.8
	0.6 E	59,037	2,070.1
	2.4 E	20,310	74.5
48	8.4 W	7,356	34.0
	5.2 W	6,517	108.7
	2.2 W	8,994	490.1
	0.0		956.6
	0.8 E	24,120	646.6
	3.8 E	14,797	500.0
106	50.0 SW	354	5.7
	41.5 SW	3,552§	7.33
	38.0 SW	1,463	39.55
	34.0 SW	7,052	19.9
	26.0 SW	3,316	38.3
	0.0		126.7

* Based on soil-surface contamination values.

† Average activity concentration for approximately 30 hr after fall-out time (UCLA sampler).

‡ High-volume directional sampler with throttle.

§ 5-hr average.

TABLE 3.14—COMPARISON OF CASCADE-IMPACTOR AND RADIOSEDIMENTATION METHODS OF PARTICLE-SIZE ANALYSIS OF MET SHOT AIRBORNE CONCENTRATIONS

Approximate distance from GZ, miles	Cascade impactor median diameter, μ	Radiosedimentation median diameter, μ
20	0.63	0.71
58	1.79	2.14
140	2.35	3.05

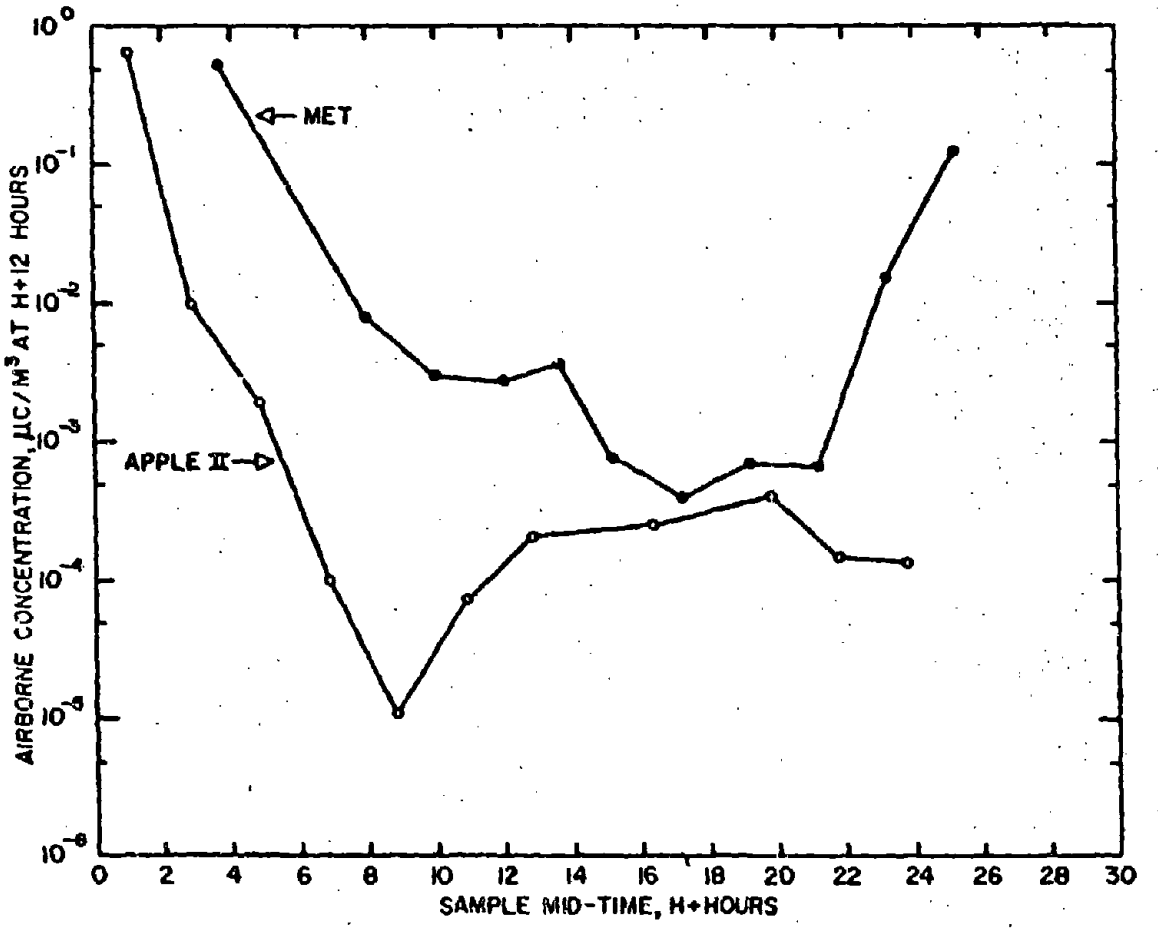

Fig. 3.35 — Variation in airborne concentration with respect to time at Met and Apple II maximum concentration stations. Met, 25.0 miles north of Indian Springs Apple II, 2.6 miles west of Mercury Highway on T-2 Access Road.

coincident with time of fall-out and occasional increases in concentration during the sampling period. The latter observation was characteristic of the Met shot. The maximum concentrations detected during the Met and Apple II sampling periods were 2.16 $\mu c/m^3$ at a sample midtime of H+3.67 hr and 12.23 $\mu c/m^3$ at a sample midtime of H+1.02 hr, respectively. The airborne concentrations corrected to H+12 hr at these two stations are plotted with respect to time in Fig. 3.35.

3.4.4 Airborne Particle-size Distributions

A serious limitation of the radiosedimentation method of radioactive particle-size analysis was the low counting efficiency of the scintillation detector, necessitating relatively high concentration levels for analysis. Consequently, cascade-impactor collections provided the primary basis for the determination of airborne particle-size distributions. Airborne concentrations were sufficiently high during the Met shot for a comparison of the two methods at three distances from GZ. These data appear in Table 3.14.

The median-diameter values determined by the radiosedimentation method were higher than those derived from cascade-impactor collections by an average factor of 20 per cent. The agreement, however, was sufficiently close to support the validity of results by either method.

The median diameters and percentage contributions of the <2- and <5-μ-diameter material originating from the Met and Apple II shots are summarized with respect to sample interval and distance from GZ in Table 3.15.

The determined median diameters ranged from 0.46 to 5.8 μ. The sequential sampling of airborne concentrations at the different locations did not indicate a consistent median-diameter trend with respect to time. However, the frequent association of smaller median diameters with initial high activity 7 miles from GZ and the occurrence of larger particle distributions at greater distances are of interest.

3.5 SOLUBILITY OF FALL-OUT AND AIRBORNE CONTAMINATION

The best results of solubility determinations performed on the predominant-size and the 0- to 5-μ-size fractions at different distances from GZ for the Turk, Tesla, Apple I, Met, and Apple II shots are given in Table 3.16.

The solubilities of the predominant-size fractions were inconsistent with respect to distance and the several solvents. In general, however, the solubilities of the 0- to 5-μ material were quite consistent over the distances considered. The maximum solubilities of the 0- to 5-μ fractions observed were as follows: distilled water, 6.4 per cent with an average of 2.4 per cent; 0.1N HCl, 36.2 per cent with an average of 22.8 per cent; 0.1N $Na_2S_2O_3$, 9.0 per cent with an average of 4.2 per cent; and in buffer solution, 15.0 per cent with an average of 5.73 per cent.

The solubilities of airborne material originating from the Met and Apple II shots determined by jet liquid-impinger samples are given in Table 3.17.

A relatively high solubility of airborne material in 0.1N HCl in comparison to the other solutions was observed. However, considerable variation occurred in relative solubilities in the remaining solvents.

A comparison of 0- to 5-μ soil and airborne activity solubilities at different distances from GZ is given in Table 3.18. (Soil- and airborne-sample locations at the several distances did not coincide in most cases.)

The comparison indicated that, for similar size ranges, the solubility of airborne material exceeded that of soil-deposited material in all solvents. The basis for this general difference in solubility is presently unknown.

3.6 RADIOACTIVITY CHARACTERISTICS OF COLLECTED SAMPLES

3.6.1 Decay and Energy Characteristics

Decay and energy characteristics of the Tesla, Turk, Bee, Apple I, Met, and Apple II samples collected at different distances from GZ are given in Tables 3.19 to 3.21.

TABLE 3.15 — PARTICLE-SIZE DISTRIBUTION OF AIRBORNE MATERIAL BY CASCADE IMPACTOR WITH RESPECT TO TIME AFTER SHOT AND DISTANCE FROM GZ

Location	Approx. distance from GZ, miles	Sample interval, H+hr	Concentration,* $\mu c/m^3 \times 10^{-6}$	Median diameter, μ	% less than 2 μ in diameter	% less than 2 μ in diameter
		Met				
22 miles N of Indian Springs AFB on Indian Springs Rd.	20	0.33 – 5.75	3,190	0.63	85.8	94.2
		5.75 – 9.25	161	1.04	82.0	96.0
		9.25 – 13.75	139	1.40	60.0	78.0
		17.75 – 19.75		1.87	51.5	67.5
14 miles N of Meadow Valley on Hwy. 93	58	1.00 – 6.00	188,000	1.79	53.0	74.0
		6.00 – 9.75	15,200	2.40	46.0	60.5
		9.75 – 15.50	93,700	1.40	56.0	67.0
6 miles N of Enterprise on Utah Hwy. 18	140	3.50 – 7.00	30,400	2.35	47.0	63.0
		7.00 – 11.58	1,870	1.65	57.0	80.0
		11.58 – 28.92	2,440	2.20	47.0	71.0
		Apple II				
4.1 miles W of Mercury Hwy. on T-2 Access Rd	7	0.13 – 8.67	21,900	0.46	99.80	100.0
		8.67 – 18.42	371	2.60	40.0	76.2
		18.42 – 31.02	129	1.83	53.5	85.0
6 miles W of Reed on Hwy. 25	48	1.83 – 6.77	23,500	5.00	24.0	50.0
		6.77 – 10.83	1,650	0.96	56.0	73.2
		10.83 – 17.75	251	3.20	37.0	69.0
		17.75 – 30.50	211	1.54	60.3	85.8
3 miles W of Reed on Hwy. 25	48	8.33 – 13.33	1,290	5.8	21.0	43.0
		13.33 – 18.42	1,220	2.6	42.5	69.8
		18.42 – 32.33	740	6.35	26.5	47.0
8 miles NE of Warm Springs on Hwy. 6	106	3.08 – 7.33	14,000	1.5	60.5	85.0
		7.33 – 11.33	4,080	2.6	43.0	67.0
		11.33 – 17.33	1,000	1.4	59.0	75.0
		17.33 – 33.33	453	3.1	42.0	58.0
0.5 mile E of Warm Springs on Hwy. 6	106	3.25 – 8.33	3,810	3.75	30.0	60.5
		8.33 – 11.33	1,170	0.96	75.5	92.0

*Determined by directional high-volume sampler with throttle.

TABLE 3.16 — SOLUBILITY - PARTICLE-SIZE RELATION, BASED ON SOIL SAMPLES COLLECTED AT DIFFERENT DISTANCES FROM GZ

Location	Approx. distance from GZ, miles	Total activity, $\mu c/ft^2$ (H + 12 hr)	Size range, μ	Solubility, %			
				Dist. water	0.1N HCl	0.1N $Na_2S_2O_3$	Buffer (pH 7.6)
		Turk					
5.8 miles NW of Tippipah Springs	11.5	1447.8	250 – 300	1.40	22.20	5.80	
			0 – 44	0.50	14.90	3.40	6.40
		Tesla					
14.7 miles S of Groom Lake Rd. on Indian Springs Rd.	20	846.04	125 – 125	0.10	1.50	0.40	
			0 – 5	1.70	17.50	2.60	1.80
50.1 miles N of Hwy. 95 on Sheep Canyon Rd.	46	673.13	88 – 125	1.60	53.60	0.60	1.10
			0 – 5	2.10	19.30	3.60	3.30
23.5 miles N of Mesquite on Hwy. 91	132	26.51	44 – 88	7.60	29.50	7.00	10.90
			0 – 5	2.00	20.40	3.90	1.90
		Apple I					
4.5 miles S of Groom Lake Rd. on Papoose Lake Rd.	13	1114.09	300 – 350	0.2	0.7	0.0	0.5
			0 – 5		27.9	3.2	4.4
48.3 miles N of Indian Springs AFB on Indian Springs Rd.	23	1094.10	250 – 300	17.8	32.5	0.3	25.0
			0 – 5		36.2	2.3	4.8
0.8 mile S of Alamo on Hwy. 93	64	259.83	125 – 177	43.8	36.5	37.9	0.0
			0 – 5	1.2	24.4	2.8	15.0
14.5 miles N of Elgin on Meadow Valley Wash	92	98.47	44 – 88	0.0	29.1	10.0	0.0
			0 – 5	0.6	20.1	1.9	2.1
7.0 miles S of Cedar City on Hwy. 91	184	13.65	44 – 88	0.0	52.5	0.0	14.5
			0 – 5		14.6		0.0
		Met					
25.0 miles N of Indian Springs on Indian Springs Rd.	20	5541.9	177 – 250	0.3	15.8	0.6	0.7
			0 – 5	3.4	18.9	9.0	10.6
14.4 miles N of Meadow Valley on Hwy. 93	58	770.66	177 – 250	0.0	5.5	0.1	13.3
			0 – 5	5.5	19.4	7.5	7.6
10.0 miles N of Enterprise on Utah Hwy. 18	140	96.36	88 – 125	0.0	4.4	6.3	0.1
			0 – 5	0.0	18.7	0.0	7.1
		Apple II					
3.6 miles W of Mercury Hwy. on T-2 Access Rd.	7	4394.20	500 – 833	33.3	2.4	0.0	23.8
			0 – 5	6.4	33.4	6.5	7.3
0.8 mile W of Reed on Old Hwy. 25	48	956.57	125 – 177	0.5	4.0	2.9	2.4
			0 – 5	3.6	28.1	6.1	6.9
42.0 miles E of Warm Springs on Hwy. 6	106	126.74	44 – 88	2.8	14.0	0.0	2.2
			0 – 5	2.7	23.7	3.4	6.5

There were no consistent differences between decay constants and energy distributions of different types of samples or of samples originating from the different detonations. Some variation in decay constant with time was detectable; the constant had a range of −0.80 to −1.07 up to approximately 100 hr postshot and a range of −1.07 to −1.59 over later time intervals. Two beta-energy components were detectable, one with a range of 0.35 to 0.96 Mev and another with a range of 1.15 to 2.30 Mev.

3.6.2 Relation of Radioactivity to Particle Size

Investigations of radioactivity particle-size relations were initiated by the separation of individual particles from Apple II gummed-paper samples. The particles were measured by optical microscopy and radioassayed individually. Only particles that were opaque and spherical or oval in shape were radioactive. Particles that were spherical but translucent were relatively inactive.

TABLE 3.17—SOLUBILITY OF MET AND APPLE II AIRBORNE CONTAMINATION, BASED ON JET LIQUID-IMPINGER SAMPLES

Location	Sample interval, H+hr	Solubility, %			
		Dist. water	0.1N HCl	0.1N $Na_2S_2O_3$	Buffer (pH 7.6)
	Met				
25.0 miles N of Indian Springs AFB	0.33– 8.75	19.5	78.2	82.7	21.2
22.0 miles N of Indian Springs AFB	0.33– 5.75	16.0	47.2	31.5	24.9
14.0 miles N of Meadow Valley on Hwy. 93	1.08– 4.25	10.1	67.1	10.0	10.3
12.0 miles N of Enterprise on Utah Hwy. 18	3.50–10.75	6.3	88.5	10.7	28.3
6.0 miles N of Enterprise on Utah Hwy. 18	3.50–11.50	11.5	41.0		19.2
1.0 miles N of Enterprise on Utah Hwy. 18	3.50–11.75	0.0	84.5	0.0	55.1
	Apple II				
4.1 miles W of Mercury Hwy. on T-2 Access Rd.	1.13– 8.87	7.9	77.4	9.8	41.1
6.0 miles W of Reed on Old Hwy. 25	1.83– 9.00	18.8	62.5	8.5	14.9
3.0 miles W of Reed on Old Hwy. 25	1.58– 8.33	36.8	67.0	28.6	27.7
8.0 miles W of Warm Springs on Hwy. 6	2.67– 8.33	24.9	85.7	40.4	51.1
0.5 mile NE of Warm Springs on Hwy. 6	3.25– 6.33	56.0	43.2	42.5	59.8
4.0 miles NE of Warm Springs on Hwy. 6	3.08– 7.92	26.2	74.8	7.2	52.4
8.0 miles NE of Warm Springs on Hwy. 6	3.67–21.33	69.3	30.7	9.7	9.5
16.0 miles NE of Warm Springs on Hwy. 6	3.08–11.50	14.7	68.7	9.0	37.6

TABLE 3.18—COMPARISON OF 0- TO 5-μ SOIL FRACTION AND AIRBORNE ACTIVITY SOLUBILITIES

Distance from GZ, miles	Sample type	Solubility, %			
		Dist. water	0.1N HCl	0.1N $Na_2S_2O_3$	Buffer (pH 7.6)
	Met				
20	Soil, 0–5 μ	3.4	18.8	9.0	10.6
	Airborne	19.5	78.2	82.7	21.2
58	Soil, 0–5 μ	5.5	19.4	7.5	7.6
	Airborne	10.1	67.1	10.0	13.5
140	Soil, 0–5 μ	0.0	18.7	0.0	7.1
	Airborne	6.3	88.5	10.7	28.3
	Apple II				
7	Soil, 0–5 μ	6.4	33.4	6.5	7.3
	Airborne	7.9	77.4	9.8	41.1
48	Soil, 0–5 μ	3.8	28.1	6.1	6.5
	Airborne	36.8	67.0	28.6	27.7
106	Soil, 0–5 μ	2.7	23.7	3.4	8.8
	Airborne	14.7	68.7	9.0	37.6

TABLE 3.19—DECAY AND ENERGY CHARACTERISTICS OF RADIOACTIVE MATERIAL AT DIFFERENT DISTANCES FROM GZ, TESLA

Location	Approx. distance from GZ, miles	Sample type	Time interval, H+hr	Decay constant*	Maximum energy† of components, Mev	Contribution, %
7.7 miles S of Groom Lake Rd. on Papoose Rd.	12	Soil, 0–2000 μ	10–60	−0.80	2.20	50.9
					0.75	49.1
			60–700	−1.39		
14.0 miles S of Groom Lake Rd. on Indian Springs Rd.	20	Soil, 0–2000 μ	10–100	−0.95	2.28	32.3
					0.82	67.7
			100–800	−1.59		
		Soil, 125–177 μ	200–1000	−1.29	1.60	35.2
					0.54	64.8
		Soil, 0–5 μ	200–700	−1.43	1.63	36.4
					0.54	63.6
50.1 miles N of Hwy. 95 on Sheep Canyon Rd.	46	Soil, 0–2000 μ	60–700	−1.21	2.20	32.7
					0.94	67.3
		Soil, 88–125 μ	200–800	−1.39	1.56	37.6
					0.56	62.4
		Soil, 0–5 μ	250–800	−1.43	1.62	43.4
					0.53	56.6
35.7 miles N of Glendale on Hwy. 93	60	Soil, 0–2000 μ	40–800	−1.28	2.30	60.2
					0.72	39.8
26.8 miles N of Hwy. 93 on Meadow Valley Wash	79	Soil, 0–2000 μ	30–150	−1.57	2.10	77.6
					0.96	22.4
			150–800	−1.43		
14.5 miles N of Hwy. 91 on Elgin Rd.	96	Soil, 0–2000 μ	20–100	−1.00	2.15	45.1
					0.69	54.9
			100–800	−1.48		
22.5 miles NE of Mesquite on Hwy. 91	132	Soil, 0–2000 μ	40–800	−1.07	2.45	47.2
					0.84	52.8

*k in expression $A = A_0 T^k$.

†Time of determination corresponds approximately to initial decay time.

TABLE 3.20—DECAY AND ENERGY CHARACTERISTICS OF RADIOACTIVE MATERIAL AT DIFFERENT DISTANCES FROM GZ FOR TURK, BEE, AND APPLE I

Location	Approx. distance from GZ, miles	Sample type	Time interval, H+hr	Decay constant*	Maximum energy† of components, Mev	Contribution, %
		Turk				
5.8 miles NW of Tippipah Springs	11.5	Soil, 250–300 μ	80–900	−1.19	1.76	42.8
					0.53	57.2
		Soil, 0–44 μ	90–900	−1.26	1.43	53.7
					0.52	46.3
		Bee				
7.0 miles N of Nye Canyon Rd.	13	Airborne	40–500	−1.17	2.20	50.9
					0.67	49.1
		Gummed paper	40–250	−1.24	1.85	50.4
					0.58	49.6
		Apple I				
5.0 miles S of Groom Lake Rd. on Papoose Rd.	13	Soil, 0–2000 μ	150–250	−1.23		
48.3 miles N of Hwy. 95 on Indian Springs Rd.	23	Soil, 0–2000 μ	150–250	−1.19		
Desert Valley	48	Soil, 0–2000 μ	150–250	−1.48		
0.8 mile S of Alamo on Hwy. 93	64	Soil, 0–2000 μ	150–250	−1.15		
15.5 miles N of Elgin on Meadow Valley Wash	92	Soil, 0–2000 μ	150–250	−1.28		

*k in expression $D = A_0 T^k$.

†Time of determination corresponds approximately to initial decay time.

TABLE 3.21—DECAY AND ENERGY CHARACTERISTICS OF RADIOACTIVE MATERIAL AT DIFFERENT DISTANCES FROM GZ, MET AND APPLE II

Location	Approx. distance from GZ, miles	Sample type	Time interval, H+hr	Decay constant*	Maximum energy† of components, Mev	Contribution, %
		Met				
25.0 miles N of Indian Springs	20	Soil, 0–2000 μ	70–800	−1.27	1.85	48.7
					0.60	51.3
		Airborne	250–450	−1.33	1.74	44.7
		Gummed paper	250–450	−1.43	2.10	27.8
					0.83	72.2
14.2 miles N of Meadow Valley on Hwy. 93	58	Soil, 0–2000 μ	50–800	−1.23	1.85	48.2
					0.64	51.8
18.0 miles N of Meadow Valley on Hwy. 93	58	Airborne	250–450	−1.39	1.20	42.2
					0.35	57.8
		Gummed paper	250–450	−1.21	1.55	43.1
					0.52	56.9
9.0 miles N of Enterprise on Utah Hwy. 18	140	Soil, 0–2000 μ	70–800	−1.35		
12.0 miles N of Enterprise on Utah Hwy. 18	140	Airborne	250–450	−1.41	2.15	23.3
					0.88	76.7
		Gummed paper	250–450	−1.17	1.58	43.3
					0.49	54.7
		Apple II				
3.2 miles W of Mercury Hwy. on T-2 Access Rd.	7	Soil, 0–2000 μ	60–300	−1.07		
4.1 miles W of Mercury Hwy. on T-2 Access Rd.	7	Airborne	35–90	−0.90	1.56	35.1
					0.57	64.9
			90–305	−1.38		
1.0 miles W of Reed on Old Hwy. 25	48	Soil, 0–2000 μ	60–300	−1.23	1.15	68.0
					0.40	32.0
16.0 miles E of Warm Springs on Hwy. 6	106	Soil, 0–2000 μ	60–300	−1.09		

*k in expression $A = A_0 T^k$.

†Time of determination corresponds approximately to initial decay time.

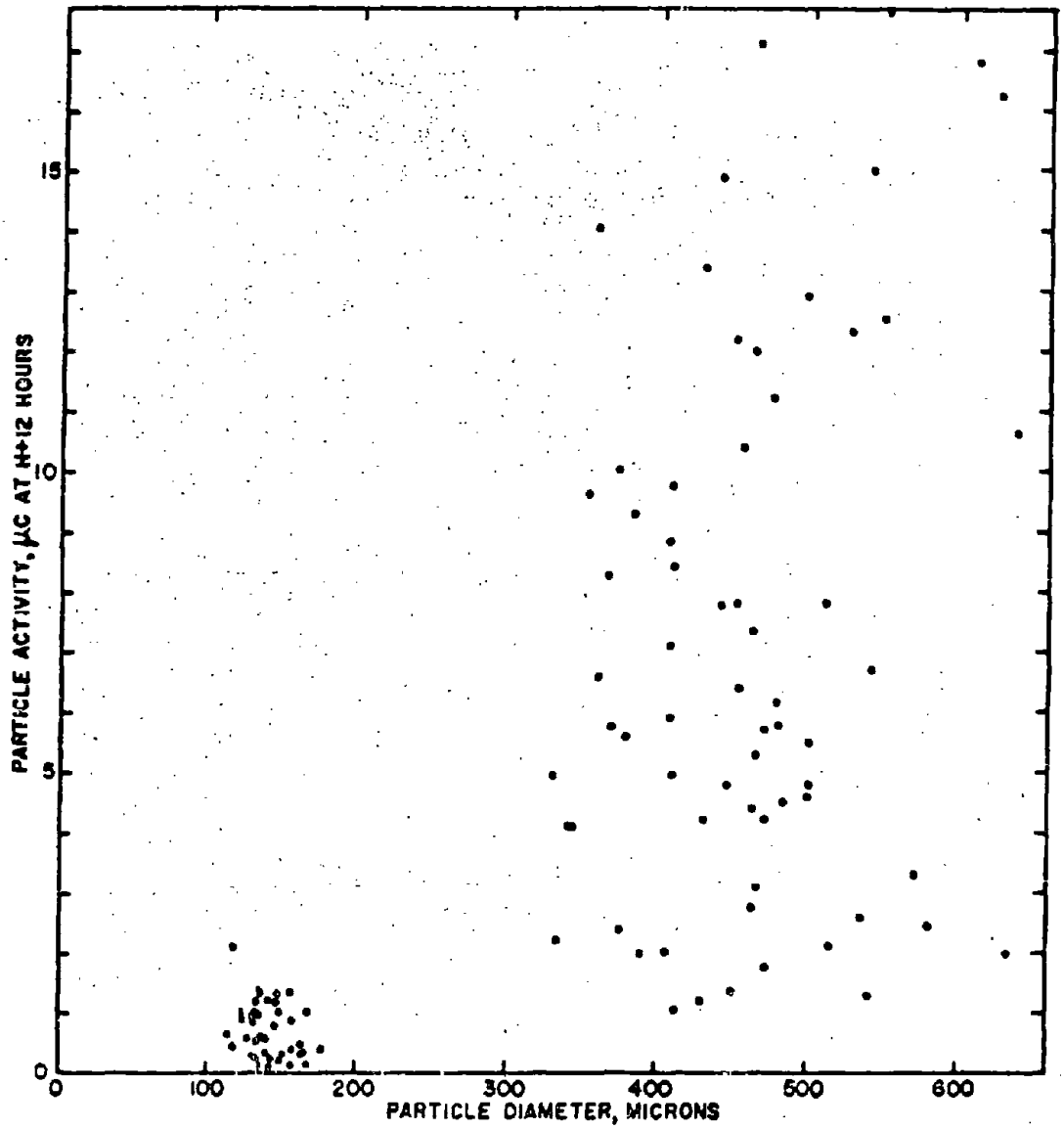

Fig. 3.36 — Variation of activity per particle with particle size for particles from Apple II shot.

The radioactivity values are plotted with respect to particle size in Fig. 3.36. The resulting scatter diagram emphasizes the highly variable nature of the radioactivity particle-size relation, although there is some indication that the particle activity changes from one power dependence of diameter to another at some diameter between 200 and 300 μ.

Additional investigations, which are directed toward widening the size ranges examined, defining the source and limits of variation, and detecting possible differences in the radioactivity particle-size relation with respect to different detonations, are in progress.

3.6.3 Magnetic Properties of Radioactive Samples

Magnetic components of soil fall-out samples originating from the Moth (2.5 kt, 300-ft tower) and Apple II shots were removed from individual fractions by the use of a small magnet. The results are given in Table 3.22.

The data indicated that more than 90 per cent of the fall-out radioactivity is separable by magnet. The variation in the percentage of fall-out activity removable in the finer fractions may be attributable to the small quantities of radioactive material present and the fact that a certain amount of physical entrapment of the radioactive material by the large mass of inert soil occurred.

Although relatively few airborne particles have been observed to date, spherical submicron particles originating from the Met shot and demonstrating high electron opacity and magnetic properties have been detected by the use of the electron microscope.

TABLE 3.22—MAGNETIC COMPOSITION OF FALL-OUT MATERIAL AS A FUNCTION OF PARTICLE SIZE

Size range, μ	% of total activity in size fraction	% of activity removed by magnet
	Moth	
0–44	0.48	74.15
88–125	0.15	5.06
420–500	24.26	99.94
500–840	55.41	99.82
840–2000	0.03	99.93
	Apple II	
20–44	0.02	73.8
44–88	0.09	18.1
88–125	0.04	3.6
125–177	0.09	91.7
177–250	0.07	97.9
250–300	0.04	80.1
300–350	0.06	35.8
350–420	0.22	96.2
420–500	3.86	93.5
500–2000	95.38	99.8

Chapter 4

DISCUSSION

On the basis of meteorological evaluation, it was possible to determine the line of maximum intensity and the width of the fall-out pattern if the space-time variations in the winds over the area of fall-out could be obtained. If it is assumed that the fall-out activity was derived from a level below the top of the cloud, this level depending on cloud height, the line of maximum intensity would be the space-time-corrected ground positions of particles falling from this level. The space-time corrections were also necessary to calculate the particle size of fall-out material, especially in regard to particles smaller than 88 μ, whose terminal velocities were low and were therefore more affected by the wind structure. By using these corrections, the observed particle sizes were found to be within a factor of 1.5 of the calculated size (Sec. 3.2.2). A comparison of calculated ground positions and isodose maps obtained from ground survey data showed that computed ground positions encompassed the fall-out pattern well within the errors of wind observations. The Turk and Bee shots were examples of such a favorable comparison.

The results of these computations are not to be construed as exact; however, it is thought that, after considering the accuracy of wind observations and ground survey techniques, the accuracy obtained here was sufficient to explain why fall-out was found in a given area and not in another. If it is desired to forecast the ground positions of particles by the preceding method, a wind forecast in time would have to be made for each layer at each station in the area under consideration. It appears that the line of maximum intensity of fall-out can then be determined as (1) the line connecting ground positions for particles falling from 5000 ft below the forecast cloud top in the case of clouds reaching approximately 30,000 ft and (2) the line connecting ground positions for particles falling from 10,000 ft below the forecast cloud top in the case of clouds reaching approximately 40,000 ft. This rule should not be extended to clouds reaching higher than 40,000 ft since no substantiating evidence is available. The intensity of fall-out will increase quite rapidly as this midline is approached at right angles from the line connecting ground positions from some higher altitude, and it will then decrease at a somewhat lesser rate as the lines connecting ground positions of particles falling from lower altitudes are approached. If the constant-layer trajectories are considered, the observed fall-out pattern was bracketed in all cases, but there was no feasible method of determining the line of maximum intensity. In predicting the fall-out pattern, it is of no more than meteorological interest to compute the constant-layer trajectories. If long-range suspension of the very small particles is of interest, then the constant-layer trajectories are the maps to be consulted.

A comparison of the observed particle sizes found in soil samples and computed predominant particle sizes gave good agreement in that the observed predominant size at a particular site was within a factor of 1.5 of the calculated predominant size. The line of maximum intensity of fall-out appeared to be where the gradient of computed predominant particle size was the strongest. Further work involving computed particle size and degree of the contamination may yield a satisfactory method of predicting the over-all fall-out pattern, the line of maximum contamination, and the degree of lateral contamination.

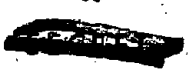

Although it may be possible to correlate fall-out intensities with distance from GZ, it would be more feasible to relate the intensity to the time of fall-out. Using this hypothesis, it was found that the fall-out intensity was inversely proportional to a function of the fall-out time. Since the relations were determined on the basis of experimental data, it was not possible to determine the equation parameters on the basis of a common time. In future tests it is planned to obtain sufficient data to determine parameters at equivalent times. In the equations developed, the constant is thought to be related to the yield and extraneous contributing contamination, and the time of fall-out is a function of cloud height and particle size.

Utilizing the same empirical equations, in the three cases where equations were available for both intensity and contamination-level relations with fall-out time, it was apparent that the ratios of mr/hr : $\mu c/ft^2$ were not the same, except in the case of Apple I, where the slopes were similar.

The quantity of radioactive material deposited from various shots should have been dependent on the yield of the device and the amount of soil and tower material that was carried into the fireball. On the basis of the plot of yield at each of two tower heights vs the total amount of contamination to be found within selected fall-out times, this relation was apparent, except in the case of Apple II. Other data indicated that the fall-out results were not complete for this shot, and the amount of fall-out was actually larger than the integrated value of 0.86×10^{12} mr/hr $\times$ ft^2 at H+12 hr. This increased value would make the point for Apple II more out of line than that indicated by the plot. It is possible that this increase in fall-out might have been caused by differences in shielding material and equipment in the tower cab.

Owing to the urgency of other analyses, it was not possible to analyze soil samples for radiostrontium content until approximately 1.75 yr after detonation. The levels were too low, using the available equipment, to determine quantitatively the Sr^{89} and Sr^{90} content separately; therefore the values listed are for total radiostrontium. Since only selected fractions were analyzed, a full comparison could not be made. However, from Tesla samples it appeared that the radiostrontium activity in the 44- to 88-μ fraction reached a peak activity approximately 5 hr after detonation. Because of the paucity of samples collected from Met fall-out, it can only be stated that the maximum radiostrontium activity in the 0- to 44-μ fraction also appeared in samples collected where the fall-out time was approximately H+5 hr.

The $NH_4C_2H_3O_2$ solubility data indicated that the radiostrontium was more soluble than the total fission-product activity. The factor of 10 increase in solubility would make it appear as if the strontium had been plated on the surface of fall-out particles, rather than being uniformly distributed throughout the volume. However, it may also be true that the radiostrontium on the surface was more readily solubilized. In the future it is planned to study such possible isotopic differentiation with particles. Indications were also seen of a possible increase in radiostrontium availability with increasing distance. This, too, requires further study.

The reason for the greater solubility of airborne activity relative to soil activity of identical particle-size ranges is unknown (see Sec. 3.5). This phenomenon was apparent irrespective of the solvent used. The large differences in particle-size distribution over the size range involved may account for this. The effects of exposure of the fall-out particles to the alkaline pH conditions of the active soil prior to dissolution may also provide an explanation. In the latter case, the solubilities of fission products such as the rare earths, which are insoluble under alkaline conditions, might be significantly altered prior to solvent treatment.

Because of the variations observed in both soil and airborne solubility results, additional investigations, with respect to methodology and correlative experiments using collected samples, are required in order to firmly establish the solubility relations.

It is apparent from the air-sampling and gummed-paper data that small amounts (<1 per cent) of radioactive materials were still being transported by the winds after the immediate fall-out. As yet it cannot be stated whether this was material still settling or whether it was material being relocated by surface winds. However, since gummed papers collected at heights of 4 ft and 6 in. above the ground surface showed similar amounts of radioactive materials, it would seem that material was still settling from the atmosphere as long as 5 hr after the first arrival of material. This added fall-out was also noticeable in the air samples collected at several stations.

Chapter 5

SUMMARY

The program as undertaken by Project 37.2 was to study the downwind concentrations of mixed fission products produced by nuclear detonations. Two phases of downwind effects were studied: (1) the material deposited on the earth's surface and (2) the material that was still being transported by the ambient wind stream.

The fall-out patterns of four tower shots were defined by surface beta-gamma survey methods. On the basis of the data from Operation Teapot and previous test series, there appeared to be an exponential relation between fall-out contamination and yield for different tower heights. Fall-out activities were generally detectable approximately 160 miles from GZ, and the maximum measurement, which calculated to an infinite dose of 180 r, was obtained 20 miles from GZ after the Met shot.

Unit-area contamination values were also used to measure the degree of fall-out contamination at different distances from GZ. These data were based on surface-soil samples, collected transversely to the fall-out pattern, which were processed to yield both total activity and size-fraction contribution. The plot of total contamination in terms of microcuries per unit area shows the same general pattern as the radiation-intensity data, i.e., a rapid decrease in activity within 50 miles with a gradual approach to an asymptotic line at further distances from GZ. There is an inverse exponential relation between both radiation-intensity and total contamination and time. Although these two measures of surface contamination are similar, there are enough variations in the $\mu c/ft^2$: mr/hr ratios to prohibit a correlation of the ratio with distance from GZ or yield.

An integral aspect of the distance effects on fall-out contamination concerns the variation in particle size of the active material. In general, it has been found that the median diameter of the fall-out material decreases with increasing distance and time. There were variations from this trend which will require further study and correlation with particle trajectories. As the median diameter decreased with distance, the percentage contribution of the 0- to 5-μ fraction to the total activity increased from 3 to 4 per cent at 20 miles to 10 to 12 per cent at approximately 150 miles from GZ for the Tesla, Apple I, and Met shots.

The radiostrontium content of selected soils from two shots did not show any relation with distance, except possibly in the 44- to 88-μ range. The percentage of radiostrontium was higher in Met fall-out than in Tesla fall-out by factors of 3 to 9. The radiostrontium was more soluble in ammonium acetate than the total fission-product mixture.

Since the contaminated soils were collected postshot, a comparison of these data to activities collected on gummed paper was made. Gummed-paper samples were collected during two shots, and the ratio of gummed-paper to soil activities was calculated to be 0.83. A study of the material deposited on gummed papers relative to time of exposure showed a later deposition of active material after the initial contamination. This was also noticeable in air samples. Further evaluation is required to determine whether this was due to continued fall-out from the cloud or translocation of deposited material.

The airborne radioactivity concentrations 4 ft above the ground were sampled by several methods. The attempt to determine the effect of near isokinetic sampling conditions on measured concentrations, the proximity to isokinetic conditions being variable due to changes in wind velocity, indicated variations in sample concentrations which have been due to the various sampling techniques but which could also be the result of nonuniformity of the fall-out materials.

The determination of concentration variation with distance from GZ and with time after shot was based on the UCLA automatic samplers, sampling for 2-hr periods both during and after the time of fall-out. Data collections for this study were made during two shots. The peak concentrations detected during Met and Apple II were 2.16 $\mu c/m^3$ at a sample midtime of H+3.67 hr and 12.23 $\mu c/m^3$ at a sample midtime of H+1.02 hr, respectively. The variation of concentration generally reflected a rapid initial decrease, followed by a less rapid or an occasional increase of concentration level with increasing time.

Based on values of the maximum allowable airborne concentrations determined by the Operation Jangle Feasibility Committee, the concentrations detected during the Operation Teapot series did not appear to represent acute inhalation hazards.

The particle-size distribution of the airborne activity, as determined by means of cascade-impactor sampling, was studied with respect to distance and time. The distance relation showed a tendency for samples within 10 miles to have small median diameters, with larger and then smaller median diameters at increasing distances. The explanation may be found in the mechanism of fall-out. At near distances the material falling from the cloud is mainly very large (300 to 500 μ), but very small particles may be brought into the air sample by means of a scrubbing action or some comparable mechanism. At greater distances the normal aerodynamic settling laws may more accurately describe the deposition of activity from the cloud, and, under these conditions, the particle size will decrease with increasing distance from GZ.

For the purpose of defining the hazard associated with solubility properties, both soil and airborne samples were treated with four solvents. No correlation between solubility and distance was apparent for any of the shots studied. However, 0.1N HCl generally removed in excess of 20 per cent of the activity of soil samples and 40 to 80 per cent of that in airborne material.

Appendix A

CHARACTERIZATION OF FALL-OUT FROM MOTH SHOT

Several samples of contaminated soil were collected and brought to Project 37.2 for size analysis and radioassay. One sample (L-48) was collected 2 miles southwest of Dry Lake on Routes 91 and 93, and another sample (L-49) was collected 2.4 miles southwest of Dry Lake. Two samples were collected by W. S. Johnson, LASL, in areas of high activity. His first sample (L-50) was collected in a region of 95 mr/hr, and his second sample (L-51) was from an area of 75 mr/hr.

Composite soil samples of 3 ft^2 were first dried for approximately 3 hr and then sieved through a 2-mm screen. Three 200-g aliquots of the <2-mm fraction were radioassayed in gas-flow proportional counters to determine the area contamination. The activity found in an aliquot was converted to $\mu c/ft^2$ at H+12 hr, including self-absorption and coincidence correction (Table A.1).

TABLE A.1 — AREA CONTAMINATION ORIGINATING FROM MOTH SHOT

Sample No.	Sample location	Activity, $\mu c/ft^2$ (H+12 hr)
L-48	2 miles SW of Dry Lake on Routes 91-93; 19.1 miles NW of Nellis AFB gate	132.18
L-49	2.4 miles SW of Dry Lake on Routes 91-93; 18.5 miles NW of Nellis AFB gate	64.33
L-50	Sample 1, collected by W. S. Johnson (95 mr/hr); 2 to 3 miles from T-3 Area	1821.9
L-51	Sample 2, collected by W. S. Johnson (75 mr/hr); 2 to 3 miles from T-3 Area	2012.9

Further 100-g samples of L-48, L-50, and L-51 were fractionated in a sieve mesh covering the range 2000 μ to < 44 μ and the air elutriator (roller separator) covering the range 44 to 0 μ. The various fractions were radioassayed for beta activity in gas-flow proportional counters; the results were corrected for sample self-absorption. The results in percentage of activity are given in Table A.2.

There appeared to be a magnetic component in the fall-out material. After magnetic separation the 0- to 44-μ fraction of sample L-48 yielded 3.70×10^5 d/min in the magnetic component and 1.29×10^5 d/min in the nonmagnetic component. Several fractions of samples L-48 and L-51 were processed in this manner, and the magnetic component was determined by radioassay in gas-flow proportional counters (Table A.3).

TABLE A.2—DISTRIBUTION OF RADIOACTIVITY WITH RESPECT TO PARTICLE SIZE

Size range, μ	Percentage of total activity: Sample L-48 2 miles SW of Dry Lake	Sample 1 (95 mr/hr)	Sample 2 (75 mr/hr)
2000–840	0.24	28.82	0.03
840–500	0.18	44.44	55.41
500–420	0.11	21.34	24.28
420–350	1.12	0.02	8.49
350–300	0.18	0.03	8.84
300–250	0.43	0.81	1.56
250–177	2.12	0.84	0.15
177–125	10.47	0.26	0.04
125– 88	46.63	0.47	0.15
88 – 44	4.03	2.45	0.59
44– 20	6.42	0.19	0.06
20– 0	29.08		
20– 5		0.01	0.21
5– 0		0.01	0.21

The magnetic fractions of sample L-51 in two ranges (420 to 500 μ and 500 to 840 μ) were further processed to separate a number of spherical particles. Six particles from each fraction were collected and weighed. The individual particles were optically measured for diameter, and the volume was computed for the single particles. On the basis of the weight of six particles and their total volume, the apparent density of the magnetic material in the 420- to 500-μ range was computed to be 1.28 g/cm^3, whereas the density in the 500- to 840-μ range was 2.23 g/cm^3.

TABLE A.3—DISTRIBUTION OF RADIOACTIVITY WITH RESPECT TO MAGNETIC AND NONMAGNETIC COMPONENTS

Sample No.	Fraction, μ	Magnetic, %	Nonmagnetic, %
L-48	0–44	74.15	25.85
L-48	88–125	5.06	94.94
L-51	420–500	99.94	0.06
L-51	500–840	99.82	0.18
L-51	840–2000	99.93	0.07

The individual particles were mounted on microscope slides and were radioassayed for beta activity in flat-plate gas-flow proportional counters. The specific activity, corrected to H + 12 hr, was determined on the basis of the measured diameter (Table A.4).

A sample of magnetic material was analyzed in a single-channel pulse-height analyzer, using a sodium iodide crystal. Three peaks were noted at 0.408-, 0.765-, and 1.02-Mev gamma. The 0.765- and 1.02-Mev peaks were about the same intensity, and the 0.408-Mev peak was three times this intensity. Absorption studies were made on the 88- to 125-μ fraction of sample L-48, the 297- to 350-μ fraction of sample L-51, and the magnetic and nonmagnetic components of the two samples. There was no apparent difference in the energy characteristics of all these samples. A beta energy of approximately 1.7 Mev was noted. Seven-tenths of the total activity was due to a gamma component with an energy whose half-thickness value was approximately 6 g/cm^2, as measured by aluminum absorbers in a G-M scaler.

TABLE A.4—RELATION OF RADIOACTIVITY TO PARTICLE SIZE, SAMPLE L-51

Particle diameter, μ	Activity per particle, μc (H+12 hr)	Specific activity, μc/g (H+12 hr)
640	7.18	42,280
780	13.91	43,500
420	6.35	157,000
1020	7.80	11,010
1040	13.91	18,630
670	10.23	51,130
620	14.25	57,030
660	8.61×10^{-2}	344.5
580	8.50	34,020
600	12.12	48,510
600	3.11×10^{-2}	124.4
600	12.86	51,490

TABLE A.5—DECAY CONSTANTS OF SEPARATED FRACTIONS

Sample No.	Decay constant, D+6 days
L-48	1.36
L-51	1.31
L-48 (88–125 μ) L-51 (297–350 μ)	1.26
L-48, nonmagnetic	1.29
L-51, nonmagnetic	1.27
L-48, magnetic	1.22
L-51	1.52

TABLE A.6—PERCENTAGE SOLUBILITY OF DIFFERENT PARTICLE-SIZE RANGES IN VARIOUS SOLUTIONS

Sample No.	Location	Size range, μ	Insoluble, %	Soluble, %		
				H_2O	0.1N HCl	6N HCl
L-48-153	2 miles SW of Dry Lake	88–125	98.44 79.03	1.56	13.73	7.24
L-48-103	2 miles SW of Dry Lake	0–20	87.88 73.19	2.12	18.13	8.68
L-50-134	Sample 1 (95 mr/hr), T-3 Area	5–20	97.20 80.76	2.80	11.66	7.58
L-50	Sample 1 (95 mr/hr), T-3 Area	0–5	98.01 72.37	1.99	18.45	9.18

The same samples were also studied by radioassay in G-M counters for their decay characteristics until D+6 days (Table A.5). There were differences to be noted in the various samples.

Solubility studies were made on solutions of distilled water and 0.1N HCl. Soil fractions, ranging in weight from 0.1 to 1.0 g, were suspended in 50 ml of solution for 30 min prior to filtration through a membrane filter. Soil treated with 0.1N HCl was leached with 50 ml of 6N HCl following the initial filtration. Aliquots (25 ml) of each solution were dried, and the beta activity was determined in G-M counters; the radioactivities of each sample were corrected for sample self-absorption (Table A.6).

On the L-48-153 sample, two additional solvents were used, namely, 0.1N sodium thiosulfate and a solution of citric acid and sodium phosphate (dibasic) buffered at pH 7.6. Only 0.80 per cent of the sample was soluble in sodium thiosulfate. However, 14.50 per cent of the sample was soluble in the buffer solution, which, together with the 0.1N HCl solubility, offers an index of biological availability.

Appendix B

ANALYSIS OF CLOUD SAMPLES FROM HORNET SHOT

B.1 SAMPLE DESCRIPTION

The samples consisted of two aluminum strips, approximately 2 in. by 24 in., taped and positioned on the right and left tank tip fins of jet aircraft Tiger Red I. Both right and left samples represented oiled and nonoiled surfaces. Contamination was accumulated by three passes through the Hornet cloud at H+1.50, H+1.67, and H+1.83 hr, with an average time of H+1.67 hr considered as the midtime of sampling. The corresponding elevations of each of the passes through the cloud were 37,000, 36,000, and 36,000 ft mean sea level.

B.2 SAMPLE VALUES

Readings of right and left oiled and nonoiled strips in mr/hr were obtained by the use of a Precision model 107 G-M survey meter calibrated by Co^{60} for gamma dose rate. Readings were taken at measured distances above the four samples at two time intervals after H-hour; gamma readings were determined with the tube shield in the closed position, and beta-gamma readings were determined with the tube shield in the open position. Values in mr/hr were extrapolated to H+1.67 hr by the use of the $T^{-1.2}$ decay factor. The mr/hr values at various distances from the sample and the beta-gamma to gamma ratios appear in Table B.1.

The readings extrapolated by the $T^{-1.2}$ decay factor at two time intervals after H-hour were similar for both gamma and beta-gamma, although both high and low variations occur. For comparable distances from the source, the four samples indicated quite similar mr/hr values, particularly where beta-gamma readings are concerned. Beta-gamma to gamma ratios decreased with distance from the source, as would be expected from the relatively greater reduction of beta radiation compared to gamma radiation by the air as an absorber. The beta-gamma to gamma ratios appeared to maximize at approximately 40:1, which was reached 9 in. from the source for the H+11- to H+12-hr reading. This ratio was generally attained at closer distances for the later readings.

B.3 CONTAMINATION PER UNIT AREA

Small portions of the four samples were radioassayed by methane-flow counters having Mylar film windows of 0.8 mg/cm^2 thickness. Owing to activity variation, samples were counted at geometries ranging from 30 to 5 per cent, as determined by aluminum-covered Ra-D and -E standards. To avoid errors incurred by energy differences between samples and standards, all values were corrected to the distance of the window by factors obtained by counting an individual cloud sample in all positions. The leading-edge samples represented those portions of the

TABLE B.1 — GAMMA AND BETA-GAMMA VALUES[a] OF FISSION-CLOUD SAMPLES, HORNET

Distance above source, in.	Top left oiled-surface sample[b]						Top left nonoiled-surface sample[c]					
	Reading at H+11.22 hr, mr/hr			Reading at H+29.58 hr, mr/hr			Reading at H+11.52 hr, mr/hr			Reading at H+29.92 hr, mr/hr		
	γ	$\beta+\gamma$	$\frac{\beta+\gamma}{\gamma}$	γ	$\beta+\gamma$	$\frac{\beta+\gamma}{\gamma}$	γ	$\beta+\gamma$	$\frac{\beta+\gamma}{\gamma}$	γ	$\beta+\gamma$	$\frac{\beta+\gamma}{\gamma}$
3.0	18.20	O.S.[d]		13.5	O.S.[d]		11.03	O.S.[d]		15.3	O.S.[d]	
4.0	10.82	O.S.[d]		10.9	353.3	32.4	7.62	O.S.[d]		12.1	O.S.[d]	
5.0	7.87	O.S.[d]		6.6	278.3	41.8	4.81	O.S.[d]		6.4	335.5	52.4
6.0	4.72	O.S.[d]		5.7	202.5	35.5	3.61	O.S.[d]		5.7	263.9	46.3
7.0	3.74	O.S.[d]		5.0	157.0	31.4	2.91	O.S.[d]		4.8	155.6	40.8
8.0	2.95	O.S.[d]		4.7	117.8	25.0	2.51	104.3	40.4	3.8	127.2	33.5
9.0	2.38	98.4	41.7	4.7	87.9	18.7	2.01	86.3	42.9	2.5	108.1	43.2
12.0	1.97	59.0	29.9	3.8	45.2	11.9	1.60	50.2	31.4	1.6	98.6	61.6
15.0	1.57	33.5	21.3	3.1	30.1	9.7	0.80	28.1	35.1	1.3	38.2	29.4
18.0	1.18	19.7	16.7	1.6	19.5	12.2	0.50	14.0	28.0	1.0	23.2	23.2

Distance above source, in.	Right oiled-surface sample[e]						Right nonoiled-surface sample[f]					
	Reading at H+11.96 hr, mr/hr			Reading at H+30.25 hr, mr/hr			Reading at H+11.74 hr, mr/hr			Reading at H+30.44 hr, mr/hr		
	γ	$\beta+\gamma$	$\frac{\beta+\gamma}{\gamma}$	γ	$\beta+\gamma$	$\frac{\beta+\gamma}{\gamma}$	γ	$\beta+\gamma$	$\frac{\beta+\gamma}{\gamma}$	γ	$\beta+\gamma$	$\frac{\beta+\gamma}{\gamma}$
3.0	14.37	O.S.[d]		9.7	O.S.[d]		11.37	O.S.[d]		9.8	O.S.[d]	
4.0	9.66	O.S.[d]		8.1	323.6	40.0	8.20	O.S.[d]		9.5	358.6	37.8
5.0	6.85	O.S.[d]		6.4	251.2	39.3	5.18	O.S.[d]		7.2	286.9	39.8
6.0	4.94	O.S.[d]		5.6	186.4	32.5	4.10	O.S.[d]		5.9	226.8	38.4
7.0	3.62	O.S.[d]		4.6	130.4	27.2	3.13	O.S.[d]		5.2	172.8	33.2
8.0	2.28	119.0	36.5	4.2	111.1	26.5	2.81	112.2	39.9	3.9	132.0	33.8
9.0	2.81	96.58	34.4	3.2	90.2	28.2	2.16	92.79	43.0	2.6	91.3	35.1
12.0	2.24	52.78	23.6	2.3	39.9	17.3	53.95	31.2	31.2	2.0	46.6	23.3
15.0	1.35	31.4	23.3	1.3	26.4	20.3	0.66	30.21	35.1	1.3	31.0	23.8
16.0	1.01	19.48	13.4	1.0	14.2	14.2	0.54	15.11	28.0	1.0	18.6	18.6

[a] These values were corrected to the midtime of sampling, H+1.67 hr, by use of the $T^{-1.2}$ decay factor.
[b] Contaminated area of 14.35 in.^{2} (92.75 cm^2).
[c] Contaminated area of 15.37 in.^{2} (99.4 cm^2).
[d] O.S. means that the dial reading was off scale.
[e] Contaminated area of 12.45 in.^{2} (80.30 cm^2).
[f] Contaminated area of 13.62 in.^{2} (90.85 cm^2).

aluminum strip which were bent around the fin, thus presenting a surface approximately perpendicular to the direction of flight. All other samples represented surfaces that were essentially parallel to the direction of flight. The activity per unit-surface area is given in terms of microcuries per square centimeter in Table B.2.

The replicate samples indicated considerable variation in $\mu c/cm^2$ levels. The most notable example was the contamination of the leading edge of the right nonoiled-surface sample contrasted to that of the immediate and more remote rear samples. It would be expected that the high leading-edge values would influence the mr/hr values. Other than the fact that positioning of the sample during the obtaining of mr/hr readings may have been unfavorable to this section of the sample, the discrepancy is unexplained. In general, the correlation between $\mu c/cm^2$ and mr/hr values is poor, which probably reflects nonrepresentative sampling of the strips.

The right oiled- and nonoiled-surface sample values in $\mu c/cm^2$ indicated a greater retention of activity by an oily surface. This relation was reversed in the top left samples, but only single samples were involved.

B.4 ENERGY AND DECAY

Energy and decay characteristics were determined by the use of methane-flow counters. Based on the use of aluminum absorbers, two primary beta components having the following maximum energies were indicated: 0.34 Mev (half-thickness = 15 mr/cm^2) and 2.0 Mev (half-

TABLE B.2—RADIOACTIVITY PER UNIT-SURFACE AREA OF FISSION-CLOUD SAMPLES, HORNET

Sample location	Sample No.	Area, cm^2	Time of count, H+hr	Sample activity, d/min*	Total activity, μc (H+6.17 hr)	Activity per unit-surface area, $\mu c/cm^2$ (H+1.67 hr)
Right leading edge (perpendicular to direction of flight)	A	2.24	32.75	6,338,690	102.4	45.7
	B	2.99	36.75	4,176,637	76.8	25.7
Approx. 1 cm to rear of right leading edge	A	1.23	39.58	449,659	9.03	7.34
Right, no oil	A	2.15	31.42	43,592	0.66	0.31
	B	2.37	36.58	61,347	1.20	0.51
	D	2.50	32.68	62,392	0.90	0.36
Right, oil	A	1.80	31.38	152,520	2.31	1.28
	B	1.59	32.72	207,961	3.33	2.09
	C	1.85	38.65	134,603	2.63	1.42
Top left, oil	A	1.66	11.23	182,089	0.61	0.49
Top left, no oil	A	1.85	11.37	509,167	2.12	1.15

*Extrapolated to distance of window.

TABLE B.3—REDUCTION OF CONTAMINATION BY VARIOUS DECONTAMINATION PROCEDURES

Sample and treatment	Sample activity, d/min	Activity remaining, %	Recovered activity, d/min	Check total, d/min
Right, oil (B) initial	138,766	100.0		
After H_2O wash	107,347	77.6	32,369	139,716
After acetone wash	93,721	67.5	6,116	99,837
After H_2O swab	14,462	10.4		
After acetone swab	5,656	4.1		
Right, no oil (D) initial	42,115	100.0		
After H_2O wash	31,195	74.1	11,520	42,715
After acetone wash	27,048	64.2	842	27,890
After H_2O swab	6,059	14.4		
After acetone swab	2,572	2.9		
Right, no oil (C) initial		*		
After H_2O wash	14,609	70.7	6,067	20,676
After masking tape	12,308	59.5	2,506	14,814
After H_2O swab	2,567	12.4		
After acetone swab	995	4.8		
Right, leading edge (A) initial	2,890,810	*		
After H_2O wash	1,476,162	70.8	609,373	2,085,535
After acetone wash	1,476,901	70.8	24,339	1,501,240
After H_2O swab	701,706	33.6		
After acetone swab	410,717	19.7		

*Based on summation total.

thickness = 125 mr/cm^2). A 0.06-Mev gamma component was also indicated. The percentages of each component, as determined by simple subtraction, approximated 75.3, 24.1, and 0.6 per cent, respectively.

Over the time interval of H+11.2 to H+89.8 hr, decay was a function of $T^{-1.08}$.

B.5 DECONTAMINATION

As a means of determining the ease of removal of contamination from the oily and nonoily surfaces, the following procedure was used: after initial counts were obtained the samples were successively subjected to running water from a wash bottle (15 ml), running acetone from a wash bottle (15 ml), swabbing with a water-moistened Kleenex, and swabbing with an acetone-moistened Kleenex. In the case of the first two treatments, washings were recovered for a comparative study of the degree of contamination removal. Each swabbing treatment used two swabs. In addition to the above treatments, in one case, Scotch masking tape was pressed on the contaminated surface, and the removal was measured. Samples were counted in gas-flow counters, with all counts pertaining to an individual sample being made at the same distance from the window. Each series of counts per sample was corrected to the midtime of the series (H+1.67 hr) by the $T^{-1.2}$ decay factor. The data are presented in Table B.3.

There appeared to be little difference in the ease of decontamination of the oily and nonoily surfaces, although the oily surface did indicate a slightly greater retentiveness with washing and a slightly less retentiveness with swabbing. The right leading-edge sample revealed the greatest opposition to decontamination, particularly of that material normally removed by swabbing. This may reflect a higher degree of impaction than that occurring in surfaces exposed to lesser wind forces.

Appendix C

FALL-OUT RADIOACTIVITY, TESLA

TABLE C.1—PARTICLE-SIZE RELATION 12 MILES FROM GZ, TESLA

Distance S of Groom Lake Rd. on Papoose Rd., miles	Activity, $\mu c/ft^2$ (H+12 hr)	% of activity in size (μ) fraction											
		0–5	5–20	20–44	44–88	88–125	125–177	177–250	250–300	300–350	350–420	420–500	500–2000
2.6	63.42	4.20	4.04	0.84	22.91	64.87	0.73	0.73	0.33	0.35	0.16	0.11	0.73
3.6	85.79	3.97	0.88	0.31	6.05	80.09	0.05	1.40	0.85	0.59	0.20	0.35	0.26
4.3	374.11	3.41	1.85	0.09	5.04	70.23	16.80	1.91	0.16	0.13	0.09	0.06	0.22
5.0	1057.98	2.95	0.32	0.06	4.94	47.27	42.37	1.50	0.08	0.23	0.10	0.02	0.12
5.3	836.16	2.14	1.19	0.20	4.52	48.76	33.41	0.62	0.05	8.98	0.06	0.01	0.07
6.7	2710.87	1.70	0.19	0.12	3.59	5.48	47.12	28.17	2.79	2.79	5.35	2.40	0.30
7.7	4334.34	0.27	0.07	0.03	3.08	2.98	5.01	29.59	26.12	6.05	23.09	1.80	1.13
7.9	4816.95	1.71	0.58	0.05	1.86	1.83	1.35	26.49	20.53	25.12	13.48	6.89	0.23
8.3	1982.01	1.67	2.04	0.12	2.05	1.53	0.72	3.26	19.16	40.46	22.14	6.21	0.63
8.6	1510.18	2.40	0.49	0.04	2.69	4.20	2.33	1.07	8.80	43.87	29.25	3.94	0.75
8.9	57.28	2.58	6.90	0.27	17.50	11.18	13.34	5.28	1.06	0.82	11.11	24.81	5.15
9.0	9.52	27.45	19.58	0.70	21.97	18.51	6.12	1.96	1.38	0.57	0.26	0.29	1.21

TABLE C.2— PARTICLE-SIZE RELATION 20 MILES FROM GZ, TESLA

Distance S of Groom Lake Rd. on Indian Springs Rd., miles	Activity, $\mu c/ft^2$ (H+12 hr)	% of activity in size (μ) fraction											
		0–5	5–20	20–44	44–88	88–125	125–177	177–250	250–300	300–350	350–420	420–500	500–2000
7.0	23.30	11.86	3.30	1.40	49.71	31.1	3.90	8.90	2.74	2.05	2.90	2.63	7.50
8.0	104.49	8.55	4.02	0.52	67.46	11.68	4.43	2.19	0.34	0.28	0.14	0.08	0.39
8.5	131.33	7.19	5.20	0.45	75.37	6.94	0.18	3.85	0.13	0.05	0.04	0.51	0.09
9.0	161.03	1.22	5.20	8.42	75.55	4.26	1.43	1.20	1.60	0.17	0.08	0.13	0.68
9.5	191.10	4.74	2.51	0.16	82.11	8.89	1.00	0.41	0.10	0.04	0.01	0.01	0.03
10.0	99.10	0.77	6.56	0.97	55.49	30.46	1.97	1.23	0.76	0.79	0.28	0.10	0.62
11.0	83.08	4.04	5.03	0.89	44.89	42.41	2.27	0.03	0.15	0.22	0.05	0.00	0.02
12.0	161.06	15.78	20.30	1.52	30.29	17.50	12.88	1.01	0.23	0.29	0.21	0.11	0.59
12.2	151.92	4.27	0.62	0.16	3.63	81.26	8.49	0.48	0.22	0.29	0.13	0.07	0.39
12.5	346.73	5.15	4.07	0.49	3.39	78.53	8.88	1.21	0.03	0.14	0.02	0.01	0.09
12.8	857.73	2.66	6.25	0.53	3.44	50.74	29.32	6.44	0.42	0.02	0.05	0.02	0.10
13.2	1681.09	7.18	0.35	1.35	8.11	18.72	59.92	1.51	0.96	1.13	0.14	0.12	0.51
13.5	2172.51	3.14	0.28	0.12	6.13	17.62	52.30	17.53	2.44	0.12	0.12	0.07	0.33
14.0	2539.46	4.03	6.73	1.89	52.74	24.33	5.59	2.34	2.10	0.08	0.04	0.04	0.08
14.4	1317.48	4.59	2.36	0.43	2.83	2.30	50.13	28.70	10.39	0.06	0.06	0.04	0.12
14.7	846.04	3.13	5.89	1.66	3.47	0.87	58.04	16.08	7.90	2.66	0.08	0.07	0.21
15.2	657.27	5.66	5.12	2.06	0.90	0.90	39.75	32.94	4.39	6.17	2.06	0.05	0.15
15.3	609.16	4.90	5.17	0.96	3.31	0.95	44.03	38.73	0.09	0.06	0.07	0.03	0.09
15.4	473.63	1.33	0.27	0.31	1.24	0.38	64.61	28.76	1.45	0.46	0.29	0.32	0.58
16.0	19.13	1.97	6.61	1.74	8.14	2.39	14.16	62.73	0.21	0.23	0.29	0.68	0.85

TABLE C.3—PARTICLE-SIZE RELATION 46 MILES FROM GZ, TESLA

Distance N of Hwy. 95 on Sheep Canyon Rd., miles	Activity, $\mu c/ft^2$ (H+12 hr)	% of activity in size (μ) fraction											
		0–5	5–20	20–44	44–88	88–125	125–177	177–250	250–300	300–350	350–420	420–500	500–2000
53.6	8.02	0.00	23.25	5.10	40.41	2.48	4.55	4.85	3.67	2.06	2.53	1.99	9.10
51.6	231.03	11.67	3.68	0.92	48.54	28.18	1.66	1.26	0.83	0.71	0.49	0.35	1.70
51.1	374.64	10.31	0.73	0.90	45.70	37.70	1.23	1.44	0.59	0.39	0.25	0.16	0.60
50.8	533.13	10.00	5.58	0.65	49.79	27.03	5.16	0.75	0.42	0.41	0.01	0.13	0.25
50.1	673.13	7.28	5.18	0.83	23.53	48.90	12.24	0.86	0.22	0.18	0.05	0.03	0.15
49.6	421.55	4.95	4.13	0.63	68.76	16.67	2.27	0.84	0.54	0.88	0.18	0.17	0.49
49.1	248.32	7.11	3.40	0.41	77.40	7.80	1.14	0.69	0.40	0.62	0.16	0.16	0.72
48.6	61.57	2.33	0.00	0.12	64.88	4.69	16.49	3.39	1.61	1.52	3.87	0.72	0.98
48.4	35.43	8.39	2.56	23.19	54.95	4.39	0.00	3.26	0.00	0.00	3.06	0.14	0.05

TABLE C.4—PARTICLE-SIZE RELATION 60 MILES FROM GZ, TESLA

Distance N of Glendale on Hwy. 93, miles	Activity, $\mu c/ft^2$ (H+12 hr)	% of activity in size (μ) fraction											
		0–5	5–20	20–44	44–88	88–125	125–177	177–250	250–300	300–350	350–420	420–500	500–2000
45.7	9.87	19.42	28.39	27.98	22.80	1.11	0.00	0.33	0.00	0.00	0.00	0.00	0.00
40.7	30.14	6.44	7.64	1.40	76.17	1.44	0.55	5.14	0.56	0.19	0.11	0.02	0.33
37.7	202.11	8.20	8.59	1.97	77.22	1.35	0.31	0.67	1.40	0.70	0.00	0.00	0.00
36.2	163.45	9.39	7.02	1.60	75.20	3.51	0.17	0.99	1.95	0.15	0.15	0.08	0.70
35.7	133.99	8.46	5.30	0.25	75.41	6.17	0.73	0.79	0.66	0.42	0.21	0.28	1.34
35.2	191.00	6.66	8.94	0.09	75.64	6.24	0.60	0.61	0.57	0.43	0.07	0.00	0.23
34.7	128.04	5.64	15.42	1.51	65.44	6.84	0.87	2.09	0.48	0.85	0.07	0.10	0.70
33.7	19.40	3.83	9.25	1.77	73.71	1.14	0.70	3.42	2.17	0.60	0.29	0.50	2.63
30.2	3.04	14.20	2.76	4.93	35.93	1.13	10.00	4.11	1.87	15.47	0.08	2.85	6.56

TABLE C.5—PARTICLE-SIZE RELATION 79 MILES FROM GZ, TESLA

Distance N of Hwy. 93 in Meadow Valley Wash, miles	Activity, $\mu c/ft^2$ (H+12 hr)	% of activity in size (μ) fraction											
		0–5	5–20	20–44	44–88	88–125	125–177	177–250	250–300	300–350	350–420	420–500	500–2000
31.7	10.07	12.37	1.22	2.07	52.62	5.18	11.40	5.26	2.24	1.74	1.36	1.12	3.48
29.7	37.98	7.87	2.31	5.26	69.12	9.57	2.40	1.18	0.34	0.34	0.29	0.20	1.10
27.8	69.17	8.08	4.43	1.81	76.40	3.40	2.38	1.35	0.65	0.40	0.30	0.27	0.56
26.8	183.70	11.88	5.43	2.61	66.54	7.36	4.13	0.72	0.30	0.32	0.22	0.16	0.34
26.7	101.93	7.87	2.84	1.15	78.77	1.48	2.40	2.29	0.65	0.21	2.03	0.13	0.19
26.0	17.25	5.44	4.68	8.97	64.05	3.56	3.80	3.09	1.15	1.44	1.10	0.83	1.55
25.3	9.73	10.06	1.49	1.04	60.25	1.96	3.89	5.01	5.12	3.41	3.29	2.16	2.33
24.9	3.53	22.08	2.68	0.00	68.35	0.17	1.37	2.15	0.58	0.41	1.57	0.67	0.00

TABLE C.6—PARTICLE-SIZE RELATION 96 MILES FROM GZ, TESLA

Distance N of Hwy. 91 on Elgin Rd., miles	Activity, $\mu c/ft^2$ (H+12 hr)	% of activity in size (μ) fraction											
		0–5	5–20	20–44	44–88	88–125	125–177	177–250	250–300	300–350	350–420	420–500	500–2000
46.8	2.62	11.34	13.08	50.67	3.77	1.47	1.99	1.85	1.11	1.46	1.03	1.81	10.43
31.8	36.61	7.10	9.53	1.70	77.54	1.01	0.77	0.26	0.13	0.19	0.21	0.16	1.40
16.0	160.66	11.05	11.63	2.27	72.41	1.90	0.04	0.38	0.07	0.06	0.00	0.04	0.14
14.5	57.02	9.51	9.14	2.27	75.35	2.75	0.00	0.98	0.00	0.00	0.00	0.00	0.00
14.0	26.16	13.59	11.61	4.91	64.25	2.07	1.05	1.58	0.23	0.08	0.08	0.08	0.08
12.5	4.71	29.95	44.13	2.89	0.29	0.00	0.00	5.41	6.41	0.00	0.00	2.68	8.25
Thayer Rd–Elgin Rd. Jct.	48.19	25.56	11.61	24.08	19.21	4.27	6.22	1.91	0.99	0.47	0.65	0.82	4.19
4.0 miles S of Thayer Rd.–Elgin Rd. Jct.	43.40	5.30	8.45	2.99	69.09	7.60	3.96	1.16	0.39	0.03	0.19	0.17	0.66

TABLE C.7—PARTICLE-SIZE RELATION 132 MILES FROM GZ, TESLA

Distance N of Hwy. 91 on Utah Hwy. 18, miles	Activity, $\mu c/ft^2$ (H+12 hr)	% of activity in size (μ) fraction											
		0–5	5–20	20–44	44–88	88–125	125–177	177–250	250–300	300–350	350–420	420–500	500–2000
5.0	14.98	18.80	3.00	68.16	6.63	3.40	0.00	0.00	0.00	0.00	0.00	0.00	0.00
3.0	22.05	4.30	11.38	69.52	5.30	1.83	3.28	0.68	0.06	0.24	0.10	0.05	0.25
1.2	43.91	8.12	11.31	57.11	17.58	2.41	2.14	0.71	0.21	0.02	0.05	0.05	0.29
0.5	33.43	3.08	1.80	63.32	24.37	2.93	1.26	2.80	0.19	0.09	0.10	0.00	0.00
35.5*	11.97	15.23	12.17	20.38	25.03	3.76	3.12	2.40	2.51	2.32	2.91	2.54	7.62
23.5*	26.51	12.15	4.08	2.49	69.69	2.66	2.68	5.56	0.17	0.06	0.15	0.11	0.19
22.5*	32.34	7.78	17.62	33.28	33.78	1.61	1.89	3.49	0.10	0.13	0.11	0.03	0.17
21.0*	34.63	2.71	1.31	0.28	52.56	2.18	2.15	0.90	0.41	0.44	0.44	2.01	34.60
19.5*	20.46	4.56	2.20	1.56	58.14	6.44	6.25	3.40	1.89	1.72	1.78	1.77	10.28
18.5*	15.34	2.81	3.93	2.81	36.44	8.91	19.11	4.64	2.36	2.40	1.91	2.25	13.25

*Miles NE of Mesquite on Hwy. 91.

Appendix D

FALL-OUT RADIOACTIVITY, TURK

TABLE D.1—PARTICLE-SIZE RELATION 11.5 MILES FROM GZ, TURK

Distance NW of Tippipah Springs at Painted Rocks, miles	Activity, $\mu c/ft^2$ (H+12 hr)	% of activity in size (μ) fraction											
		0–5	5–20	20–44	44–88	88–125	125–177	177–250	250–300	300–350	350–420	420–500	500–2000
5.3	872.9	6.65	4.37	0.14	4.70	6.11	64.00	10.38	3.11	0.18	0.13	0.07	0.16
5.8	1447.81	10.40	2.15	0.38	4.17	6.11	61.10	9.76	0.90	3.11	0.32	0.30	1.29
6.8	1853.36	9.94	4.70	0.35	4.25	3.65	55.55	18.78	0.45	0.56	0.35	0.26	1.15
10.6	1225.27	4.34	0.57	0.68	2.34	17.23	58.40	11.42	1.04	1.24	0.69	0.55	1.50

Appendix E

FALL-OUT RADIOACTIVITY, APPLE I

TABLE E.1—PARTICLE-SIZE RELATION 13 MILES FROM GZ, APPLE I

Distance S of Groom Lake Rd. on Papoose Rd., miles	Activity, $\mu c/ft^2$ (H+12 hr)	% of activity in size (μ) fraction											
		0–5	5–20	20–44	44–88	88–125	125–177	177–250	250–300	300–350	350–420	420–500	500–2000
2.8	709.80	0.02	0.88	0.40	4.16	1.02	0.86	15.30	30.30	17.68	1.41	21.82	6.52
4.5	1114.09	4.86	6.63	1.23	2.98	0.42	0.22	0.44	19.08	29.80	12.66	11.32	10.38
5.0	917.66	5.29	4.19	0.95	1.39	0.84	0.33	0.81	3.69	13.37	16.99	7.55	44.62

TABLE E.2—PARTICLE-SIZE RELATION 23 MILES FROM GZ, APPLE I

Distance N of ISAFB* on Indian Springs Rd., miles	Activity, $\mu c/ft^2$ (H+12 hr)	% of activity in size (μ) fraction											
		0–5	5–20	20–44	44–88	88–125	125–177	177–250	250–300	300–350	350–420	420–500	500–2000
45.5	20.42	13.48	9.72	1.23	0.14	9.81	0.34	1.92	0.87	0.56	0.11	57.46	0.37
46.7	155.00	1.56	14.11	0.17	7.34	1.75	1.01	3.35	9.25	28.79	0.06	32.52	0.09
47.3	246.60	9.27	7.99	0.49	6.25	2.07	1.74	27.63	4.35	3.88	33.65	2.30	0.36
47.8	706.97	3.49	21.26	0.20	9.65	1.22	1.55	27.96	7.02	7.43	11.03	14.45	0.13
48.3	1094.10	5.41	2.47	0.12	5.96	1.85	2.45	24.04	30.06	22.89	4.44	0.07	0.17
49.2	465.25	12.89	1.05	0.68	2.03	0.79	2.16	40.56	26.43	5.65	6.55	0.17	1.03
49.5	508.15	3.25	10.98	1.00	0.73	0.58	25.69	29.27	19.31	8.28	0.06	0.05	0.80
49.8	144.06	4.43	2.86	0.23	5.74	2.29	1.69	41.26	2.16	6.03	9.84	0.03	23.45
50.3	182.49	0.47	6.48	0.01	3.70	9.11	6.95	64.77	0.58	6.77	0.20	0.14	0.23
50.8	146.78	3.98	2.19	0.21	3.64	1.41	0.06	47.06	20.29	20.29	0.12	0.00	0.06
52.8	172.77	4.91	0.94	0.39	1.04	2.74	55.08	13.89	1.24	18.16	0.58	0.46	0.78
54.1	122.12	0.02	1.49	0.05	3.04	2.45	76.50	13.26	1.26	1.06	0.07	0.00	0.01

* Indian Springs Air Force Base.

TABLE E.3—PARTICLE-SIZE RELATION 64 MILES FROM OZ, APPLE I

Distance S of Alamo on Hwy. 93, miles	Activity, $\mu c/ft^2$ (H + 12 hr)	% of activity in size (μ) fraction											
		0–5	5–20	20–44	44–88	88–125	125–177	177–250	250–300	300–350	350–420	420–500	500–2000
4.0	16.80	13.13	26.63	5.72	16.91	4.08	11.19	10.98	2.35	1.43	0.83	1.25	5.53
3.0	130.34	17.76	11.47	1.75	3.61	2.60	56.78	0.33	5.67	0.00	0.00	0.00	0.04
2.5	203.89	0.43	7.76	1.89	12.00	18.02	50.99	3.89	0.64	0.56	0.45	0.36	2.01
2.0	143.10	11.02	8.62	1.82	3.66	5.15	61.22	8.15	0.15	0.02	0.05	0.02	0.11
1.5	247.16	10.09	0.69	4.93	13.56	5.49	60.33	0.79	0.48	0.43	0.29	0.17	2.74
1.2	345.61	9.71	17.53	2.19	4.17	6.01	55.33	4.49	0.04	0.08	0.02	0.01	0.33
1.0	259.20	14.08	25.08	5.13	8.29	12.44	31.14	2.45	0.13	0.20	0.10	0.14	0.82
0.8	259.63	4.23	12.57	0.83	8.28	4.32	67.27	0.59	0.27	0.28	0.23	0.17	0.95
0.5	183.02	17.91	5.72	0.83	0.67	15.94	54.78	0.71	0.34	0.28	0.33	0.22	2.36
0.3	206.64	12.31	9.21	1.53	2.86	16.70	51.87	0.58	0.48	0.75	0.27	0.56	2.90
Alamo	180.84	9.35	17.20	1.93	15.15	19.97	36.10	0.15	0.06	0.00	0.02	0.04	0.04
0.4*	371.53	19.63	9.95	0.88	6.18	4.66	56.13	2.37	0.00	0.03	0.11	0.00	0.06
1.0*	264.88	2.92	1.86	0.49	8.22	39.13	35.49	3.58	3.74	0.53	1.08	0.39	2.52
1.5*	217.89	17.09	2.98	12.49	4.78	29.21	25.86	4.24	0.30	0.24	0.26	0.29	2.26
2.0*	138.20	28.07	3.97	1.66	3.32	15.60	27.79	10.45	0.36	7.56	0.32	0.28	0.62
2.5*	121.52	17.66	12.02	3.25	4.83	33.37	22.46	..77	0.29	0.25	0.40	0.38	3.35
3.5*	131.18	24.25	6.84	3.43	17.08	32.98	13.60	0.39	0.01	0.12	0.12	0.21	0.77
4.5*	80.22	6.78	2.08	9.79	13.44	50.01	6.73	0.60	0.29	0.54	0.67	0.76	8.31
6.5*	100.69	26.73	8.28	5.40	5.75+	36.64	7.17	5.85	0.33	0.13	0.35	0.60	2.77
10.7*	40.89	12.80	4.37	4.12	29.00	31.32	4.92	1.72	0.89	1.38	1.40	1.20	6.77
Hiko	16.27	8.98	3.83	1.38	61.11	6.13	7.78	4.15	1.58	1.55	0.78	0.54	2.19

* Miles N of Alamo on Hwy. 93.

TABLE E.4—PARTICLE-SIZE RELATION 92 MILES FROM GZ, APPLE I

Distance N of Elgin in Meadow Valley Wash, miles	Activity, $\mu c/ft^2$ (H+12 hr)	% of activity in size (μ) fraction											
		0–5	5–20	20–44	44–88	88–125	125–177	177–250	250–300	300–350	350–420	420–500	500–2000
9.0	5.34	15.37	25.25	8.05	7.56	32.15	7.41	1.64	0.00	1.47	0.48	0.00	0.62
11.0	15.33	9.63	3.51	3.39	10.58	34.35	6.64	5.89	9.38	3.29	3.00	2.51	7.86
12.0	76.86	7.42	7.95	0.10	39.93	43.29	0.79	0.11	0.01	0.26	0.07	0.00	0.07
13.0	49.61	19.40	33.38	6.75	16.75	19.35	3.69	0.13	0.00	0.09	0.02	0.01	0.44
14.0	44.80	13.51	8.10	7.41	15.22	35.16	9.80	1.88	1.10	0.92	0.73	0.64	5.53
14.5	98.47	16.90	21.49	4.53	27.04	22.01	2.69	1.77	0.64	0.60	0.49	0.30	1.54
15.0	47.52	9.14	19.14	14.07	11.47	22.45	0.94	2.13	1.26	1.18	0.48	0.71	16.65
15.5	58.58	8.61	2.93	6.61	38.85	19.08	7.77	4.90	1.00	1.58	1.14	1.51	7.70
16.0	82.10	10.17	6.97	1.22	50.54	25.47	3.45	0.51	0.20	0.10	1.09	0.04	0.24
16.5	69.43	24.19	14.40	3.22	23.29	28.89	2.06	1.40	0.16	0.06	0.10	0.97	1.12
17.5	50.69	11.01	10.95	3.56	42.66	9.60	9.87	2.04	1.28	0.98	0.90	0.96	6.20
18.5	6.54	43.57	3.87	0.61	13.85	32.77	3.41	1.06	0.73	0.00	0.00	0.00	0.13
20.5	37.82	7.66	1.66	0.19	61.56	20.27	1.86	2.74	0.94	0.06	0.04	0.08	2.94
Caliente	1.49	6.22	6.66	1.15	64.34	2.17	2.73	11.98	0.98	0.73	0.56	0.81	1.67
2.0	20.20	4.10	7.93	1.94	6.67	78.30	0.46	0.21	0.04	0.04	0.03	0.13	0.14
4.0	12.66	23.05	5.72	9.28	40.08	15.15	0.90	1.24	0.46	0.60	0.45	0.26	2.83
6.0	19.04	3.70	11.67	1.76	5.47	0.79	0.31	0.17	0.08	1.11	74.83	0.02	0.09

TABLE E.5--PARTICLE-SIZE RELATION 140 MILES FROM GZ, APPLE I

Distance along Utah Hwy. 18, miles	Activity, $\mu c/ft^2$ (H + 12 hr)	% of activity in size (μ) fraction											
		0–5	5–20	20–44	44–88	88–125	125–177	177–250	250–300	300–350	350–420	420–500	500–2000
0.8*	0.52	12.83	20.39	5.48	20.96	10.48	13.71	7.65	1.41	2.01	0.00	0.00	5.09
1.9*	0.85	7.83	15.65	7.07	24.89	7.94	10.81	9.11	3.54	0.63	1.97	0.61	9.94
2.9*	0.51	1.88	18.32	3.90	29.69	12.34	8.63	5.48	4.69	10.15	1.12	0.78	3.01
2.0†	5.02	12.60	17.59	14.36	26.30	2.79	2.91	3.27	1.35	1.66	1.57	1.51	14.31
4.7†	7.90	7.44	9.66	4.32	46.67	11.25	4.13	3.35	1.84	1.65	1.44	0.31	7.24
2.0‡	11.66	4.85	14.14	5.13	46.36	6.79	2.37	5.18	1.64	1.00	1.11	0.34	10.53
1.4§	2.24	11.01	14.07	4.63	41.96	4.77	10.63	1.92	2.49	4.74	1.48	0.59	1.50
4.9§	23.00	0.53	0.15	0.03	35.79	7.99	9.41	17.22	5.64	8.09	3.05	3.77	8.28
5.4§	9.63	4.19	12.23	6.74	19.57	2.21	27.13	1.86	0.12	0.17	0.57	0.13	1.04
9.7§	6.51	8.22	12.61	7.93	42.18	7.09	9.03	3.78	2.97	2.11	1.95	1.04	1.09

* Miles N of Veyo. † Miles N of Central. ‡ Miles S of junction with Utah Hwy. 130. § Miles S of Beryl junction.

107–108

TABLE E.6--PARTICLE-SIZE RELATION 165 MILES FROM GZ, APPLE I

Distance S of Cedar City on Hwy. 91, miles	Activity, $\mu c/ft^2$ (H + 12 hr)	% of activity in size (μ) fraction											
		0–5	5–20	20–44	44–88	88–125	125–177	177–250	250–300	300–350	350–420	420–500	500–2000
14.2	5.05	10.29	12.60	9.69	32.20	12.91	10.88	6.99	2.50	1.34	0.00	0.50	0.10
12.2	5.78	6.30	14.07	7.08	52.19	6.70	6.09	2.65	1.56	1.50	0.23	0.00	1.73
10.2	7.48	4.07	18.60	1.58	61.70	3.50	3.94	2.45	0.07	1.30	0.23	0.51	2.05
9.2	9.70	11.85	15.96	15.56	27.51	5.63	7.90	3.85	3.10	2.12	1.39	0.02	4.42
8.1	5.64	1.61	2.89	32.19	27.81	8.07	12.01	10.37	3.24	0.28	0.71	0.75	0.08
7.5	10.34	12.11	15.47	4.61	49.12	2.56	2.91	3.18	2.19	2.72	0.91	1.10	3.13
7.0	13.65	6.76	14.52	10.80	49.46	3.21	4.52	2.96	1.82	1.35	1.09	0.90	2.52
6.5	4.05	11.19	12.34	0.00	46.38	2.65	4.14	0.00	1.41	0.17	3.21	3.06	16.46
6.0	3.91	7.77	10.98	5.67	37.40	4.03	17.16	3.48	2.91	3.77	2.23	1.53	3.07
5.0	5.26	3.56	3.51	3.29	81.03	2.89	2.97	0.95	0.29	0.16	0.00	0.61	0.73
4.0	17.77	17.77	15.19	5.20	21.65	5.71	6.43	11.34	5.15	4.47	1.22	2.11	3.77
2.0	0.74	3.91	15.97	8.13	21.71	9.11	11.27	7.10	3.50	5.60	6.24	2.89	4.75

Appendix F

FALL-OUT RADIOACTIVITY, MET

TABLE F.1—PARTICLE-SIZE RELATION 20 MILES FROM GZ, MET

Distance N of ISAFB on Indian Springs Rd., miles	Activity, $\mu c/ft^2$ (H+12 hr)	% of activity in size (μ) fraction											
		0–5	5–20	20–44	44–88	88–125	125–177	177–250	250–300	300–350	350–420	420–500	500–2000
27.5	19.17	16.43	8.34	5.59	5.58	6.07	20.83	23.90	3.60	3.22	1.06	0.89	1.47
27.0	15.02	9.57	15.90	15.04	19.67	11.97	16.26	9.10	0.82	0.66	0.09	0.30	0.62
26.5	229.95	15.68	12.98	2.57	1.79	6.18	2.12	2.36	14.51	41.58	0.11	0.03	0.09
26.0	666.38	5.98	9.49	1.63	2.38	1.10	2.47	5.99	20.37	37.35	13.17	0.04	0.03
25.8	2645.20	2.75	4.08	0.46	1.53	0.47	1.23	12.06	26.94	41.38	7.66	1.17	0.02
25.2	4365.63	2.60	2.05	0.20	1.67	0.66	0.84	9.39	28.17	42.13	8.21	0.01	4.05
25.0	5541.90	3.76	0.90	0.29	1.37	0.53	0.99	10.38	21.39	36.06	13.22	12.23	0.21
24.6	3930.27	0.00	0.20	0.42	1.09	0.50	1.93	18.13	25.39	32.29	5.32	7.53	7.20
24.2	1810.70	4.28	1.91	0.79	2.00	0.01	2.97	23.99	19.23	29.07	5.84	1.00	7.91
24.1	2988.10	3.10	0.95	0.62	1.97	1.40	5.94	8.35	10.62	17.77	19.95	1.89	27.43
24.0	1334.50	0.79	0.20	0.07	0.50	0.33	3.94	12.52	12.87	5.30	4.98	43.54	14.04
23.5	259.45	4.77	6.96	1.89	4.87	1.42	1.05	27.80	2.26	0.98	0.82	46.87	0.29
22.0	8.69	9.13	21.97	4.90	33.30	10.17	18.17	4.48	2.73	1.54	0.80	0.00	1.80

TABLE F.2—PARTICLE-SIZE RELATION 58 MILES FROM GZ, MET

Distance N of Meadow Valley on Hwy. 93, miles	Activity, $\mu c/ft^2$ (H+12 hr)	% of activity in size (μ) fraction											
		0–5	5–20	20–44	44–88	88–125	125–177	177–250	250–300	300–350	350–420	420–500	500–2000
25.5	14.33	19.42	10.76	2.51	27.84	18.91	14.58	0.32	1.84	0.55	0.08	0.44	2.75
20.0	196.88	7.09	2.78	0.80	8.35	36.91	37.91	4.59	0.24	0.45	0.27	0.31	1.39
18.0	321.45	8.80	3.46	1.32	13.79	28.67	32.91	7.18	1.37	0.35	0.40	0.29	1.45
16.0	658.43	2.44	1.38	5.71	30.03	24.80	13.41	16.45	2.63	0.24	0.11	0.24	0.57
15.0	803.01	9.60	3.41	0.79	5.44	19.67	26.90	31.50	0.79	0.37	0.31	0.21	1.01
14.8	890.50	6.37	1.34	0.70	2.67	6.45	24.80	38.67	1.21	16.55	0.22	0.23	0.78
14.6	667.38	5.83	3.35	0.26	2.77	4.92	33.80	38.80	8.95	0.43	0.78	0.06	0.31
14.4	770.66	8.52	0.97	0.85	5.15	6.46	32.86	36.75	16.33	1.37	0.20	0.12	0.43
14.2	824.10	5.91	0.62	0.60	3.78	3.42	42.74	23.81	15.45	1.28	0.35	0.36	1.67
14.0	376.53	6.61	2.09	0.38	3.62	13.58	42.33	18.47	7.46	4.73	0.16	0.11	0.42
13.8	414.66	4.85	0.81	0.36	3.72	1.87	12.85	71.88	3.13	0.18	0.05	0.08	0.23
13.6	397.00	6.39	0.54	0.62	4.65	3.58	23.39	53.34	6.37	0.28	0.24	0.21	0.38
13.4	279.19	4.35	3.19	0.33	3.72	2.19	24.94	42.53	17.48	0.55	0.11	0.27	0.33
13.2	180.59	1.50	3.78	0.52	3.41	10.30	11.54	4.44	64.07	0.32	0.05	0.02	0.04
13.0	90.09	9.02	1.31	0.38	3.76	0.74	19.48	40.30	14.32	15.94	0.52	0.39	2.14
12.0	9.14	16.89	10.93	4.39	36.00	9.77	8.23	3.74	1.10	2.04	0.98	1.64	5.28
10.0	2.19	21.18	3.00	18.36	16.95	5.65	8.05	7.51	3.94	3.55	2.68	1.58	7.55
8.0	1.82	12.69	4.82	3.50	23.92	9.08	10.58	14.51	2.13	3.15	3.12	3.76	9.74

TABLE F.3—PARTICLE-SIZE RELATION 140 MILES FROM GZ, MET

Distance N of Enterprise on Hwy. 18, miles	Activity, $\mu c/ft^2$ (H+12 hr)	% of activity in size (μ) fraction											
		0–5	5–20	20–44	44–88	88–125	125–177	177–250	250–300	300–350	350–420	420–500	500–2000
23.0	7.68	15.25	12.37	0.96	38.15	7.40	16.77	2.79	1.29	0.95	0.76	0.46	2.88
18.0	51.75	8.78	1.33	1.39	33.70	25.36	21.92	1.97	1.07	0.66	0.60	0.52	2.78
16.0	67.04	8.72	1.47	0.46	39.52	20.85	14.43	2.53	5.86	0.63	0.62	0.45	4.47
12.0	100.48	0.24	0.03	0.21	6.08	6.92	18.67	16.17	2.66	2.50	11.60	6.71	28.21
10.0	98.36	12.24	11.49	0.19	14.31	53.66	7.41	0.13	0.05	0.12	0.02	0.09	0.27
9.0	71.09	28.33	8.17	3.52	8.01	31.86	21.37	0.37	0.09	0.04	0.01	0.03	0.26
8.0	71.46	7.87	11.77	1.10	8.08	17.15	9.83	18.25	1.10	23.68	0.36	0.24	0.33
6.0	38.18	11.50	8.25	0.78	8.89	43.89	2.40	1.93	19.23	1.24	0.49	0.54	1.03
5.0	8.54	11.08	64.31	1.37	12.89	4.43	2.79	2.44	0.72	0.00	0.00	0.00	0.00
1.0	1.04	10.09	36.3+	2.44	19.54	5.37	5.50	5.63	3.40	2.08	2.05	2.16	5.42
Enterprise	0.62	9.84	36.46	3.08	10.84	3.45	3.52	2.72	1.29	21.23	1.96	0.97	4.65

Appendix G

FALL-OUT RADIOACTIVITY, APPLE II

TABLE G.1 — PARTICLE-SIZE RELATION 7 MILES FROM GZ, APPLE II

Distance W of Mercury Hwy. on T-2 Access Rd., miles	Activity, $\mu c/ft^2$ (H+12 hr)	% of activity in size (μ) fraction											
		0–5	5–20	20–44	44–88	88–125	125–177	177–250	250–300	300–350	350–420	420–500	500–2000
4.7	1292.36	0.32	0.22	0.02	0.54	0.01	0.35	0.33	3.72	60.57	26.29	4.96	2.67
4.1	2475.51	0.52	0.31	0.10	0.48	0.20	0.42	0.39	0.15	0.29	19.71	29.09	20.52
3.6	4394.20	0.52	0.31	0.10	0.48	0.20	0.42	0.39	0.15	0.29	19.71	29.09	48.34
3.2	5913.77	0.36	0.12	0.08	0.33	0.18	0.38	0.24	0.15	0.32	0.15	14.31	83.37
2.9	1183.22	1.27	1.13	0.10	0.59	0.20	0.98	0.87	0.95	0.55	1.21	16.58	75.48
2.6	2070.10	0.08	0.05	0.02	0.09	0.04	0.09	0.07	0.04	0.06	0.22	3.66	95.38
2.4	759.38	0.10	0.10	0.14	0.65	0.36	0.53	0.56	0.39	0.09	0.32	0.53	95.63
0.8	74.51	0.85	0.00	0.00	2.15	0.00	0.00	0.00	0.00	0.00	0.00	15.69	81.31

TABLE G.2 — PARTICLE-SIZE RELATION 48 MILES FROM GZ, APPLE II

Distance W of Rec on Old Hwy. 25, miles	Activity, $\mu c/ft^2$ (H+12 hr)	% of activity in size (μ) fraction											
		0–5	5–20	20–44	44–88	88–125	125–177	177–250	250–300	300–350	350–420	420–500	500–2000
12.0	20.00	10.08	4.56	0.62	65.86	9.71	7.14	0.88	0.04	0.00	0.00	0.26	0.97
9.0	34.00	3.63	5.84	0.29	5.67	41.53	2.95	0.59	0.31	0.59	0.40	34.02	4.19
6.0	108.69	4.40	12.18	0.10	1.75	75.48	6.05	0.00	0.00	0.00	0.00	0.00	0.05
3.0	490.13	1.86	13.51	0.62	2.12	62.34	17.62	0.89	0.05	0.09	0.08	0.08	0.54
2.4	525.49	11.38	2.77	1.32	2.10	55.66	23.86	0.69	0.22	0.21	0.20	0.18	1.52
1.5	508.87	7.80	3.65	0.38	4.04	38.87	41.94	1.21	0.13	1.15	0.48	0.11	1.32
1.5	698.29	12.88	5.99	0.68	1.95	31.06	43.35	1.19	1.05	0.19	0.20	0.15	1.41
1.4	580.06	10.41	3.38	0.32	0.08	36.75	45.68	0.72	0.20	0.16	0.16	0.09	1.34
1.0	922.82	16.60	3.92	0.19	4.13	67.00	4.31	0.72	0.74	0.12	0.14	0.17	1.97
0.8	956.57	5.58	11.51	1.29	1.22	36.31	41.01	0.54	0.25	0.34	0.23	0.23	1.47
Reed	646.6	13.08	1.82	0.36	2.16	24.98	49.32	2.79	1.03	1.22	0.69	0.50	2.05
2.0*	495.92	7.86	1.17	3.35	3.56	16.24	64.07	2.60	0.09	0.16	0.07	0.08	0.25
4.5*	599.17	12.84	4.91	0.72	2.65	1.05	72.33	3.39	0.21	0.17	0.16	0.14	1.34
5.5*	253.04	11.84	4.81	0.33	1.90	3.48	71.86	3.32	0.18	0.15	0.03	0.02	1.50
8.5*	681.78	3.56	5.81	0.45	2.00	14.98	64.06	1.59	0.16	6.97	0.05	0.06	0.32

*Miles E of Reed.

TABLE G.3— PARTICLE-SIZE RELATION 160 MILES FROM GZ, APPLE II

Distance NE of Warm Springs on Hwy. 6, miles	Activity $\mu c/ft^2$ (H + 12 hr)	% of activity in size (μ) fraction											
		0–5	5–20	20–44	44–88	88–125	125–177	177–250	250–300	300–350	350–420	420–500	500–2000
8.0	19.91	25.84	3.16	42.67	4.07	8.84	2.26	9.48	1.26	0.78	0.40	0.34	0.90
12.0	13.39	17.01	2.80	1.39	66.34	1.61	1.93	1.20	0.00	0.53	0.77	0.28	6.01
16.0	39.78	6.70	0.36	0.34	89.50	1.96	0.49	0.00	0.05	0.26	0.06	0.26	0.00
24.0	25.51	26.86	7.64	30.38	24.95	2.60	1.48	1.25	0.34	0.74	0.51	0.43	2.81
28.0	53.18	9.88	2.03	0.70	80.08	5.33	0.38	0.41	0.13	0.00	0.07	0.03	0.97
32.0	60.72	3.59	3.72	3.93	74.60	8.13	1.91	1.18	0.59	0.68	0.52	0.00	1.14
37.0	72.84	23.33	7.11	0.00	61.02	8.63	0.00	0.09	0.00	0.00	0.00	0.00	0.00
42.0	126.74	14.22	3.33	2.42	60.98	8.10	6.27	1.17	0.63	0.33	1.12	0.21	1.21
47.0	38.89	17.28	12.12	1.11	63.29	2.97	1.18	0.58	0.33	0.36	0.22	0.20	0.36

Appendix H

AIRBORNE ACTIVITY CONCENTRATIONS, BEE

TABLE H.1 — AIRBORNE ACTIVITY CONCENTRATIONS AT VARIOUS DISTANCES FROM GZ, BEE

Location	UCLA sampler		High-volume samplers[a]			
	Sample time, H + hr	Activity, $\mu c/m^3 \times 10^{-6}$ (H + 12 hr)	Sample time, H + hr	Activity, $\mu c/m^3 \times 10^{-6}$ (H + 12 hr) Fixed-T	Dir-NT	Dir-T
4 miles N of Nye Canyon Rd. on road 13 miles E of GZ	1.00 – 2.00	25,400				
	2.00 – 4.00	10,300				
			1.00 – 5.08	30,900	31,100	27,000
	4.00 – 6.00	594				
	6.00 – 8.00	518				
			5.08 – 9.99	194	65.9	150
	8.00 – 10.00	30.9				
	10.00 – 12.00	6.82				
			9.99 – 12.46	235	122	256
	1.00 – 12.00	8,141	1.00 – 12.46	10,443	10,429	9,058
7 miles N of Nye Canyon Rd. on road 13 miles E of GZ	1.50 – 2.00	113,000				
	2.00 – 4.00	4,750				
			1.50 – 5.67			113,000
	4.00 – 6.00	178				
	6.00 – 8.00	32.3				
	8.00 – 10.00	31.4				
	10.00 – 12.00	42.3				
			5.67 – 9.42			239
			9.42 – 12.00			164
	1.50 – 12.00	19,672				
			1.50 – 12.00			37,801
6 miles N of Hwy. 95 on Indian Springs Rd. 30 miles E of GZ	1.80 – 2.00	1,030				
	2.00 – 4.00	1,140				
	4.00 – 6.00	96.8				
	6.00 – 8.00	11.8				

[a] Fixed-T, fixed-directional sampler with throttle; Dir-NT, directional sampler without throttle; Dir-T, directional sampler with throttle.

Appendix I

AIRBORNE ACTIVITY CONCENTRATIONS, MET

TABLE I.1—AIRBORNE ACTIVITY CONCENTRATIONS AT VARIOUS DISTANCES FROM OR ALONG THE MIDLINE OF PREDICTED FALL-OUT, MET

Location	UCLA sampler		High-volume samplers[a]			
	Sample time, H + hr	Activity, $\mu c/m^3 \times 10^{-6}$ (H + 12 hr)	Sample time, H + hr	Activity, $\mu c/m^3 \times 10^{-3}$ (H + 12 hr) Fixed-T	Dir-NT	Dir-T
35.0 miles N of Indian Springs AFB on Indian Springs Rd.	0.33– 7.00	320,000	0.33– 7.0	NS	NS	563,000
	7.00– 9.00	7,670	7.00– 8.75	NS	NS	13,300
	9.00–11.00	3,830				
	11.00–13.00	2,560				
	13.00–14.25	2,550	8.75–14.25	NS	NS	1,690
	14.25–16.25	731				
	16.25–18.25	405				
	18.25–20.25	493				
	20.25–22.25	677				
	22.25–24.25	14,200				
	24.25–26.25	116,000				
23.0 miles N of Indian Springs AFB on Indian Springs Rd.	0.50– 1.58	16,500				
	1.58– 3.67	232				
	3.67– 5.75	66.5	0.33– 5.75	4,250	5,750	8,190
	5.75– 7.75	29.2				
	7.75– 9.75	101	5.75– 9.25	331	27.2	161
	9.75–11.75	17.5				
	11.75–13.75	222	9.75–13.75	268	282	181
	13.75–15.75	216				
	15.75–17.75	172				
	17.75–19.75	142				
			13.75–19.75	NS	NS	NS
18.0 miles N of Meadow Valley Rd. Jct. on Hwy. 93	1.00– 3.75	143,000				
	3.75– 4.75	221,000				
	4.75– 5.75	15,700				
			1.00– 5.75	NS	NS	139,000
	5.75– 8.75	14,100				
	8.75–10.75	3,900				
			5.75–10.05	NS	NS	18,800
	10.75–12.75	2,440				
	12.75–14.75	2,100				
	14.75–16.00	2,288				
			10.05–16.00	NS	NS	2,020
	16.00–18.00	1,880				
	18.00–20.00	2,670				
	20.00–22.00	31,100				
14.0 miles N of Meadow Valley Rd. Jct. on Hwy. 93	1.08– 3.75	155,000				
	3.75– 4.75	38,000				
	4.75– 5.75	11,400				
			1.08– 5.00	221,000	405,000	188,000
	5.75– 8.75	6,450				
	8.75–10.75	13,500				
	10.75–12.75	6,390				
	12.75–15.50	2,700				
			5.00– 9.75	10,400	15,200	15,200
			9.75–15.50	16,400	18,600	23,700
	15.50–17.50	2,020				
	17.50–19.50	2,670				
	19.50–21.50	185				
	21.50–23.50	11,000				
	23.50–25.50	14,400				
	25.50–27.50	21,600				
			15.50–30.25	17,600	17,500	14,100
13.0 miles N of Enterprise on Utah Hwy. 18	3.50– 5.00	133,000				
	5.00– 7.00	3,320				
			3.50– 7.92	NS	NS	38,000
	7.00– 9.00	4,040				
	9.00–10.92	263				
			7.92–10.75	NS	NS	5,260
	10.92–12.92	1,070				
	12.92–14.92	154				
	14.92–16.92	1,580				
	16.92–18.92	964				
	18.92–20.92	191				
	20.92–22.92	1,400				
	22.92–24.92	3,820				
	24.92–27.25	4,550	10.75–27.50	NS	NS	328
6.0 miles N of Enterprise on Utah Hwy. 18			3.50– 7.00	10,500	114,000	30,400
			7.00–11.58	7,930	1,880	1,870
			11.58–25.92	5,260	3,290	2,440
1.0 mile N of Enterprise on Utah Hwy. 18			3.50– 5.67	NS	NS	1,260
			5.67–11.92	NS	NS	218
			11.92–25.92	NS	NS	69.5

[a] Fixed-T, fixed-directional sampler with throttle; Dir-NT, directional sampler without throttle; Dir-T, directional sampler with throttle.

Appendix J

AIRBORNE ACTIVITY CONCENTRATIONS, APPLE II

TABLE J.1 — AIRBORNE ACTIVITY CONCENTRATIONS AT VARIOUS DISTANCES FROM GZ, APPLE II

Location	UCLA sampler		High-volume samplers[a]			
	Sample time, H + hr	Activity, $\mu c/m^3 \times 10^{-6}$ (H + 12 hr)	Sample time, H + hr	Activity, $\mu c/m^3 \times 10^{-6}$ (H + 12 hr) Fixed-T	Dir-NT	Dir-T
4.1 miles W of Mercury Hwy. on T-3 Access Rd.	0.13 – 1.83	175,000				
	1.83 – 3.83	3,530				
	3.83 – 5.83	908				
	5.83 – 7.83	532				
			0.13 – 8.78	95,000	53,800	31,900
	7.83 – 9.83	3,100				
	9.83 – 11.83	5,100				
	11.83 – 13.83	118				
	13.83 – 15.83	160				
			8.78 – 18.42	582	340	271
	18.42 – 20.42	66.5				
	20.42 – 22.42	52.7				
	22.42 – 24.42	125				
	24.42 – 26.42	33.3				
	26.42 – 28.42	0.0				
	28.42 – 30.42	20.8				
	30.42 – 31.08	181				
			18.42 – 31.08	196	92.1	139
3.6 miles W of Mercury Hwy. on T-3 Access Rd.	0.90 – 1.83	627,000				
	1.83 – 3.83	9 940				
	3.83 – 5.83	1,550				
	5.83 – 7.83	108				
	7.83 – 9.83	10.7				
	9.83 – 11.83	70.0				
	11.83 – 13.83	219				
	13.83 – 15.83	344				
			0.90 – 9.55			107,000
			9.83 – 18.83			251
	15.83 – 20.83	407				
	20.83 – 22.83	134				
	22.83 – 24.83	139				
			15.83 – 20.27			299
0.8 mile W of Mercury Hwy. on T-3 Access Rd.	0.83 – 1.83	276,000				
	1.83 – 3.83	6,730				
	3.83 – 5.83	2,000				
	5.83 – 7.83	77.1				
	7.83 – 9.83	53				
	9.83 – 11.83	54.3				
			0.38 – 10.27			44,100
	11.83 – 13.83	28.6				
	13.83 – 15.83	159				
			10.27 – 19.00			226
	19.00 – 21.00	277				
	21.00 – 23.00	284				
	23.00 – 25.00	224				
	25.00 – 27.00	125				
	27.00 – 29.00	15.5				
	29.00 – 30.42	24.6				
			19.00 – 30.42			207
13.0 miles W of Road on Hwy. 95			1.50 – 7.83			6,480
			7.83 – 13.16			1,060
			13.16 – 18.33			205
			18.33 – 30.83			118
9.0 miles W of Road on Hwy. 95	1.67 – 3.33	2,640				
	3.33 – 5.33	1,750				
	5.33 – 7.33	788				
			1.67 – 7.33			5,065
	7.33 – 9.33	681				
	9.33 – 11.33	220				
			1.67 – 7.33			87.9
	11.33 – 13.33	216				
	13.33 – 15.33	2,150				
	15.33 – 16.17	240				
			13.66 – 18.66			243
	16.17 – 20.17	56.3				
	20.17 – 22.17	0.0				
	22.17 – 24.17	0.0				
	24.17 – 26.17	0.0				
	26.17 – 28.17	429				
	28.17 – 30.17	3.94				
	30.17 – 31.50	649				
			18.00 – 31.42			210
8.0 miles W of Road on Hwy. 95	1.83 – 3.33	43,500				
	3.33 – 5.33	3,060				
	5.33 – 7.33	1,660				
			1.83 – 8.77	60,900	60,700	33,500
	7.33 – 9.33	94.6				
	9.33 – 11.33	30.6				
			8.77 – 16.83	3,430	6,450	1,656
	11.33 – 13.33	428				
	13.33 – 15.33	1,230				
	15.33 – 17.33	3,180				
			16.83 – 17.78	583	763	881

TABLE J 1.—(Continued)

Location	UCLA sampler		High-volume samplers[a]			
	Sample time, M + hr	Activity, $pc/m^3 \times 10^{-6}$ (H + 12 hr)	Sample time, M + hr	Activity, $pc/m^3 \times 10^{-3}$ (H + 12 hr) Fixed-T	Dir-MT	Dir-T
3.0 miles W of Reed on Hwy. 25	1.58 – 5.33	6,150				
	5.50 – 6.67	2,330				
	6.67 – 7.83	370				
			1.58 – 8.33	40,000	340,000	24,100
	7.83 – 10.00	10.0				
	10.00 – 10.17	146				
			8.33 – 13.33	1,060	4,610	1,220
	10.17 – 14.33	45.5				
	14.33 – 18.33	20.6				
			13.33 – 18.33	777	4,730	1,280
	18.33 – 20.33	256				
	20.33 – 22.33	0				
	22.33 – 24.33	13.1				
	24.33 – 26.33	0				
	26.33 – 28.33	63.8				
	28.33 – 34.33	312				
			18.43 – 33.33	841	2,880	740
Reed (on Hwy. 25)	1.67 – 4.11	290,000				
	4.11 – 6.89	8,490				
			1.67 – 8.00			109,000
	6.89 – 9.67	2,460				
	9.67 – 12.48	346				
			8.00 – 13.00			8,040
	12.48 – 15.29	1,230				
	15.29 – 18.00	3,020				
			13.00 – 17.83			4,380
	18.00 – 20.00	2,170				
	20.00 – 22.00	343				
	22.00 – 24.00	311				
	24.00 – 26.00	760				
	26.00 – 28.00	1,830				
	28.00 – 30.00	2,440				
	30.00 – 31.43	4,060				
			17.68 – 30.83			2,770
3.0 miles E of Reed	1.67 – 3.33	170,000				
	3.33 – 11.33	3,130				
			1.67 – 7.67			80,600
			7.67 – 12.83			3,190
	11.33 – 13.33	551				
	13.33 – 15.33	1,290				
	15.33 – 17.33	340				
	17.33 – 19.33	335				
			12.83 – 17.33			2,030
	19.33 – 21.33	172				
	21.33 – 23.33	204				
	23.33 – 25.33	336				
	25.33 – 27.33	179				
	27.33 – 29.33	673				
	29.33 – 30.33	670				
			17.33 – 30.33			1,110
8.0 miles W of Warm Springs on Hwy. 8	3.67 – 4.33	4,470				
	4.33 – 6.33	537				
	6.33 – 8.33	18				
			3.67 – 8.33			4,750
	8.33 – 10.33	0				
	10.33 – 12.33	0				
	12.33 – 14.33	0				
	14.33 – 16.33	31				
	16.33 – 17.83	0				
			8.33 – 10.83			1,870
			12.83 – 17.83			201
	17.83 – 19.83	61.1				
	19.83 – 21.83	70.2				
	21.83 – 23.83	20.8				
	23.83 – 25.83	4.53				
	25.83 – 27.83	96.5				
	27.83 – 29.83	0				
	29.83 – 30.83	11.1				
			17.83 – 30.83			106
0.5 mile NE of Warm Springs on Hwy. 8	3.83 – 4.33	3,010				
	4.33 – 6.33	1,110				
	6.33 – 8.33	628				
			3.33 – 8.33	1,290	1,304	2,010
			8.33 – 11.83	737	1,700	1,110

TABLE J.1—(Continued)

Location	UCLA sampler		High-volume samplers*			
	Sample time, E + hr	Activity, $\mu c/m^3 \times 10^{-4}$ (E + 12 hr)	Sample time, E + hr	Activity, $\mu c/m^3 \times 10^{-4}$ (E + 12 hr) Fixed-T	Dir-NT	Dir-T
4.0 miles NE of Warm Springs on Hwy. 6	3.04 – 3.83	588				
	3.83 – 5.83	16,600				
	5.83 – 7.83	883				
			5.06 – 7.92			10,800
	7.83 – 9.83	1,190				
	9.83 – 11.83	556				
			7.92 – 11.17			833
	11.83 – 13.83	383				
	13.83 – 15.83	429				
	15.83 – 17.00	226				
			11.17 – 16.92			340
	17.00 – 19.00	90.8				
	19.00 – 21.00	143				
	21.00 – 23.00	220				
	23.00 – 25.00	134				
	25.00 – 27.00	104				
	27.00 – 29.00	120				
	29.00 – 30.00	227				
			16.92 – 30.00			175
8.0 miles NE of Warm Springs on Hwy. 6	3.08 – 4.83	18.5				
	4.83 – 6.33	199,000				
	6.33 – 8.33	350				
	8.33 – 10.33	477				
			5.06 – 7.83	21,100	13,000	14,000
			7.33 – 11.33	1,770	1,970	4,000
	10.33 – 12.33	130				
	12.33 – 14.33	641				
	14.33 – 16.33	93.8				
	16.33 – 17.08	930				
			11.33 – 17.33	530	563	1,000
	17.08 – 19.08	148				
	19.08 – 21.08	97.8				
	21.08 – 23.08	140				
	23.08 – 25.08	93.5				
	25.08 – 27.08	96.3				
	27.08 – 29.08	130				
	29.08 – 31.08	429				
	31.08 – 32.83	85.4				
			17.33 – 29.33	541	516	463
16.0 miles NE of Warm Springs on Hwy. 6	3.08 – 4.33	40,200				
	4.33 – 6.33	331				
			3.06 – 7.46			55,700
	6.33 – 8.33	1,810				
	8.33 – 10.33	1,900				
			7.46 – 11.50			4,530
	10.33 – 12.33	644				
	12.33 – 14.33	126				
	14.33 – 16.33	257				
	16.33 – 17.33	7,630				
			11.50 – 17.50			1,640
	17.33 – 19.33	178				
	19.33 – 21.33	96.9				
	21.33 – 23.33	72.8				
	23.33 – 25.33	104				
	25.33 – 27.33	55.2				
	27.33 – 29.33	121				
	29.33 – 31.33	94.1				
	31.33 – 33.67	35.6				
			17.50 – 33.50			348

* Fixed-T, fixed-directional sampler with throttle; Dir-NT, directional sampler without throttle; Dir-T, directional sampler with throttle.